

AN ABSTRACT OF THE THESIS OF

Dah-Cheng Lin for the degree of Master of Science in Chemical Engineering
presented on August 24, 1990

Title: Fouling Characteristics of A Desalted Crude Oil

Redacted for privacy

Abstract approved:


James G. Knudsen

The fouling characteristics of a desalted crude oil were investigated in a systematic investigation. There are two main parts in this study, the dry bulk tests (dehydrated crude oil) and the wet bulk tests (to which desalter brine was added). Three barrels of desalted crude oil provided by Amoco Oil Company were studied.

For the dry bulk tests, no brine was added to the crude oil. The effects of fluid velocity and surface temperature on fouling were investigated. The higher the surface temperature the greater the fouling was observed. Fouling decreased with an increase of fluid velocity. Fluid velocity had a stronger effect on fouling at low surface temperatures than at high surface temperatures. It was also observed that the fouling behavior of crude oil depended on small difference in composition. The threshold surface temperatures for the initiation of fouling were 400 - 450 °F (3.0 ft/sec), 525 - 550 °F (5.5 ft/sec), 550 - 600 °F (8.0 ft/sec) and about 600 °F (10.0 ft/sec) for Barrel No. 2 and Barrel No. 3. For Barrel No. 1 however, the threshold surface temperatures were about 550 °F (3.0 ft/sec) and 600 °F (5.5 ft/sec).

For the wet bulk tests, a certain amount desalter brine (weight percentage = 0.8%) was added to the crude oil for each run. The effects of fluid velocity, surface temperature and the presence of brine on fouling were investigated. Higher surface temperature enhanced fouling considerably. Fouling was reduced as fluid velocity was increased. It was shown that brine had a strong effect on fouling. No fouling occurred for velocities of 5.5 and 8.0 ft/sec at a surface temperature of 350 °F which was a condition for which an aqueous phase was present and the salt remained in solution. Significant fouling occurred for velocities of 5.5 and 8.0 ft/sec at a surface temperature operated at a low 400 °F ($T_b = 300$ °F) which was a condition for which the aqueous phase at the heat transfer surface was dissolved or boiled to extinction and the salt was deposited on the heat transfer surface.

Fouling Characteristics of A Desalted Crude Oil

by

Dah-Cheng Lin

A THESIS

submitted to

Oregon State University

in partial fulfillment of
the requirements for the
degree of

Master of Science

Completed August 24, 1990

Commencement June 1991

Approved:

Redacted for privacy

Professor of Chemical Engineering in Charge of Major

Redacted for privacy

Head of Department of Chemical Engineering

Redacted for privacy

Dean of Graduate School

Date thesis is presented: August 24, 1990

Typed by: Dah-Cheng Lin

ACKNOWLEDGEMENTS

There has been a lot of help and encouragement from others during this investigation, therefore I wish to take this opportunity to express my sincere appreciation to the following:

My advisor, Dr. James G. Knudsen, for his advice and guidance throughout the duration of this study. The opportunity to be his research assistant will not be forgotten.

Dr. Dawn Peters for her very valuable time and suggestions.

Heat Transfer Research Inc., Alhambra, California, for their funding of this project.

The faculty members in the Chemical Engineering Department, especially Dr. Levenspiel and Dr. Kimura, for their suggestions.

My family and my wife for their encouragement, especially for my wife's care of our baby during this period.

TABLE OF CONTENTS

CHAPTER 1	INTRODUCTION.....	1
CHAPTER 2	THEORETICAL ASPECTS AND LITERATURE SURVEY	3
2.1	Heat Transfer under Boiling Conditions	3
2.2	Classification of Fouling.....	5
2.3	Physical Parameters in Chemical Reaction Fouling.....	7
2.3.1	Velocity Effect	8
2.3.2	Surface Temperature Effect	10
2.3.3	Bulk Temperature Effect.....	11
2.3.4	Boiling Effect.....	12
2.4	Mechanism of Fouling	13
2.4.1	Existing Models of Chemical Reaction Fouling	16
2.4.2	Basic Equation for Determining Fouling Resistance	22
CHAPTER 3	EXPERIMENTAL EQUIPMENT	27
3.1	Test Section.....	27
3.2	Flow Rate Measurement	30
3.3	Storage Vessel.....	31
3.4	Circulation Pump	33
3.5	By-Pass Systems	33
3.6	Heating and Cooling of Bulk Fluid.....	33
3.7	Safety Measures.....	34
CHAPTER 4	EXPERIMENTAL PROCEDURE.....	36
4.1	Fluid Investigated.....	36

4.2	Cleaning and Recalibration of Heaters	36
4.3	Heat Transfer Test (Boiling Test).....	42
4.4	Operating Conditions.....	43
4.5	Run Initiation.....	44
4.6	Data Acquisition and Processing.....	49
4.7	Process Monitoring.....	50
4.8	Run Termination	51
CHAPTER 5	RESULTS AND DISCUSSION.....	52
5.1	Heat Transfer Test (Boiling Test).....	52
5.2	Dry Bulk Tests on Amoco Crude Oil.....	60
5.2.1	Fouling Tests with Barrel No. 1.....	60
5.2.1.1	Effect of Surface Temperature.....	60
5.2.1.2	Effect of Velocity	65
5.2.2	Fouling Tests with Barrel No. 2.....	65
5.2.2.1	Effect of Surface Temperature.....	65
5.2.2.2	Effect of Velocity	71
5.2.2.3	Determination of Threshold Fouling Temperature for Sample from Barrel No. 2	76
5.2.3	Fouling Tests with Barrel No. 3.....	76
5.2.3.1	Threshold Temperature at 8.0 ft/sec.....	78
5.2.3.2	Threshold Temperature at 3.0 ft/sec.....	78
5.2.3.3	Threshold Temperature at 5.5 ft/sec.....	78
5.2.3.4	Threshold Temperature at 10.0 ft/sec.....	81
5.2.4	Threshold Surface Temperature for Amoco Crude Oil from Barrel No. 2 and Barrel No. 3	81
5.3	Wet Bulk Tests on Amoco Crude Oil	85

5.4	Effect of Reusing the Sample with the Dry Bulk Test	89
5.5	Fouling Deposit Characteristics	92
CHAPTER 6	CONCLUSIONS AND RECOMMENDATIONS	94
6.1	Conclusions	94
6.2	Recommendations for Future Work	95
BIBLIOGRAPHY	97
APPENDICES		
APPENDIX A	HEATER CALIBRATION	103
APPENDIX B	COMPUTER PROGRAM	107
APPENDIX C	RESULTS OF HEAT TRANSFER TESTS	115

LIST OF FIGURES

<u>Figure</u>	<u>Page</u>
2.1 A 5x5 fouling matrix.....	14
2.2 Typical fouling resistance versus time curves.....	15
2.3 An overview of chemical reaction fouling mechanism.....	18
2.4 Definition of various terms for thermal fouling.....	23
3.1 Flow diagram of experimental equipment.....	28
3.2 Test section schematic diagram.....	29
3.3 Electrical resistance divider.....	32
4.1 Specific gravity of dry crude oil	37
4.2 Typical Wilson plot	39
4.3 Calibration equipment diagram	40
4.4 Definition of terms for thermal fouling	38
5.1 Heat transfer tests on crude oil from Barrel No. 1 Runs AMO-FDC(263)-BO-01 through -BO-04 (Fresh feed used).....	54
5.2 Heat transfer tests on crude oil from Barrel No. 2 Runs AMO-FDC(263)-BO-05, -BO-06, -BO-09 and -BO-10 (Reused oil)	56
5.3 Heat transfer tests on crude oil from Barrel No. 2 Runs AMO-FDC(263)-BO-07, -BO-08, -BO-11 and -BO-12 (Reused oil)	57
5.4 Heat transfer tests on crude oil from Barrel No. 2 Runs AMO-FDC(263)-BO-05, -BO-06, -BO-11 and -BO-12 (Reused oil)	58
5.5 Heat transfer tests on crude oil from Barrel No. 2 Runs AMO-FDC(263)-BO-13 through -BO-16 (Fresh feed used).....	59
5.6 Effect of surface temperature on fouling from Barrel No. 1 Comparison of Runs AMO-FDC(263)-01, -02, -04 and 07	66
5.7 Effect of surface temperature on fouling from Barrel No. 1	

	Comparison of Runs AMO-FDC(263)-05 and -08.....	67
5.8	Effect of velocity on fouling from Barrel No. 1 Comparison of Runs AMO-FDC(263)-04 and -05.....	68
5.9	Effect of velocity on fouling from Barrel No. 1 Comparison of Runs AMO-FDC(263)-07, -08 and -09.....	69
5.10	Effect of surface temperature on fouling from Barrel No. 2 Comparison of Runs AMO-FDC(263)-13 and -15.....	70
5.11	Effect of surface temperature on fouling from Barrel No. 2 Comparison of Runs AMO-FDC(263)-14, -16 and -25.....	72
5.12	Effect of velocity on fouling from Barrel No. 2 Comparison of Runs AMO-FDC(263)-10, -13 and -14.....	73
5.13	Effect of velocity on fouling from Barrel No. 2 Comparison of Runs AMO-FDC(263)-22, -24 and -25.....	74
5.14	Effect of velocity on fouling from Barrel No. 2 Comparison of Runs AMO-FDC(263)-12 and -16.....	75
5.15	Determination of threshold fouling temperature for oil from Barrel No. 2 Comparison of Runs AMO-FDC(263)-27 through -32 (8.0 ft/sec).....	77
5.16	Determination of threshold fouling temperature for oil from Barrel No. 3 Comparison of Runs AMO-FDC(263)-33 through -38 (8.0 ft/sec).....	79
5.17	Determination of threshold fouling temperature for oil from Barrel No. 3 Comparison of Runs AMO-FDC(263)-39 through -42 (3.0 ft/sec).....	80
5.18	Determination of threshold fouling temperature for oil from Barrel No. 3 Comparison of Runs AMO-FDC(263)-43 through -50 (5.5 ft/sec).....	82
5.19	Determination of threshold fouling temperature for oil from Barrel No. 3 Comparison of Runs AMO-FDC(263)-51 through -57 (10.0 ft/sec).....	83
5.20	The effect of velocity on the threshold surface temperature from Barrel No. 2 and Barrel No. 3.....	84
5.21	Determination of threshold fouling temperature for wet bulk test from Barrel No. 3. Comparison of Runs AMO-FDC(263)-58 through -62 (5.5 ft/sec).....	87
5.22	Determination of threshold fouling temperature for wet bulk test from Barrel No. 3. Comparison of Runs AMO-FDC(263)-63 through -67 (8.0 ft/sec).....	88
5.23	Effect of feed re-use on fouling from Barrel No. 2 Comparison of Runs AMO-FDC(263)-16, -17, and -18.....	90
5.24	Effect of feed re-use on fouling from Barrel No. 2 Comparison of Runs AMO-FDC(263)-19 through -23..	91

LIST OF TABLES

<u>Table</u>	<u>Page</u>
4.1 Summary of operating conditions	45
5.1 Summary of heat transfer tests (boiling tests).....	53
5.2 Summary of dry crude tests.....	61
5.3 Initial heat transfer coefficients for dry bulk tests	63
5.4 Summary of wet crude tests.....	86

NOMENCLATURE

A	heat transfer area, ft^2
A_1 to A_6	constants in Equation 2.5, 2.9, 2.11, 2.12 and 2.17
ACS	cross section area of tube, ft^2 (in Equation 3.2)
C, C^* , C^{**}	property constants
C_{fi}	concentration of foulant at the solid-liquid interface, mol/liter or lb_m/ft^3
C_{pb} , C_w	concentration of fouling precursors in bulk fluid and at the wall, mol/liter
D	inside diameter of clean tube, ft
D_e	equivalent diameter of annulus, ft
E	activation energy, cal/mol, Btu/ lb_m or kJ/mol
E_b	enhancement factor due to boiling
f	friction factor
G	mass flow rate, lb_m/hr or lb_m/sec
h	convection heat transfer coefficient, Btu / $\text{hr ft}^2 \text{ } ^\circ\text{F}$
J	mass flux of fouling precursors (in Equation 2.10)
k	reaction rate constant, $\text{L}^{1-n} \text{ mol}^{1-n} \text{ hr}^{-1}$
k_f	thermal conductivity of fouling deposit, Btu/hr $\text{ft}^2 \text{ } ^\circ\text{F}$
K_p	mass transfer coefficient of precursors, ft/hr
m_f	mass of deposit per unit surface, lb_m/ft^2
P	pressure, lb_f/in^2
q	power (heat) to be transfered to the bulk fluid, Btu/hr
R	gas-law constant
R^2 (RSQURD)	regression coefficient
Re	Reynolds number
R_f	thermal resistance of fouling deposit, $\text{hr ft}^2 \text{ } ^\circ\text{F}/\text{Btu}$

R_w	wall thermal resistance, $\text{hr ft}^2 \text{ } ^\circ\text{F}/\text{Btu}$
S	sticking probability (in Equation 2.11)
Sc	Schmidt number
SPGR	specific gravity
S_b	brine solubility in crude oil at T_b
S_s	brine solubility in crude oil at T_s
t	time, hours
t_d	deduction time, hours
T	temperature, $^\circ\text{F}$, $^\circ\text{C}$ or K
T_{bb}	boiling temperature of salt saturated brine
T_{wb}	boiling temperature of water
U	overall heat transfer coefficient, $\text{Btu}/\text{hr ft}^2 \text{ } ^\circ\text{F}$
u , u_b , v	fluid velocity, ft/sec or GPM (gallon per minute)
w	total brine amount (weight percentage) in crude oil
X_f	thickness of deposit layer, ft
$\text{hr ft}^2 \text{ } ^\circ\text{F}/\text{Btu}$	refers to unit of fouling resistance ($\text{hr ft}^2 \text{ } ^\circ\text{F}/\text{Btu}$) in figures

Greek symbols

δ	thickness of boundary layer, ft
λ	parameters in Equation 2.14 and 2.15
μ	fluid viscosity, $\text{lb}_m/\text{hr ft}$ or cp
ϕ	parameter in Equation 2.15
ρ	fluid density, lb_m/ft^3
π_1	parameter in Equation 2.13
π_2	parameter in Equation 2.13
β_5	constant in Equation 2.16

subscripts

b	bulk
b	boiling
f	fouling deposit
f	at fouled condition
i	liquid-solid interface
o	at clean condition
p	precursor
s	surface
w	wall

FOULING CHARACTERISTICS OF A DESALTED CRUDE OIL

CHAPTER 1

INTRODUCTION

Fouling often occurs on heat exchanger surfaces in contact with hydrocarbon fluids in the chemical, petroleum refinery and food industries. Fouling increases the overall thermal resistance in a heat exchanger and reduces the efficiency of the equipment. Hence, additional heat transfer surface is provided during design to account for expected fouling during a production process.

Chemical reaction fouling is still not well understood although numerous investigations have been reported in the literature. The current practice in heat exchanger design for fouling is to select fouling resistance values (R_f) from T.E.M.A. [1] tables and to add these to the total clean surface resistance. These tables give little recognition to the variation of R_f with such important process variables as fluid velocity, bulk temperature, fluid composition, surface temperature of heater and heat exchanger geometry.

This work was sponsored by Heat Transfer Research Inc., Alhambra, CA. Three barrels of desalted crude oil supplied by Amoco Oil Company were tested. The objective of this research is the determination of the fouling behavior of desalted crude oil and the threshold surface temperatures for the initiation of fouling at different velocities. The effects of fluid velocity, brine, surface temperature of heater rod and bulk temperature of crude oil are of interest in this investigation.

This thesis is divided into six chapters. Chapter 2 is a literature review of the relevant work reported in the field of chemical reaction fouling. The background of fouling on heat transfer surfaces is also described in this chapter. Chapter 3 presents a detailed description of experimental equipment which is designed to study the fouling characteristics of organic fluids ranging from styrene in heptane to heavy crude oil. The experimental procedures and operating conditions are presented in Chapter 4.

Chapter 5 discusses the results of both dry bulk tests and wet bulk tests. Some important parameters affecting fouling such as fluid velocity, surface temperature and the presence of desalted brine are investigated. The threshold surface temperature for the initiation of fouling at different velocities are also determined with a systematic study.

Finally, Chapter 6 summarizes the results of this work. Some recommendations for future work are also included in this chapter.

CHAPTER 2

THEORETICAL ASPECTS AND LITERATURE SURVEY

Fouling is the formation of undesirable deposits on heat transfer surfaces. The phenomenon has been known since fire was discovered. The investigation of fouling has been more systematic since 1920s [2] but although the knowledge of fouling has been accumulating, it is still a major unsolved problem in heat transfer and is impossible to predict accurately [3,5].

The economic penalties associated with the fouling of heat transfer equipment have been reported in the literature. The financial penalties are based on the additional capital, energy, maintenance, anti-foulant additives, and shutdown costs that result from fouling. Pritchard [6] estimated the total cost of fouling in the United Kingdom to be 300-500 million pounds per year based on 1978 values. Von Nostrand et al. [7] estimated the total cost of fouling for petroleum refineries in the U.S. and non-Communist countries respectively to be \$ 1.36 billion/year and \$ 4.41 billion/year. Smith and Driks [8] investigated the costs of heat exchanger fouling in the U.S. industries and reported that the annual cost of fouling was estimated to be between \$ 4.2 and \$ 10 billion.

2.1 Heat Transfer under Boiling Conditions

Under boiling conditions, heat transfer coefficients and rates are generally much larger than those which are characteristic of convection heat transfer without phase change. High heat transfer rates can be achieved with small temperature differences under boiling conditions.

The heat-transfer curve (either heat flux or convective heat transfer coefficient versus superheat) for a liquid has four distinct regions, namely: natural convection, nucleate boiling, transition (unstable film boiling) and stable film boiling (radiation). When surface temperature is increased up to a specific value, the curve will change from a low slope straight line to a steep slope straight line which indicates that heat transfer has changed from natural convection mode to a nucleate boiling mode. In the nucleate boiling region, the heater surface becomes densely populated with bubbles which will induce considerable fluid mixing near the surface, and substantially increases the convective heat transfer coefficient (or heat flux). References [53,54,55] provide a good survey and explanation of this boiling phenomenon.

Lemmert and Chawla [9] studied the influence of flow velocity on the surface boiling heat transfer coefficient in a forced convection loop. Their data showed that heat transfer coefficient depends on flow velocity, especially at low superheat. At low superheats, increasing flow velocity will enhance the heat transfer coefficient. At high superheats (heat flux), the heat transfer coefficient is virtually independent of flow velocity. Kenning and Hewitt [10] investigated the boiling heat transfer for water in annular flow at 160 and 390 kpa in a 9.6 mm bore tube. They concluded that below the nucleate boiling region, the heat transfer coefficient was independent of heat flux and depended on the flow rate. Similar results were obtained by Steiner and Ozawa [11], in which flow boiling heat transfer in horizontal and vertical tubes was studied.

Due to the bubble formation, heat transfer will be enhanced at boiling conditions. Converse to the boiling phenomenon, fouling will reduce the heat transfer rate. The fouling deposit also will change the characteristics of heat transfer surface. The deposition of solid materials on heat transfer surface will provide favorable conditions that may initiate vapor bubble formation. In addition, the fouling deposit also changes the interfacial

roughness and surface tension between the bubbles and heat transfer surface. Reference [56] provides a good explanation of roughness effect on nucleate boiling. Berenson [12] investigated the effect of surface roughness for n-pentane boiling on copper and concluded that nucleate-boiling heat transfer coefficient could be changed by 500-600 percent due to changes in surface roughness. Increasing the roughness of the surface will enhance heat transfer coefficient. Roy-Chowdhury and Winterton [13] studied the surface effects in pool boiling of saturated water or methanol on copper. A similar conclusion was reached from their study.

Insinger and Bliss [14] found that reducing surface tension increased the heat transfer coefficient in distilled water by adding wet agent (Triton W-30). Al-Roubaie et al. [20] presented a detailed study of surface tension effect on the deposition of solids from milk on heated surface. It was concluded that reducing surface tension would reduce the amount of deposit attachment on heated surfaces.

2.2 Classification of Fouling

Six primary categories of fouling phenomena which have been identified are described briefly as follows [16,57].

a. Precipitation (Crystallization) Fouling:

This type of fouling is concerned in the crystallization of dissolved substances in a flowing fluid onto the heat transfer surface when the fluid becomes supersaturated with respect to the deposit material. It is also called scaling when this type of fouling involves the deposition of inorganic salts from water. There are two types of solubility for inorganic salts, normal solubility (solubility increasing with temperature) and inverse solubility (solubility decreasing with temperature). The precipitation of normal solubility salts will occur on a subcooled surface. Inverse solubility salts precipitate on a heated surface.

Reviews of precipitation fouling have been given by Epstein [16], Hasson [17], and Marschall [18].

b. Particulate Fouling:

Particulate fouling is the accumulation of fine particles from a fluid containing suspended solids onto the heat transfer surface. Due to settling by gravity in a few cases, the process is also referred to as sedimentation fouling. Reviews of this type of fouling have been presented by Gudmundsson [19] and Beal [20].

c. Freezing Fouling:

This type of fouling refers to the solidification of a pure liquid in contact with a cold surface or the deposition of a high-melting-point constituent of a multi-component solution in contact with a cooled surface. Due to limited application, little work has been reported on this type of fouling. Bott [21] presented a review of this type of fouling.

d. Chemical Reaction Fouling:

Chemical reaction fouling is generally defined as a deposition process that results from a chemical reaction which forms the deposit directly, or is involved in forming the deposit. This type of fouling deposit formation at the heat transfer surface occurs in which the surface material of heat exchanger is not a reactant. Chemical reaction fouling can occur in many fields. Food and petroleum refinery processes are two typical areas involving this type of fouling. Lund and Sandu [22] presented a detailed review of chemical reaction fouling in the food processing industry. Forment [23] reviewed the fouling of heat transfer surface caused by coke formation and resulting from cracking of heavy hydrocarbons in petrochemical reactors (petroleum refining process).

e. Corrosion Fouling:

Corrosion fouling occurs when the heat transfer surface itself reacts with the heating or cooling fluid and produces corrosion product on the surface. Due to the damage

of the heat transfer surface, it is necessary to replace the heat exchanger because it is impossible to get the original heat transfer efficiency by cleaning the surface. This type of fouling has been reviewed by Lister [24] and Somerscales [25].

f. Biofouling:

Biofouling (biological fouling) occurs due to the attachment of microorganisms onto the heat transfer surface. The conditions of the heat exchanger surface are often suitable for promoting the biofouling. It is difficult to control biofouling in cooling systems using sea or river water as coolant. Characklis [26] presented a detailed process analysis of biofouling.

Even though fouling phenomena are classified into six primary categories, most fouling is due to two or more different types of fouling. It becomes increasingly complicated when different fouling types occur simultaneously on a heat transfer surface.

2.3 Physical Parameters in Chemical Reaction Fouling

Most of the literature on chemical reaction fouling is related to hydrocarbon streams. In general, organic fouling is affected significantly by two major factors: chemical species effects (complicated variables in themselves) and physical parameters. Chemical species effects generally include the effects of hydrocarbon stream composition under oxygenated and de-oxygenated conditions, the effects of dissolved oxygen and oxygenated species, sulphur species, nitrogen species, dissolved metallic ions and tube wall materials. A detailed review of these chemical species effects has been presented by Watkinson [27].

In addition to chemical species effects, among the physical parameters known to have an influence on organic fluid fouling are bulk fluid velocity past through heat transfer surface, bulk temperature of fluid, surface temperature of heat transfer surface, presence of

boiling and so on. The effects of some parameters are discussed below to the extent that they have been reported in the literature.

2.3.1 Velocity Effect

The results of velocity effects on organic fouling are contradictory in the literature. Fouling rates are reported to decrease with increasing velocity in some cases and to increase with velocity in other cases. The fouling rates increase with velocity if mass transfer controls the reaction fouling rates. In case of independence of mass transfer, the fouling rates decrease with increasing velocity due to the increase of shear stress which enhances the removal rate of fouling deposit.

Watkinson and Epstein [28] investigated the velocity effect in a gas-oil thermal fouling process. At given constant surface temperatures and heat fluxes, the initial fouling rate decreased with increasing velocity. The initial fouling rate was well correlated by the equation:

$$\left(\frac{dR_f}{dt} \right)_{t=0} = \frac{1.347 \times 10^9 e^{-28730/RT_s}}{G^{1.07}} \quad (2.1)$$

where,

T_s = surface temperature of inner tube wall (K)

G = mass flow rate (lb_m / sec)

R = gas-law constant (cal / mole-K)

In crude oil coking studies, Scarborough et al. [29] observed effect of mass velocity on coking at a constant film temperature (405 °C). They reported that increasing mass velocity significantly reduced the coking rate, in which the 750 kg/sec-m² mass velocity condition had a coking rate of about 2.5 times that of the 1500 kg/sec-m² mass

velocity test. Oufer [30], in a study of chemical reaction under boiling conditions using styrene dissolved in n-heptane, found that higher fluid velocity past the heat transfer surface considerably reduced fouling and the initial fouling rates were inversely proportional to the velocities at each surface temperature.

Smith [31] investigated the fouling rates for kerosene fuels at Reynolds numbers in the range of 4500-10000 and showed that the thermal resistance of the fouling deposit increased as the mass flow rate increased at any given time after initiation of the experiment. For determination of coking rate in jet fuel, Vanos et al. [32] correlated coking data and showed coking rate increased with Reynolds numbers over the range $600 < Re < 10000$ at temperatures of 300 and 500 °F. No obvious dependence upon flow regime was indicated as flow changed from laminar to turbulent fluid. Different tube diameters were investigated at temperatures of 300 and 500 °F. Correlation of their data showed:

$$\left(\frac{dR_f}{dt} \right)_{t=0} = 0.006 Re^{0.566} \quad \text{at } T_s = 300 \text{ °F} \quad (2.2)$$

$$\left(\frac{dR_f}{dt} \right)_{t=0} = 0.054 Re^{0.605} \quad \text{at } T_s = 500 \text{ °F} \quad (2.3)$$

Crittenden et al. [33] indicated that the dependence of initial fouling rate on flow rate is complex. In the polymerization fouling studies (1% v/v styrene in kerosene) with flow through a single horizontal tube (0.02 m I.D.), a strong effect of flow rate on initial fouling rate at relatively high surface temperature was obtained for Reynolds numbers ranging from 1100 to 5200. The initial fouling rate increased with mass flow rate at all temperatures over 100 °C, but decreased slightly with increasing mass flow rate at temperatures below 100 °C. They concluded that deposition rates may be strongly affected by mass transfer at relatively low flow rates and high surface temperatures.

2.3.2 Surface Temperature Effect

It is well known that increasing temperature always increases the chemical reaction rate. The surface temperature of a heat transfer surface is clearly a key variable for chemical reaction fouling. The other parameters affecting fouling processes should be controlled in any study of surface temperature effect. The relationship between surface temperature and fouling rate is usually expressed by in terms of Arrhenius type equations, in which the activation energy is involved. Activation energies have been reported from about 20 to 120 kJ/mole for chemical reaction fouling [40].

Temperature effects had been investigated for chemical reaction fouling, in which all other variables were fixed. The fouling rate always increases with surface temperature. For gas-oil fouling, Watkinson and Epstein [28] correlated their fouling data to obtain Equation (2.1) which is a typical Arrhenius form. The temperature effects can be expressed as:

$$\left(\frac{dR_f}{dt} \right)_{t=0} \propto e^{-28730/RT_s} \quad (2.4)$$

where R is in cal/mole-K and T_s is in K.

In a study of styrene polymerization fouling, Crittenden et al. [38] obtained an Arrhenius-type equation to predict the initial fouling rate which was expressed as follows:

$$\left(\frac{dR_f}{dt} \right)_{t=0} = A_1 \exp\left(\frac{-E}{RT_s} \right) \quad (2.5)$$

where A_1 is a constant and E (activation energy) is about 25 kJ/mole for flow rates below 512 kg/s-m² and increases to about 37 kJ/mole for flow rates above 512 kg/s-m². Oufier [30] developed a complex equation in terms of an Arrhenius-type relationship for

determining the initial fouling rate in a styrene polymerization fouling study. It was concluded that higher surface temperature always increases the fouling rate.

Hausler and Thalmayer [34] studied the fouling rate in three different petroleum feedstocks. The equation relating surface temperature and initial fouling rate was expressed as :

$$\left(\frac{dR_f}{dt} \right)_{t=0} = 3.7 \times 10^{-7} \exp\left(\frac{T_s - 100}{100} \right) \quad (2.6)$$

where the initial fouling rate is in $\text{ft}^2\text{-}^\circ\text{F/Btu}$ and T_s is in $^\circ\text{F}$. Scarborough et al. [29], in a crude oil coking study, investigated the surface temperature effect and concluded that coking rate increased at higher surface temperatures. At a flow rate of 750 kg/sec-m^2 , the coking rate is doubled for an approximate 40°C increase in surface temperature.

Compared to thermal cracking data in which the reaction rate doubles approximately for every 15°C increase in temperature, the dependence of coking rate on surface temperature is relatively small.

2.3.3 Bulk Temperature Effect

The bulk temperature effect on organic fouling has not been well elucidated in the literature. In general, the bulk temperature of the fluid affects the polymerization rate, chemical reaction rate, solubility and mass transfer rate. It is believed that this effect plays an important role on organic fouling. Garrett-Price et al. [64] indicate that fouling rate generally increases with bulk temperature.

Eaton and Lux [35] performed a fouling study for hydrocarbon feedstocks in which the bulk temperature effect was investigated. It was shown that the fouling rate of paraffin oil was high in which bulk and probe temperature were 38°C and 274°C

respectively, and there was no fouling when both bulk and probe temperature were 267 °C. Another experiment using Blue Island Crude Oil showed that increasing bulk temperature decreased fouling at the same initial probe temperature. At a probe temperature of 241 °C, the asymptotic fouling resistance for a bulk temperature of 71 °C was three times higher than for a bulk temperature of 144 °C. The data also showed that higher bulk temperatures had higher initial fouling rate. In a polymerization (styrene dissolved in n-heptane) fouling study, Oufer [30] observed that higher bulk temperatures increased the initial fouling rates at constant surface temperatures. The initial fouling rate increased about 1.5 times as the bulk temperature was increased from 175 °F to 190 °F at a surface temperature of 360 °F.

2.3.4 Boiling Effect

It is believed that the main effect of boiling on fouling is due to the high turbulent mixing caused by bubbles at the interface of the liquid and the heat transfer surface. This turbulent behavior not only increases the heat transfer but also enhances the mass transfer rate which is usually an important step in fouling processes.

Even though heat transfer at boiling conditions has been studied extensively, the effects of boiling on fouling are still not well known. The study of fouling under nucleate boiling conditions is one of the most poorly investigated areas [3]. There are still some disagreement on boiling effects in some reported papers of hydrocarbon fouling. Crittenden and Khater [36] investigated fouling studies in a vaporizing kerosene process. Low fouling rates were observed at locations when surface temperature was close to the final boiling point. In general, higher initial fouling rates occurred when saturated boiling did not occur.

2.4 Mechanism of Fouling

Fouling is a complicated phenomenon which involves at least five distinct steps.

Somerscales [37] has proposed the following steps:

- (a) Processes in the bulk fluid.
- (b) Transport to the heat transfer surface.
- (c) Attachment or formation of the deposit onto the heat transfer surface.
- (d) Removal of the fouling deposit from the heat transfer surface.
- (e) Transport of removed deposit from the heat transfer surface back to the bulk.

Epstein [38,39] classified a fouling processes in five sequential events (initiation, transport, attachment, removal and aging) and combined these in a 5x5 matrix which included the five major types of fouling. This fouling matrix is shown in Figure 2.1. Among these 25 terms, column 1 (crystallization fouling) and row 2 (transport) have received most of the study, but column 4 (corrosion fouling) and row 5 (aging) may have been the most neglected.

The fouling deposit is the solid material which accumulates on the heat transfer surface. The fouling resistance versus time curves are shown in Figure 2.2, where linear, falling rate and asymptotic are generally the typical behaviors. The "saw-tooth" configuration is occasionally obtained with commercial cooling towers [3,4]. There are three ways to express the amount of fouling deposit on the heat transfer surface, namely mass per unit surface (m_f), thickness (X_f), or unit thermal resistance (R_f). These three quantities are related to each other as follows:

$$m_f = \rho_f X_f = \rho_f k_f R_f \quad (2.7)$$

where,

R_f = thermal resistance of deposit.

	1. Crystallization Fouling	2. Particulate Fouling	3. Chemical Reaction Fouling	4. Corrosion Fouling	5. Biological Fouling
1. Initiation	1,1	1,2	1,3	1,4	1,5
2. Transport	2,1	2,2	2,3	2,4	2,5
3. Attachment	3,1	3,2	3,3	3,4	3,5
4. Removal	4,1	4,2	4,3	4,4	4,5
5. Aging	5,1	5,2	5,3	5,4	5,5

Figure 2.1 A 5x5 fouling matrix [44].

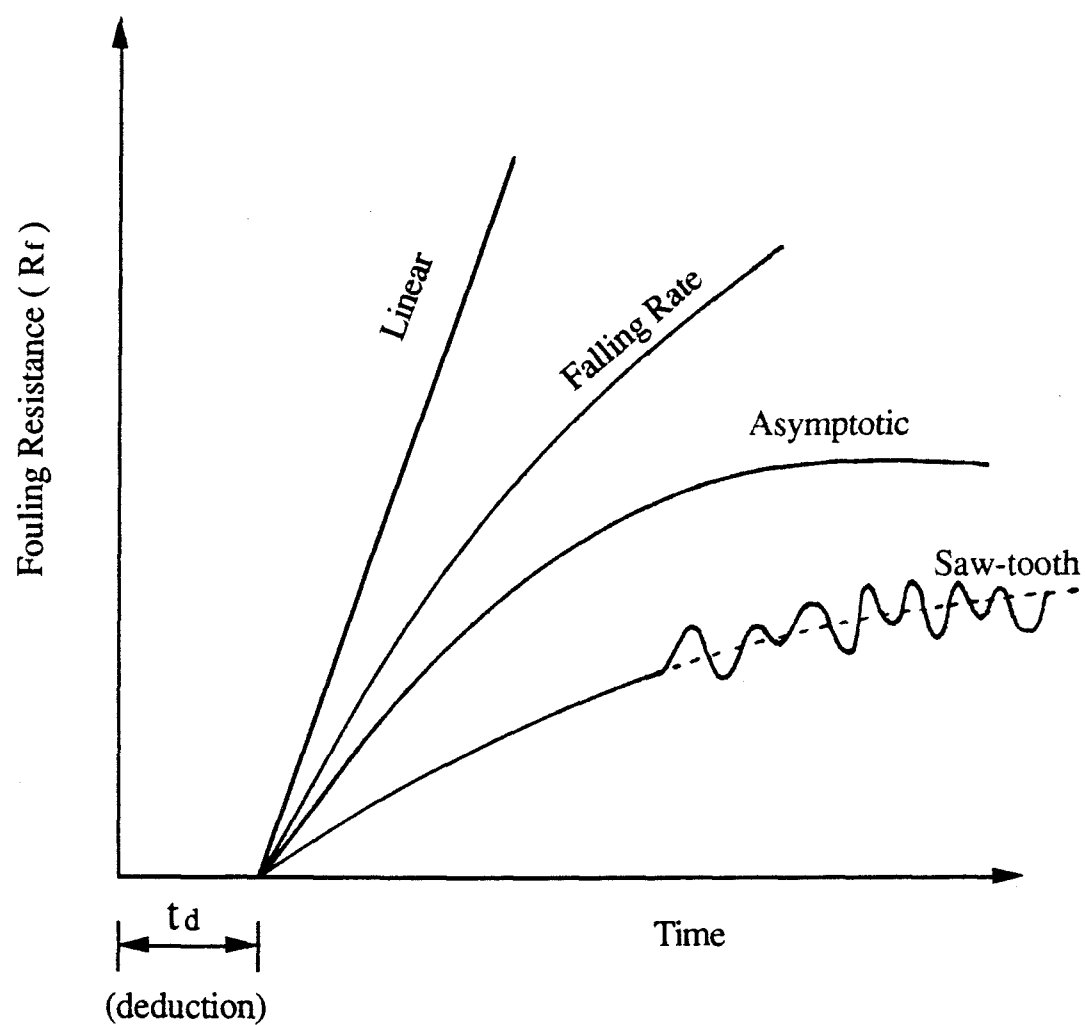


Figure 2.2 Typical fouling resistance versus time curves.

m_f = mass of deposit per unit surface.

ρ_f = density of deposit material.

k_f = thermal conductivity of deposit material.

X_f = thickness of deposit layer.

Assuming that ρ_f and k_f remain constant during the deposition period, the accumulation rate is given by:

$$\frac{dR_f}{dt} = \frac{1}{\rho_f k_f} \frac{dm_f}{dt} = \frac{1}{k_f} \frac{dX_f}{dt} \quad (2.8)$$

This assumption is not always met in practical operations, since ρ_f and k_f usually vary with the time and thickness (X_f). In general, the fouling deposit near the heat transfer surface is harder than near the interface of deposit-liquid. Epstein [16] indicates that the thermal method is advantageous over the other two methods for the designer or operator of heat transfer equipment. The major data sources of fouling data for heat exchanger design are the T.E.M.A. tables [1] which list the R_f values for various types of fluid.

2.4.1 Existing Models of Chemical Reaction Fouling

Mathematical modeling for chemical reaction fouling is complex. Many variables which may be related to each other are involved in a fouling process at the heat transfer surface. Due to the complexity of fouling phenomena, it is impossible to correlate all the variables into one model by using regression methods. In most models, fouling rates were modeled in terms of a single set of parameters such as surface temperature, flow velocity, foulant concentration, deposit properties, etc. All such models proposed to date have deficiencies and no single model can be expected to describe the complexities of chemical reaction fouling [40]. Crittenden et al. [41] have summarized a number of available models and given a detailed review of them. An overview of chemical reaction fouling is shown in

Figure 2.3. In the reported models, an overall mechanism of the fouling process generally consists of a deposition and removal term, in which mass transfer and surface reaction are involved. In order to simplify the problem, assumptions are usually made in mathematical models due to the complexities of fouling processes. A brief description of reported chemical reaction fouling models is given below.

Nelson [42], in an oil refining study, didn't consider the removal term and proposed a model in which the coking rate depended on the thickness of thermal boundary layer because the thicker the boundary layer the greater the volume of oil exposed to the higher temperature. There are two factors accounted for in the model, the thickness and temperature of the boundary. It was observed that coking rate could be decreased by increasing fluid velocity, but no correlation with velocity effect was made in Nelson's study.

Watkinson and Epstein [28] developed a model which included deposition and removal term. The deposition was considered to be caused by mass transfer of suspended particles to the wall region and followed by adhesion to the wall. The first order Kern-Seaton shear removal term was utilized in the removal rate. Their initial fouling rate equation is given by:

$$\left(\frac{dR_f}{dt} \right)_{t=0} = A_2 J S \quad (2.9)$$

where,

$$J = \text{mass flux of fouling precursors} = K_c (C_b - C_w) = \frac{u_b f^{1/2}}{11.8 Sc^{2/3}} \quad (2.10)$$

$$S = \text{sticking probability} = \frac{A_3 e^{-E/RT_s}}{u_b^2 f} \quad (2.11)$$

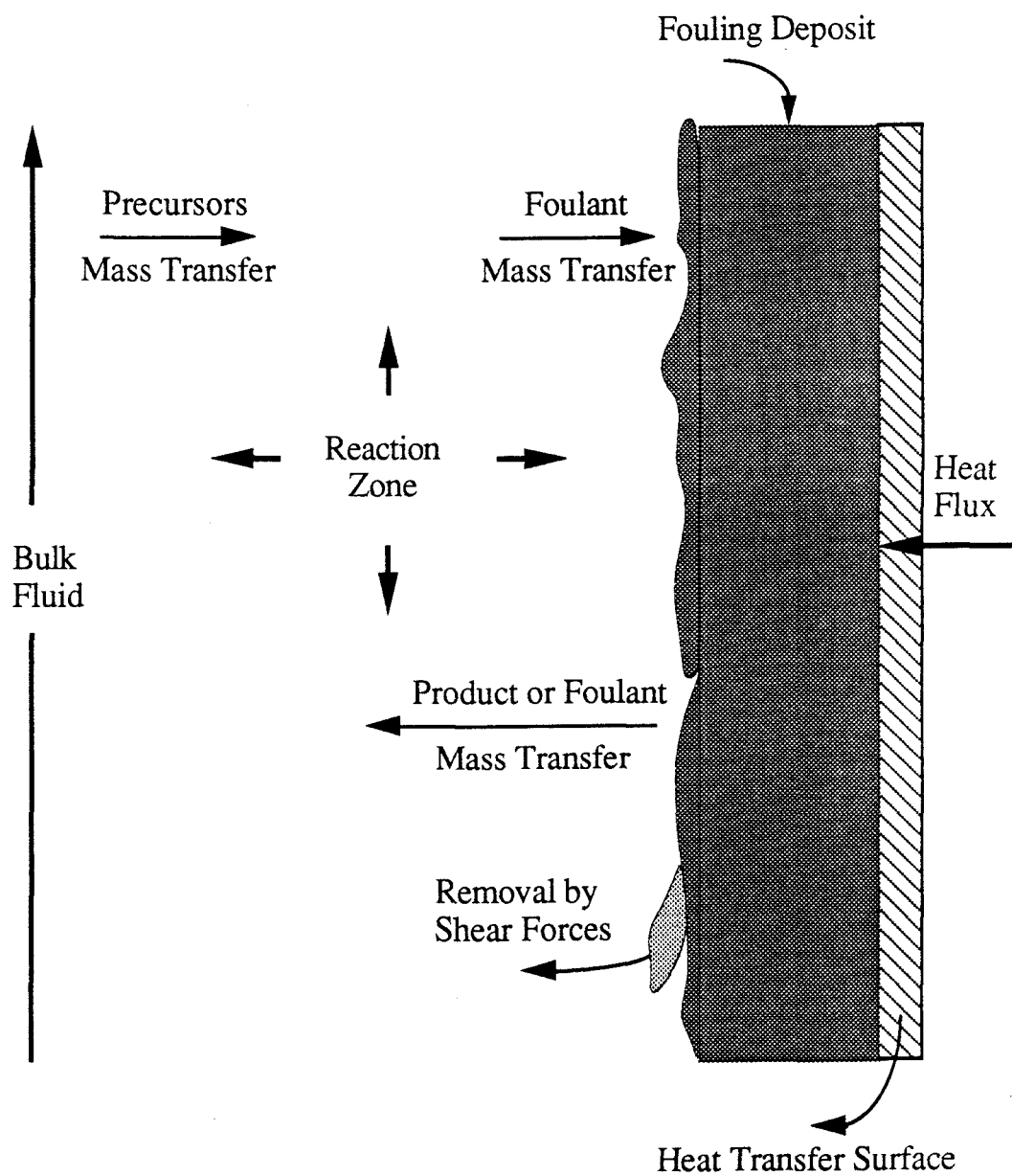


Figure 2.3 An overview of chemical reaction fouling mechanism.

Neglecting the variation of k_f with X_f and of f with u_b , rearranging Equation (2.9) gives:

$$\left(\frac{dR_f}{dt} \right)_{t=0} = \frac{A_4 (C_b - C_w) e^{-E/RT_s}}{G} \quad (2.12)$$

where,

$A_2, A_3, A_4 = \text{constant}$

$C_b, C_w = \text{concentration of fouling precursors in bulk fluid and at the wall.}$

$u_b = \text{bulk fluid velocity.}$

$G = \text{mass flow rate.}$

$f = \text{friction factor.}$

$E = \text{activation energy.}$

$T_s = \text{surface temperature.}$

$Sc = \text{Schmidt number.}$

Equation (2.12) is in good agreement with experimental observations for the initial fouling rate of gas oil (Equation (2.1)).

Sundram and Froment [43] presented one model to predict the coking rate for the thermal cracking of propane in a mixed flow reactor, in which removal term was not considered. The coke deposition was considered to be formed by a consecutive mechanism and it was shown that the numerically simulated data were in good agreement with observations made in industry. The coke deposition rate is assumed to be determined by first order kinetics control for concentration of propylene (a product of primary cracking reaction) and surface temperature are important variables.

Crittenden and Kolackowski [44] extended a two-step, mass and kinetics, model to include convection of the foulant from the wall back into the bulk fluid. They assumed that the deposition reaction was of first order and occurred at the solid-fluid interface. Mass transfer coefficients were expressed in terms of flow rate and fluid physical properties by

using Chilton-Colburn analogy. The foulant removal rate was considered to have a first order dependence on deposit thickness. Their final equation for hydrocarbon fouling was given by:

$$\left(\frac{dR_f}{dt} \right) = \pi_1 - \pi_2 R_f \quad (2.13)$$

where,

π_1 = deposition rate

$$= \frac{1}{\rho_f k_f} \left\{ \frac{C_{pb}}{\frac{\rho(D - 2X_f)^{1.8} Sc_p^{0.67}}{1.213 \lambda \mu^{0.2} G^{0.8}} + \frac{1}{A_5 \exp(-E/RT_s)}} - \frac{1.213 \lambda \mu^{0.2} G^{0.8} C_{fi}}{\rho(D - 2X_f)^{1.8} Sc_p^{0.67}} \right\} \quad (2.14)$$

π_2 = removal rate

$$= \frac{0.607 \lambda \mu^{0.2} G^{1.8}}{\rho \psi k_f (D - 2X_f)^{3.8}} \quad (2.15)$$

where,

C_{pb} = concentration of precursor in bulk fluid.

C_{fi} = concentration of foulant at the solid-liquid interface.

Sc = Schmidt number.

μ = fluid viscosity.

ρ = fluid density.

D = inside diameter of clean tube.

ψ = f (deposit structure).

λ = f (surface roughness).

A_5 = constant

G = mass flow rate

Subscript (p) and (f) represent the precursor and foulant respectively. The other quantities are the same as those previously defined.

Peterson and Fryer [45] proposed a model to explain their observations of chemical reaction fouling for skimmed milk. Their model treated the fouling rate as being controlled by the size of the boundary layer (viewed as a differential chemical reactor) and used a sticking probability approach. The idea of the boundary layer was originally proposed by Nelson [42]. The thickness of the boundary layer is assumed to be equal to the volume of reactor per unit wall area. The equation is given by:

$$\left(\frac{dR_f}{dt} \right)_{t=0} = \frac{\beta_5 \exp\left(\frac{-E}{RT_s} \right)}{u_b} \quad (2.16)$$

where,

β_5 = constant.

E = activation energy.

T_s = surface temperature.

u_b = velocity of bulk fluid.

Finally, Oufer [30] developed a model without any parameter fitting for the polymerization fouling of styrene, in which the boiling effect was considered as one factor affecting fouling rate. By application of the general Kern-Seaton approach, the net fouling rate is a combination of deposition and removal terms. His model treats the fouling process as follows: the foulant precursor (styrene) is brought to the reaction zone by convective flow and diffusion, then the polymer either adheres to the heat transfer surface or returns to the bulk fluid due to wall shear forces or by diffusion. It is believed that the removal term not only depends on velocity but also surface temperature. The model has the form :

$$\left(\frac{dR_f}{dt}\right)_{t=0} = \frac{1}{\rho_f k_f} \frac{[-E_b K_p + (E_b^2 K_p^2 + 4 E_b k K_p C_{pb} \delta)^{0.5}]^2}{4 k \delta} \quad (2.17)$$

where,

$$k = A_6 \exp\left(\frac{-E}{RT_s}\right)$$

$$\delta = \text{thickness of boundary layer} = \frac{5 D_e}{Re \left(\frac{f}{2}\right)^{0.5}}$$

E_b = enhancement factor due to boiling.

K_p = mass transfer coefficient of precursor.

ρ_f, k_f = density and conductivity of fouling deposit, respectively.

D_e = equivalent diameter of annulus.

Re = Reynolds number.

f = fanning friction factor.

E = activation energy.

T_s = surface temperature.

A_6 = constant.

2.4.2 Basic Equation for Determining Fouling Resistance

By using thermal methods, the thermal resistance of fouling deposit (R_f) can be determined even if ρ_f and k_f are unknown and vary with time and thickness (X_f). The thermal method relies on flow rate and temperature measurements of the test section in the experiment. The definition of terms for thermal fouling are shown in Figure 2.4. The subscript (o) and (f) refer respectively to clean and fouled condition of the heat transfer surface.

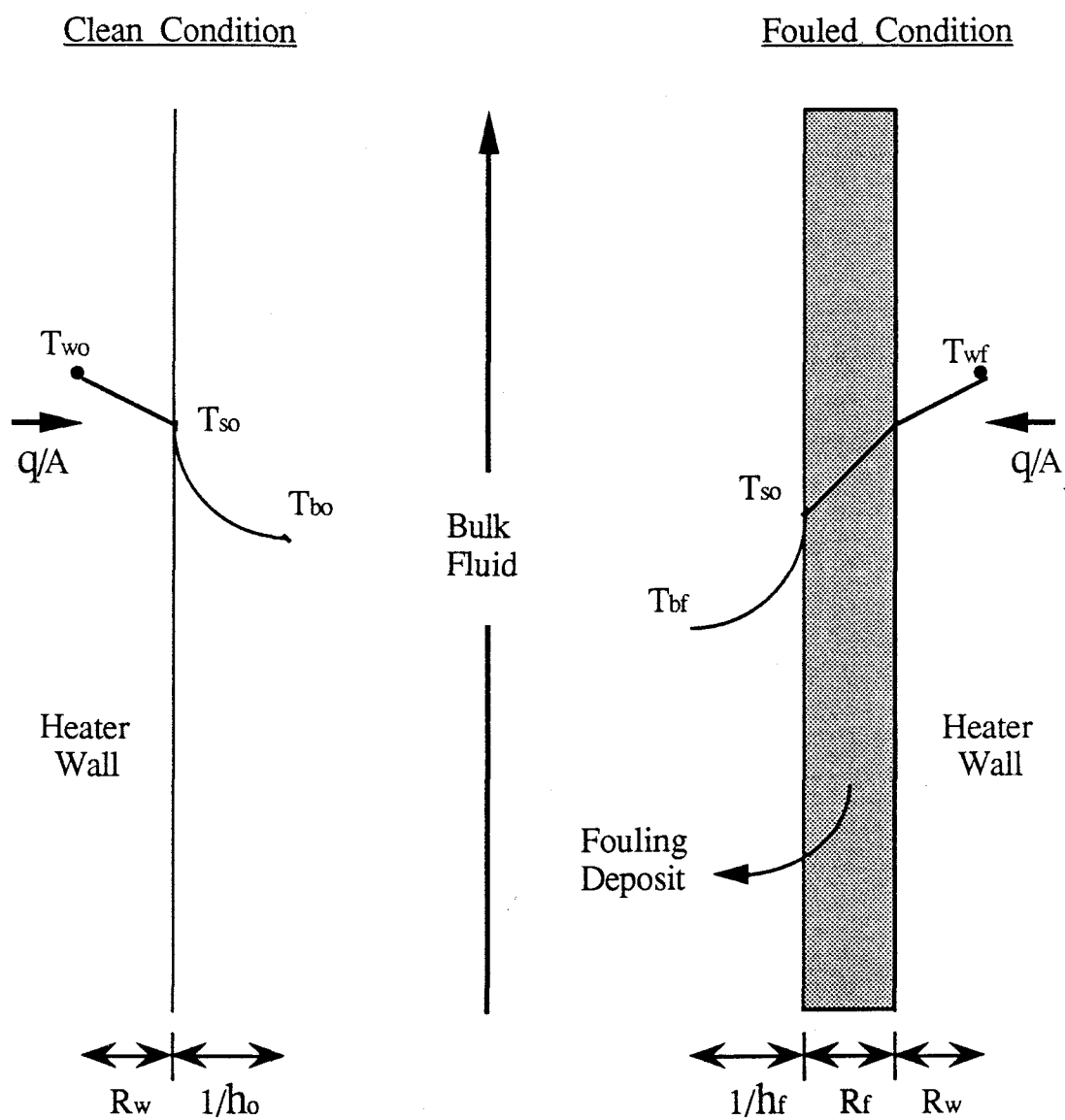


Figure 2.4 Definition of various terms for thermal fouling.

In Figure 2.4, the wall temperature (T_w) can be determined by a thermocouple embedded in the heater wall. For clean and fouled condition, the heat transfer between bulk fluid and heater wall can be expressed as follows:

$$\text{At clean conditions : } \left(\frac{q}{A}\right)_o = U_o (T_{wo} - T_{bo}) = \frac{1}{R_w + \frac{1}{h_o}} (T_{wo} - T_{bo}) \quad (2.18)$$

$$\text{At fouled conditions : } \left(\frac{q}{A}\right)_f = U_f (T_{wf} - T_{bf}) = \frac{1}{R_w + R_f + \frac{1}{h_f}} (T_{wf} - T_{bf}) \quad (2.19)$$

where,

q = power (heat) to be transferred to the bulk fluid.

A = heat transfer surface area.

U = overall heat transfer coefficient.

T_w = inner wall temperature of heater.

T_b = bulk temperature of fluid.

R_w = wall resistance = $\frac{\text{wall thickness}}{\text{wall thermal conductivity}}$

h = convection heat transfer coefficient.

R_f = thermal resistance of fouling deposit.

Rearranging Equation (2.18) and Equation (2.19) give :

$$\frac{1}{U_o} = \frac{T_{wo} - T_{bo}}{\left(\frac{q}{A}\right)_o} = R_w + \frac{1}{h_o} \quad (2.20)$$

$$\frac{1}{U_f} = \frac{T_{wf} - T_{bf}}{\left(\frac{q}{A}\right)_f} = R_w + R_f + \frac{1}{h_f} \quad (2.21)$$

Subtracting Equation (2.20) from Equation (2.21) gives :

$$R_f = \frac{T_{wf} - T_{bf}}{\left(\frac{q}{A}\right)_f} - \frac{T_{wo} - T_{bo}}{\left(\frac{q}{A}\right)_o} - \frac{1}{h_f} + \frac{1}{h_o} \quad (2.22)$$

In some cases of interest, heat flux and bulk temperature of fluid are maintained constant during the fouling study. In this situation, Equation (2.22) can be simplified as follows :

$$R_f = \frac{T_{wf} - T_{wo}}{\left(\frac{q}{A}\right)_o} - \frac{1}{h_f} + \frac{1}{h_o} \quad (2.23)$$

Based on the further assumption that the convection heat transfer coefficient of the fluid does not change when the fouling deposit attaches to the heat transfer surface, Equation (2.23) reduces to a simpler form as follows :

$$R_f = \frac{T_{wf} - T_{wo}}{\left(\frac{q}{A}\right)_o} \quad (2.24)$$

Hence, the thermal resistance of the fouling deposit can be easily determined at any specific time by Equation (2.24) which only relies on the inner wall temperature difference of heater between clean and fouled conditions.

Equation (2.24) assumes no change in convection coefficient (h) due to fluid velocity and surface roughness caused by the fouling deposit on the heat transfer surface. The fluid velocity will be increased when the thickness of deposit layer increases, which will reduce the cross-section area of the flow channel. It is well known that the increase in velocity at constant mass flow rate caused by blockage will increase the convection coefficient (h) [16].

For the surface roughness effect, it is not always negligible. Bott and Gudmundsson [46] suggested that the enhanced heat transfer was attributed to the increased roughness caused by a ripped silica fouling deposit. A similar phenomenon was proposed by Hasson [47] for Na_2SO_4 scaling. Turakhia et al. [48] proposed that convective thermal resistance would be decreased due to deposit roughness. A more recent study of surface roughness effect on fouling was investigated by Crittenden and Alderman [49].

CHAPTER 3

EXPERIMENTAL EQUIPMENT

The equipment used in this investigation was designed to study the fouling characteristics of organic fluids ranging from styrene in heptane to heavy crude oil. The thermal method of analysis which relies on temperature measurements was used in this study.

The experimental equipment developed by Oufer [30] for his Ph.D. study was used in this investigation, although some modifications were made in the equipment and computer program. One by-pass valve device has been added to the equipment. The modification of the computer program is described in Appendix B.

The modified equipment is a closed-loop circulation system shown in Figure 3.1. It consists of a test section, a flow rate measurement device, a storage vessel, a circulation pump, two by-pass devices, a heating and cooling system, an IBM personal computer for data acquisition and control along with a parallel manual data measurement system composed of electronic meters. The data acquisition and processing will be described in Chapter 4.6. The brief description of the other components in the system is as follows.

3.1 Test Section

The test section schematic diagram is shown in Figure 3.2. It consists of an annular duct formed by a 15-inch, 1-inch OD, 0.771-inch ID stainless steel outer tube. The

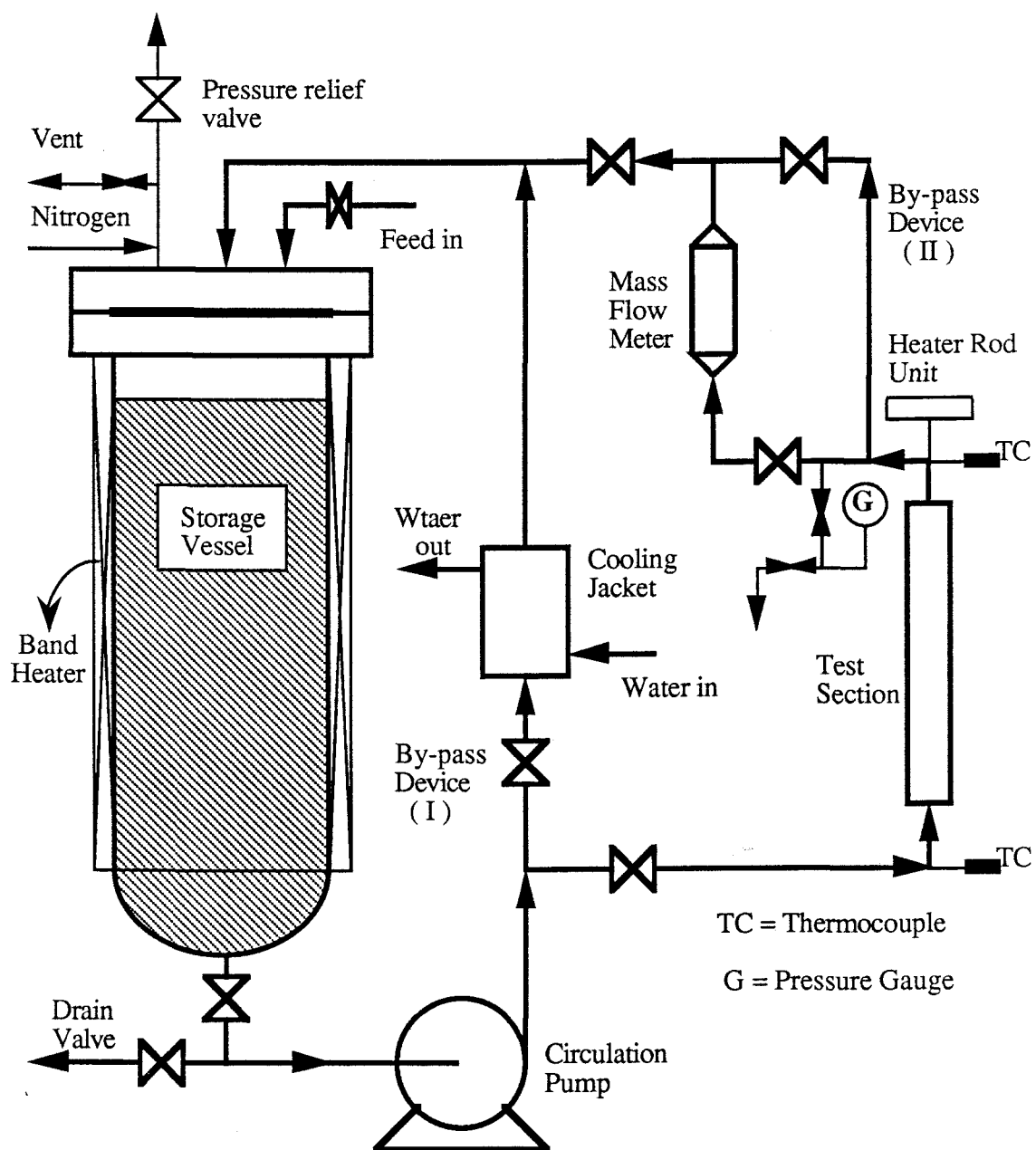


Figure 3.1 Flow diagram of experimental equipment

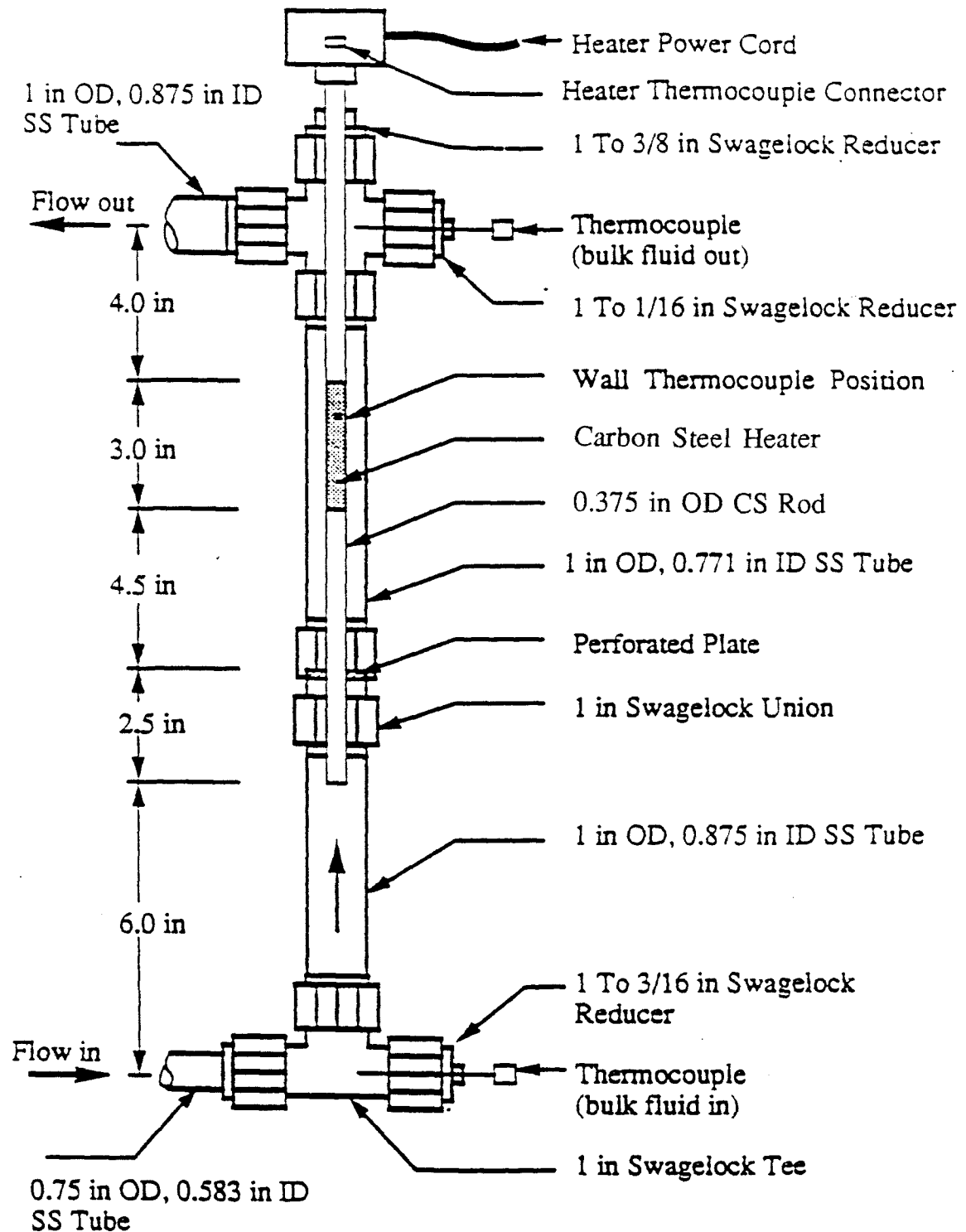


Figure 3.2 Test section schematic diagram

heater rod is located on the center of tube and is made of carbon steel material purchased from Dew Industrial Division, Boonton, New Jersey.

The heater rod, an electrical resistance heater located about seven inches from the lower end, and is capable of heating a 3-inch long rod section at constant heat flux and is rated at 1200 watts at 120 volts AC. A variable transformer controls the amount of power supplied to the 3-inch heated section of the rod. There is also one chromel-constantan thermocouple embedded in the wall of the rod to measure the wall temperature.

In this study, surface temperature is more important than wall temperature. In order to determine the surface temperature of each run, recalibration is required after cleaning the heater surface following each test. The method and procedure of calibration will be discussed in Chapter 4.1.

Another important aspect is that the heater rod is centered by a screen sandwiched between the lower end of outer tube and the inside ring of 1-inch union. This permits uniform flow of fluid around the surface of heater rod when it approaches the test section.

3.2 Flow Rate Measurement

In this study, a traditional flow rate meter can't be used due to the high viscosity and high bulk temperature of crude oil. Thus, a mass flow rate meter (type D100S) was purchased from Micro Motion, Inc., Boulder, Colorado. The operating temperatures of this meter are from -400 °F to +400 °F with an operating pressure of less than 2250 psi.

The mass flow meter consists of a sensor unit composed of two U-shaped tubes, a drive coil, two position detectors and a remote electronics unit (REU). The twist angle of the tubes is proportional to the mass flow rate when fluid flows through the tubes. Position detectors send signals to the REU which processes and converts the signals into voltage.

The analog output voltage from the REU is 0-5 volts corresponding to 0-55 pounds per minute. The A/D converter of the Adalab data acquisition card uses a voltage range of -1 voltage to +1 voltage for temperature, power and volumetric flow rate measurement. In order for the computer to record the data, it is necessary to use a single electrical resistance divider (shown in Figure 3.3) to scale down the output voltage to 0-1 volt.

A DC power supply was used to find the exact correction factor because the ratio of $R2/(R1+R2)$ is not exactly equal to 1/5. A 5 volt signal from the DC power supply gives an 1.0015 volt output from the divider. An independent venturi flow rate meter was used to calibrate the mass flow rate meter and showed that a correction factor of 1.474 had to be included. Based on this correction method, the final equation to convert the voltage output (in millivolts) from the divider to a mass flow rate (in pounds per minute) is as follows:

$$lb_m / min = mV \times \frac{55}{1001.5} \times 1.474 \quad (3.1)$$

In the other words,

$$ft / sec = lb_m / min + (SPGR \times 62.4 \times ACS \times 60) \quad (3.2)$$

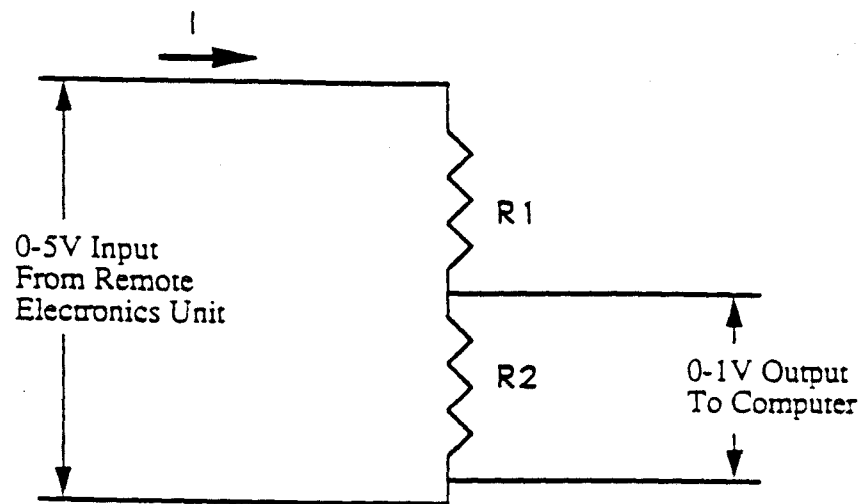
where,

SPGR : specific gravity of crude oil at operation condition.

ACS : cross section area of tube.

3.3 Storage Vessel

The storage vessel was constructed out of a 27-inch long, 6-inch schedule 80 (5.671-inch ID) 316 stainless steel pipe. The bottom and top of the pipe were respectively welded a 6-inch schedule 80 stainless steel cap and a fifteen hundred pound stainless steel



R1=410.5 ohms
R2=102.5 ohms

$$V_{out} = \frac{R2}{R1+R2} V_{in} = \frac{102.5}{410.5+102.5} V_{in} = \frac{1}{5.005} V_{in}$$

Figure 3.3 Electrical resistance divider

flange. There are three holes drilled in the top of the flange. Two 1-inch holes were used to charge the system and for the return line. One 3/4-inch hole was used for pressurizing, venting the system and for a safety valve device.

3.4 Circulation Pump

A magnetically driven seal/less pump was used for recirculating the fluid being studied. The pump is equipped with a 3-HP, 3600 rpm explosion proof motor. The specified design of the pump can allow it to be operated under fluid temperatures up to 600 °F and pressures up to 750 psig. Based on past operation experience, the pump is known to be very sensitive to electricity fluctuation. Sometimes the system will shut down automatically due to fluctuations in electric power.

3.5 By-Pass Systems

There are two by-pass devices in the experiment system. The first one is used to adjust the flow rate. The second is designed for the higher bulk temperature operating conditions in the future because the highest operating temperature for the mass flow rate meter is only +400 °F. It is also necessary to use both by-pass devices for isolating the test section in order to clean the heater rod and reuse the crude oil.

3.6 Heating and Cooling of Bulk Fluid

Installed on the storage vessel are three pairs of band heaters which were purchased from Watlow, Inc.. They are rated at 2300 watts at 120 volts AC with a density of 7 watts per square inch and controlled by a Variac. The storage vessel and heater assembly are insulated by a 1.5-inch thick foam-glass layer. In order to heat the large mass of the

stainless steel flanges, similar band heaters are also clamped around the bottom and top flanges of storage vessel.

To avoid heat losses from the pipes which make bulk temperature unstable, there are silicon rubber heaters of various wattage ratings of 200, 300 or 400 watts and widths of 1, 2 or 4 inches surrounding the 1-inch OD circulation pipe, the Swagelok fittings, the pump head and flanges. It is especially important to control stable flow rate and bulk temperature under conditions of high viscosity fluid and high bulk temperature. All silicon rubber heaters are controlled by a separate Variac. The whole system is insulated with fiber glass tape to avoid excessive heat losses. Finally, the aluminum paper tape is used to fix the fiber glass tape in place.

3.7 Safety Measures

Due to the high pressure and temperature operating condition, experimental equipment requires safety measures to handle emergency situations. There is an adjustable pressure relief valve which is connected to a venting bucket by a 1/4- inch stainless steel tube for venting excessive pressures in the system. The heaters in the storage vessel and silicon rubber heaters interconnected with the circulation pump. In case of power or pump failure, all heaters will shut off automatically.

The wall temperature of the carbon steel heater in the test section will rise when the fouling resistance becomes significant. To avoid excessive wall temperature which will burn out the heater, it is necessary to set maximum allowable temperature in the computer program. A signal will be sent from the computer to cut off the power to the heater rod when the wall temperature is higher than the set point value. In case of pump failure, the power will also shut off automatically. An alarm is activated when the circulation pump is overheating.

All open electrical circuits and devices are enclosed in a hermetically sealed box. Inlet and outlet wiring are made through openings drilled at the bottom of the box. The remote electronics unit of the mass flow rate meter and two voltage amplifiers for the temperature measurement are also installed in the box.

CHAPTER 4

EXPERIMENTAL PROCEDURE

4.1 Fluid Investigated

In this investigation of the fouling characteristics of a crude oil, FDC.263, 400+, provided by Amoco Oil Company were conducted. The specific gravity of the crude oil is shown in Figure 4.1.

Three 55-gallon drum of crude oil sample were provided by Amoco. Barrel No. 1 was only partially full and the crude oil in it was used for Runs AMO- FDC(263)-01 through -09. The crude oil in Barrel No. 2 and Barrel No. 3 was used for Runs AMO-FDC(263)-10 through -32a and for Runs AMO-FDC(263)-33 through -67, respectively. Runs AMO-FDC(263)-01 through -57 were the dry bulk tests, in which no desalter brine was added to the crude oil. In the dry bulk tests, the crude oil is essentially dehydrated and no liquid water exists or a second phase in the sample. Runs AMO-FDC(263)-WW-58 through AMO-FDC(263)-SDW-67 were the wet bulk tests where a small amount of desalter brine was added to the crude oil for each run. In the wet bulk tests, liquid water (as desalter brine) is present as a second phase in the system.

4.2 Cleaning and Recalibration of the Heaters

It is important to make certain that the heater surface is clean before an experiment is initiated. The method used for cleaning fouling deposit is to submerge the heater into the Lacquer Thinner thus dissolving most deposits. Next, a 400 grit 3M wet/dry sand paper is

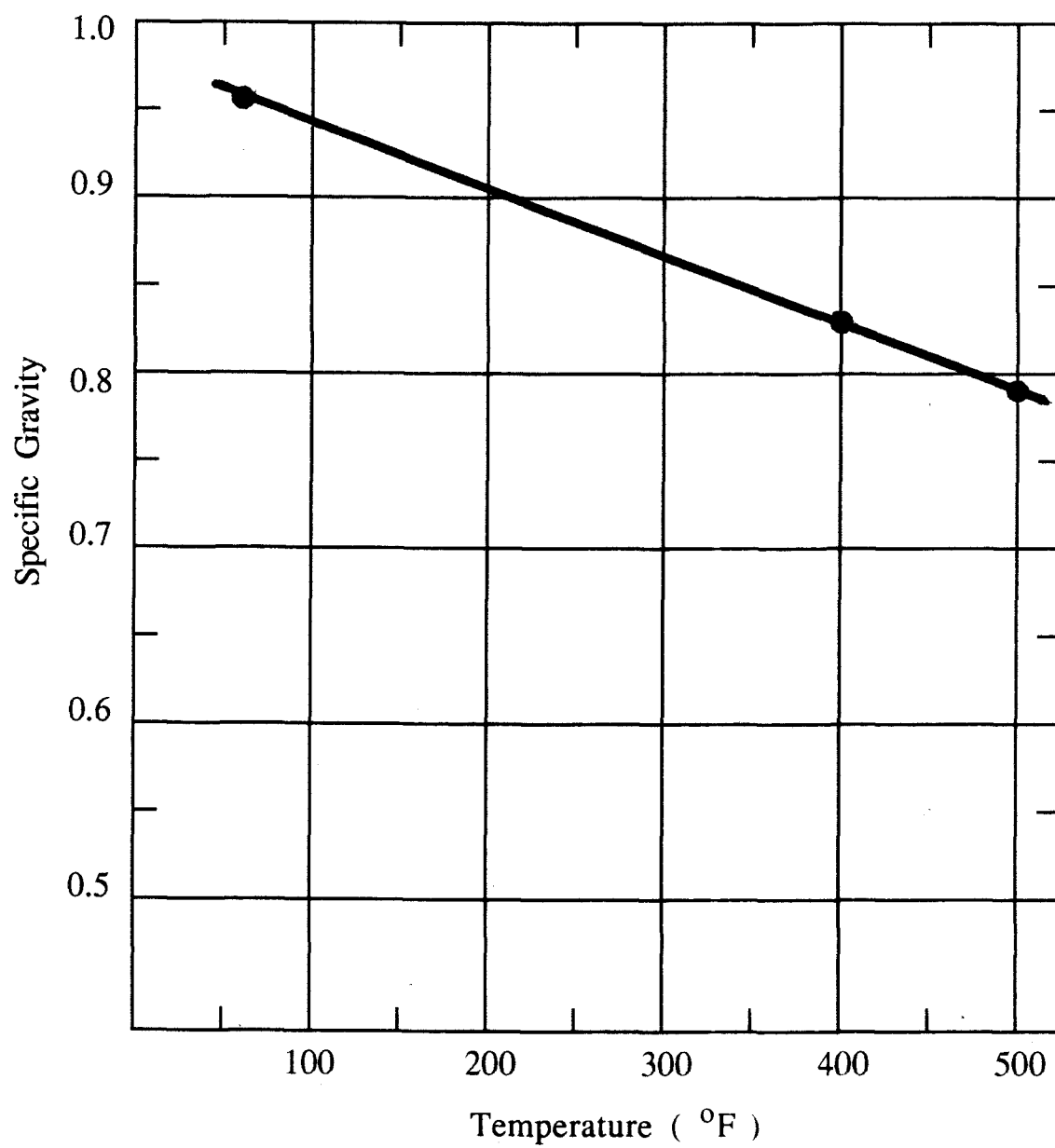


Figure 4.1 Specific gravity of dry crude oil

used to remove any deposits left. In order to get uniform smoothness, the heater surface is polished by 600 grit 3M wet/dry sand paper as a final step.

The thermal resistance (or conductance) of the heater wall between the thermocouple junction and the surface of heater may change after the surface is cleaned. Hence, it is necessary to recalibrate the heater and to determine the new R_w (wall resistance) value. The calibration method used is described by Knudsen [50]. He used the typical Wilson plot [51] (Figure 4.2) to determine the R_w value. The calibration equipment is shown in Figure 4.3.

This method is used to determine the wall resistance (R_w) and to evaluate the change of heat transfer coefficient (h) due to fouling deposits on the heater surface. Evaluating the change of heat transfer coefficient is discussed in Appendix A.

The definition of terms for thermal fouling are shown in Figure 4.4. By maintaining constant velocity, constant bulk temperature and constant heat flux, the heat transfer coefficient remains essentially constant if thickness and roughness of the deposit film are neglected. Thus, the surface temperature remains constant and the wall temperature increases as fouling occurs.

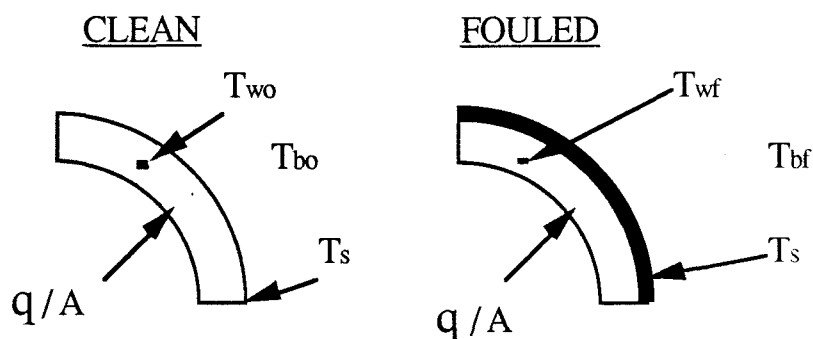


Figure 4.4 Definition of terms for thermal fouling

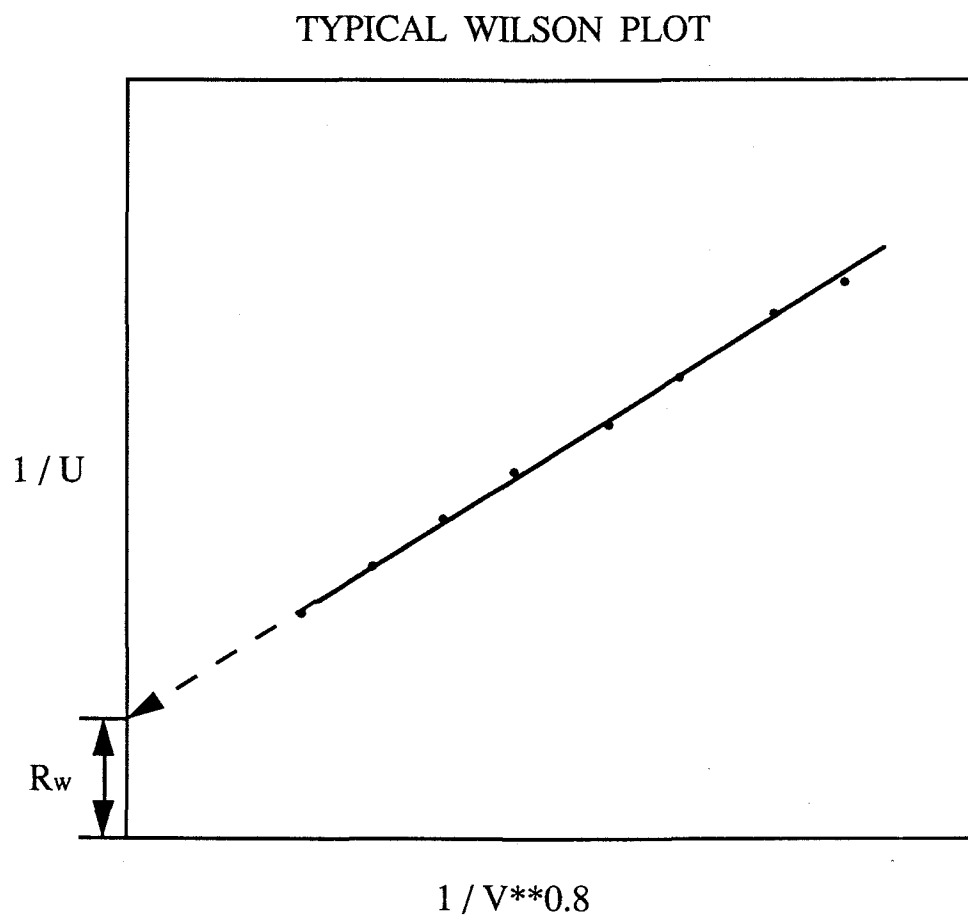


Figure 4.2 Typical Wilson plot [56]

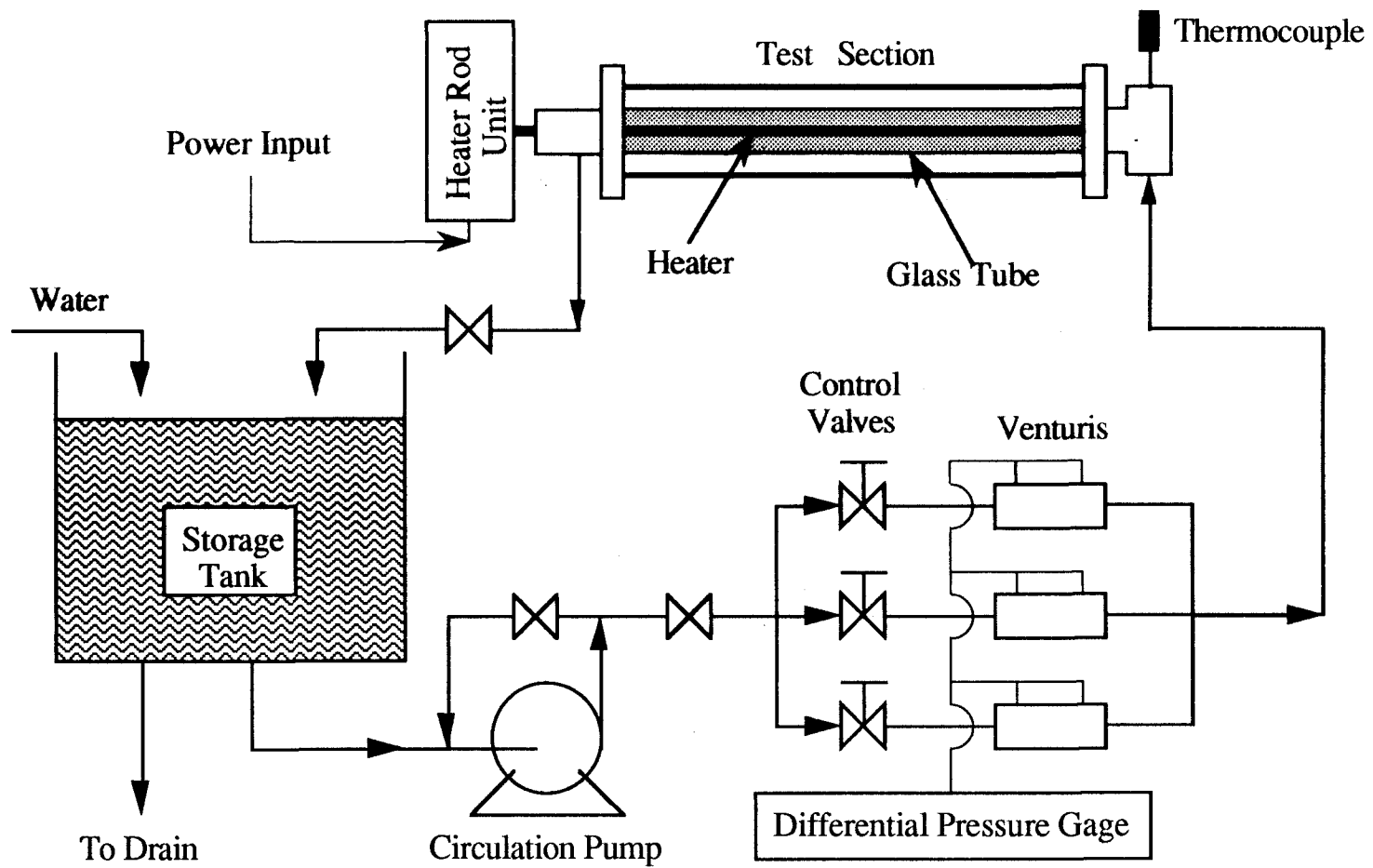


Figure 4.3 Calibration equipment diagram.

For the clean condition : $q / A = U_o (T_{wo} - T_{bo})$ (4.1)

For the fouled condition : $q / A = U_f (T_{wf} - T_{bf})$ (4.2)

where :

$$\frac{1}{U_o} = R_w + \frac{1}{h_{bo}} \quad (4.3)$$

$$\frac{1}{U_f} = R_w + R_f + \frac{1}{h_{bf}} \quad (4.4)$$

Knudsen and Katz [58] recommend the equation proposed by Wiegand [52] for predicting the heat-transfer coefficient for a fluid flowing in a smooth annulus with heat flowing through the smooth inner tube :

$$\frac{h D_e}{k} = 0.023 \left(\frac{D_e \rho v}{\mu} \right)^{0.8} \left(\frac{C_p \mu}{k} \right)^{0.4} \left(\frac{D_2}{D_1} \right) \quad (4.5)$$

where, all properties of fluid are evaluated at bulk temperature. d_2 and d_1 are respectively the outside and inside diameters of annulus and $D_e = D_2 - D_1$ is the equivalent diameter.

Rearranging equation (4.5) gives :

$$h = 0.023 \frac{k}{D_e} \left(\frac{D_e \rho v}{\mu} \right)^{0.8} \left(\frac{C_p \mu}{k} \right)^{0.4} \left(\frac{D_2}{D_1} \right) \quad (4.6)$$

Simplifying all the properties which are constants, equation (4.6) becomes to :

$$h = C v^{0.8} \quad (4.7)$$

where C is a constant, a function of the annulus geometry and fluid properties at bulk temperature.

Substitution equation (4.7) into equation (4.3) and equation (4.4) give :

$$\text{For the clean condition : } \frac{1}{U_o} = R_w + \frac{1}{C^* v^{0.8}} \quad (4.8)$$

$$\text{For the fouled condition : } \frac{1}{U_f} = R_w + R_f + \frac{1}{C^{**} v^{0.8}} \quad (4.9)$$

where C^* and C^{**} are property constants which depend on these two conditions.

By using equation (4.8), wall resistance (R_w) can be obtained from the plot of $\frac{1}{U_o}$ versus $\frac{1}{v^{0.8}}$ at the clean condition. R_w is equal to the intercept and $\frac{1}{C^*}$ is equal to the slope in the linear plot. At the fouled condition, the same method is used to get the result in which $(R_w + R_f)$ is equal to the intercept and $\frac{1}{C^{**}}$ is equal to the slope in the linear plot of $\frac{1}{U_f}$ versus $\frac{1}{v^{0.8}}$.

For the previous constant heat transfer coefficient assumption, $\frac{1}{C^*}$ should be equal to $\frac{1}{C^{**}}$. It is necessary to check the difference between $\frac{1}{h_{bo}}$ and $\frac{1}{h_{bf}}$. The change is discussed in the Appendix A.

4.3 Heat Transfer Test (Boiling Test)

As previously discussed in Chapter 2.1, it is important to determine that a fouling test is under local boiling or non-boiling at the operating condition before the experiments is started.

By using the band heaters around the storage vessel, the crude oil is heated up to the desired bulk temperature. At this moment, the flow rate is adjusted by the by-pass valve and nitrogen is supplied to raised the pressure to their desired values. Heat transfer tests begin when all the conditions are met.

The procedure of the heat transfer test is to increase the power input of heater rod in the test section gradually and to record the wall temperature at each power level. In the calibration process, the wall resistance of heater rod can be determined at the clean condition. Therefore, the surface temperature can be determined at each power level and wall temperature. Thus, both the wall superheat ($T_s - T_b$) and the convective heat transfer coefficient (h) can be obtained by using the basic heat transfer equation.

4.4 Operating Conditions

In this study, experiments were separated into two major parts, the dry bulk test and the wet bulk test. The wet bulk test consists of wet wall test and semi-dry wall test. The definitions for these tests are as follows :

For dry bulk test : no brine in the crude oil.

For wet bulk test : a certain amount of brine is added to the crude oil.

a : wet wall test : (1) no brine boiling : $w > S_b, w > S_s, T_s < T_{bb}$.

(2) wall brine boiling : $w > S_b, w > S_s, T_s > T_{bb}$.

b : semi-dry wall test : (1) no brine boiling : $w > S_b, w < S_s, T_s < T_{bb}$.

(2) wall brine boiling : $w > S_b, w < S_s, T_s > T_{bb}$.

where

T_b : bulk temperature of crude oil.

T_s : surface temperature of heater rod.

T_{wb} : boiling temperature of water.

T_{bb} : boiling temperature of salt saturated brine.

w : total brine amount (weight percentage) in crude oil.

S_s : brine solubility in crude oil at T_s .

S_b : brine solubility in crude oil at T_b .

In this study, 57 dry tests, 4 wet wall tests, and 6 semi-dry wall tests were completed. Velocities are ranged from 3.0 ft/sec to 10.0 ft/sec and pressures are ranged from 30 psig to 285 psig. The bulk temperatures of crude oil and surface temperature of heater rod are ranged from 300 °F to 400 °F and 350 °F to 700 °F, respectively. Table 4.1 summarizes the operating conditions of the fouling tests.

4.5 Run Initiation

The crude oil sent from Amoco Oil Company by 55-gallon barrel is liquid at the room temperature with high viscosity. It can be charged into the system even with its high viscosity. To avoid additional pollution, the oil is charged into the storage vessel without any preheating process. Due to the limit amount of sample available, 3.75 gallons of crude oil was used for each run following the first 14 runs which used 4 gallons per run.

By using a trial and error method, the desired surface temperature of the heater rod was achieved when all the operating conditions were met. In order to avoid fouling at this moment, this procedure should take as little time as possible. The wall resistance (R_w) can be determined by the calibration method before each run is initiated. Hence, the desired surface temperature of heater rod can be obtained from the relation between the power input and wall temperature. This relation is as follows :

Table 4.1 Summary of operating conditions

DRY BULK TEST Run No.	Time (hours)	Velocity (ft / sec)	Surface Temp. T _s (F)	Bulk Temp. T _b (F)	Pressure P (psig)	h _o (*)	Remarks (**)
<u>BARREL No. 1 - AMOCO CRUDE FDC(263)</u>							
AMO-FDC(263)-01	40.00	3.0	500	400	250	138	RH
AMO-FDC(263)-02	116.00	3.0	549	400	250	142	REU
AMO-FDC(263)-03	61.00	3.0	599	400	250	158	REU
AMO-FDC(263)-04	84.00	3.0	600	400	250	142	
AMO-FDC(263)-05	59.50	5.5	601	400	250	215	
AMO-FDC(263)-06	65.50	5.5	650	400	250	229	REU
AMO-FDC(263)-07	74.50	3.0	650	400	250	133	
AMO-FDC(263)-08	56.00	5.5	650	400	250	217	
AMO-FDC(263)-09	54.25	8.0	651	400	250	320	
<u>BARREL No. 2 - AMOCO CRUDE FDC(263)</u>							
AMO-FDC(263)-10	20.00	3.0	700	400	250	136	
AMO-FDC(263)-11	97.50	5.5	699	400	250	355	
AMO-FDC(263)-12	87.00	3.0	551	400	250	228	
AMO-FDC(263)-13	7.45	8.0	702	400	250	339	
AMO-FDC(263)-14	17.35	5.5	699	400	250	225	
AMO-FDC(263)-15	20.35	8.0	599	400	250	508	
AMO-FDC(263)-16	39.50	5.5	549	400	250	358	
AMO-FDC(263)-17	90.00	5.5	551	400	250	194	REU
AMO-FDC(263)-18	353.00	5.5	551	400	250	181	REU
AMO-FDC(263)-19	54.50	3.0	499	400	250	119	
AMO-FDC(263)-20	104.00	3.0	500	400	250	212	RH
AMO-FDC(263)-21	51.00	3.0	500	400	250	166	REU
AMO-FDC(263)-22	106.00	3.0	500	400	250	215	
AMO-FDC(263)-23	66.50	3.0	500	400	250	100	REU

Table 4.1 Summary of operating conditions (Continued)

DRY BULK TEST Run No.	Time (hours)	Velocity (ft / sec)	Surface Temp. Ts (F)	Bulk Temp. Tb (F)	Pressure P (psig)	h o (*)	Remarks (**)
<u>BARREL No. 2 - AMOCO CRUDE FDC(263)</u>							
AMO-FDC(263)-24	40.50	10.0	500	400	250	397	
AMO-FDC(263)-25	110.00	5.5	500	400	250	153	REU
AMO-FDC(263)-26	141.00	5.5	500	400	250	158	REU
AMO-FDC(263)-27	24.00	8.0	350	300	30	179	
AMO-FDC(263)-28	35.25	8.0	400	300	30	209	REU
AMO-FDC(263)-29	25.00	8.0	450	400	155	390	REU
AMO-FDC(263)-30	45.00	8.0	500	400	155	343	REU
AMO-FDC(263)-31	47.50	8.0	550	400	155	437	REU
AMO-FDC(263)-32	62.25	8.0	600	400	155	499	REU
AMO-FDC(263)-32a	0.00	8.0	601	400	155	747	REU
<u>BARREL No. 3 - AMOCO CRUDE FDC(263)</u>							
AMO-FDC(263)-33	24.00	8.0	350	300	30	197	
AMO-FDC(263)-34	24.00	8.0	400	300	30	214	REU
AMO-FDC(263)-35	24.00	8.0	449	400	155	424	REU
AMO-FDC(263)-36	40.25	8.0	500	400	155	418	REU
AMO-FDC(263)-37	50.50	8.0	550	400	155	466	REU
AMO-FDC(263)-38	99.90	8.0	600	400	155	478	REU
AMO-FDC(263)-38a	32.00	8.0	600	400	155	717	REU
AMO-FDC(263)-39	24.00	3.0	350	300	30	108	
AMO-FDC(263)-40	31.00	3.0	400	300	30	120	REU
AMO-FDC(263)-41	41.75	3.0	450	400	155	114	REU
AMO-FDC(263)-41a	53.50	3.0	449	400	155	95	REU
AMO-FDC(263)-42	44.00	3.0	475	400	155	93	REU
AMO-FDC(263)-43	24.00	5.5	350	300	30	143	

Table 4.1 Summary of operating conditions (Continued)

DRY BULK TEST Run No.	Time (hours)	Velocity (ft/sec)	Surface Temp. Ts (F)	Bulk Temp. Tb (F)	Pressure P (psig)	ho (*)	Remarks (**)
<u>BARREL No. 3 - AMOCO CRUDE FDC(263)</u>							
AMO-FDC(263)-44	25.00	5.5	399	300	30	156	REU
AMO-FDC(263)-45	43.00	5.5	450	400	155	173	REU
AMO-FDC(263)-46	24.00	5.5	475	400	155	173	REU
AMO-FDC(263)-47	52.25	5.5	500	400	155	173	REU
AMO-FDC(263)-48	43.00	5.5	524	400	155	189	REU
AMO-FDC(263)-49	112.00	5.5	550	400	155	277	REU
AMO-FDC(263)-50	134.00	5.5	575	400	155	290	REU
AMO-FDC(263)-51	51.00	10.0	350	300	30	235	
AMO-FDC(263)-52	40.00	10.0	400	300	30	272	REU
AMO-FDC(263)-53	24.00	10.0	450	400	155	488	REU
AMO-FDC(263)-54	46.00	10.0	499	400	155	538	REU
AMO-FDC(263)-55	46.00	10.0	549	400	155	619	REU
AMO-FDC(263)-56	70.00	10.0	601	400	155	726	REU
AMO-FDC(263)-57	171.00	10.0	625	400	155	667	REU

* Btu / (hr ft² °F)

** RH : Test fluid reused from a series of boiling tests.

REU : Test fluid reused from previous run.

Table 4.1 Summary of operating conditions (Continued)

WET BULK TEST (BARREL NO. 3)	WET BULK $w > S_b$									
	WET WALL $w > S_s$				SEMI-DRY WALL $w < S_s$					
	WALL BRINE BOILING $T_s > T_{bb}$		NO BRINE BOILING $T_s < T_{bb}$		WALL BRINE BOILING $T_s > T_{bb}$		NO BRINE BOILING $T_s < T_{bb}$			
T_b , (F)	300		300		300		300		300	
T_s , (F)	350		350		400		400		425	
w , (wt %)	0.8		0.8		0.8		0.8		0.8	
S_b , (wt %)	0.4		0.4		0.4		0.4		0.4	
S_s , (wt %)	0.6		0.6		1.2		1.2			
Pressure, (psig)	85		285		135		285		285	
T_{wb} , (F)	328		417		358		417		417	
T_{bb} , (F)	338		427		368		427		427	
h_o , (*)	182	266	133	176	212	269	137	238	144	263
Remark, (**)					REU	REU	REU	REU	REU	REU
Time, (hours)	46	42	48	64	105	144	92	119	72	76
Velocity, (ft/sec)	5.5	8.0	5.5	8.0	5.5	8.0	5.5	8.0	5.5	8.0
RUN No.	AMO-FDC(263)-WW-58	AMO-FDC(263)-WW-63	AMO-FDC(263)-WW-60	AMO-FDC(263)-WW-65	AMO-FDC(263)-SDW-59	AMO-FDC(263)-SDW-64	AMO-FDC(263)-SDW-61	AMO-FDC(263)-SDW-66	AMO-FDC(263)-SDW-62	AMO-FDC(263)-SDW-67

* Btu / (hr ft² °F)

** REU : Test fluid reused from previous run.

$$\text{At initial (clean) condition : } T_{so} = T_{wo} - \left(\frac{q}{A}\right)_o R_w \quad (4.10)$$

where R_w : wall resistance.

T_{so} : surface temperature.

T_{wo} : initial wall temperature.

The computer program is started when all the operating conditions (velocity, pressure, bulk temperature, and surface temperature of heater rod) are met. In order to maintain the constant bulk temperature, it is necessary to decrease the power input to band heaters which is determined by excessive power supply of the heater rod. Based on the operating experience, bulk temperature fluctuation is only 2 °F departure from the set point for the optimum control of band heaters and silicon rubber heaters.

4.6 Data Acquisition and Processing

An IBM personal computer is used to control and monitor the equipment. An Adalab- PC data acquisition and control board, purchased from Interactive Microwave Inc. (IMI), was installed in the PC. This is required for the computer to automatically compile and process the acquired data through the computer program. The computer program is written in basic language and is shown in Appendix B.

The computer receives the information which is in the form of voltages from various measurement sensors. There are three temperature signals from three different thermocouples. Two thermocouples measure the bulk temperature of crude oil in and out of the test section. Another thermocouple is used to detect the wall temperature of heater rod. The mass flow meter is the sensor of flow rate measurement. Due to constant power

supplied to the heater rod in each run, it is necessary to input the power value sensed by a wattmeter when the computer program is initiated.

The experimental data is also monitored by electronic analog instruments except for the computer system. The electronic analog instruments include a digital thermometer and a digital multimeter. The thermometer displays the bulk temperature of the fluid and the wall temperature of heater rod through an Omega thermocouple switch. The digital multimeter displays the measured flow rate and power supplied to the heater rod (in volts). Sometimes it is necessary to compare the data displayed on the computer screen and electronic analog instruments to assure that all operating conditions are constant.

The computer program processes all the voltage signals from the sensors into information in the form of degrees F (temperature), pounds per minute or feet per second (flow rate), and watts (power supplied for the heater rod). Based on the current data sent from sensors, the computer program will calculate fouling resistance by using the basic Equation (2.24) and display the results continuously on the monitor. The data are recorded on a hard disk and printed on the printer at given time intervals which can be changed on the screen at any time. The main purpose for recording and printing out the data at the same time is to prevent loss of data in case of a power outage.

4.7 Process Monitoring

Although the computer will monitor the experimental process and record all the data, it is still necessary to check the process periodically. It is especially necessary to examine the process and find the optimum power input of band heaters on the storage vessel in order to keep constant bulk temperature at the beginning of each run. Due to

unstable electricity power and environment temperature change, it is necessary to occasionally adjust the power input of the storage vessel and heater rod.

4.8 Run Termination

Termination of each run depends on many factors. An experiment is usually terminated manually when the fouling resistance has reached an asymptotic value. The power to the heater rod will be cut off by the computer automatically when the wall temperature is above the maximum allowable temperature (set point). The set point of maximum allowable temperature is 910 °F. At times the experiment is terminated manually when it is operated for a sufficient time and there is no fouling.

All the power input of heaters are cut off when the experiment is terminated. There are two ways to deal with crude oil. The first one is to reuse the crude oil and clean the heater if fouling has occurred. In this situation, the test section is isolated by the two by-pass devices and cooled down to low temperature in order to remove the heater. Another way is to recharge the fresh sample for next run. Based on this choice, the cooling heat exchanger jacket is used to cool the whole system down to a low temperature (about 200 °F). All of the used crude oil is drained away and then the heater rod is removed out from the test section.

In order to analyze fouling deposits on the carbon steel heater surface, it must be scraped off carefully. Fouling deposits and liquid samples were sent to the Research and Development Department of Amoco Oil Company, Naperville, Illinois for analysis.

CHAPTER 5

RESULTS AND DISCUSSION

5.1 Heat Transfer Test (Boiling Test)

In all, sixteen heat transfer tests (Runs AMO-FDC(263)-BO-01 through AMO-FDC(263)-BO-16) were completed with velocities ranging from 3.0 ft/sec to 10.0 ft/sec. Pressure and bulk temperature were respectively 250 psig and 400 °F. All the tests are summarized in Table 5.1. The data for these boiling tests and a computer program used for calculations are shown in Appendix C.

Figure 5.1 shows a plot of the heat transfer coefficient (h) versus the superheat ($T_s - T_b$) for the first 4 boiling tests (Runs AMO-FDC(263)-BO-01 through -BO-04) conducted on fresh sample from Barrel No. 1. The superheats are ranged from 11 °F to 468 °F. The curves in Figure 5.1 are typical of convection heat transfers and indicate that no boiling occurs in any of the tests.

Using the crude oil from Barrel No. 2, a series of 12 heat transfer tests were conducted. Runs AMO-FDC(263)-BO-05 through -BO-12 were completed on reused crude oil sample following a fouling test (AMO-FDC(263)-19). Velocities of 3.0, 5.5, 8.0 and 10.0 ft/sec were investigated in ascending order on four tests (Runs -BO-05 through -BO-08), in which the crude oil had been exposed for sometime to high heater temperatures at high velocities of 8.0 and 10.0 ft/sec. After cleaning and recalibrating the heater, four subsequent tests (Runs -BO-09 through -BO-12) were studied in inverse order of the velocities, in which 10.0 ft/sec was investigated first, then 8.0 ft/sec, then 5.5 ft/sec and finally 3.0 ft/sec. This procedure was used to determine if fouling may have been

Table 5.1 Summary of heat transfer tests (boiling tests)

Run No.	Velocity (ft/sec)	Bulk Temp. T _b (F)	Pressure P (psig)	Remarks (*)
(Barrel No. 1)				
AMO-FDC(263)-BO-01	3.0	400	250	
AMO-FDC(263)-BO-02	5.5	400	250	
AMO-FDC(263)-BO-03	8.0	400	250	
AMO-FDC(263)-BO-04	10.0	400	250	
(Barrel No. 2)				
AMO-FDC(263)-BO-05	3.0	400	250	REU-19
AMO-FDC(263)-BO-06	5.5	400	250	REU-19
AMO-FDC(263)-BO-07	8.0	400	250	REU-19
AMO-FDC(263)-BO-08	10.0	400	250	REU-19
AMO-FDC(263)-BO-09	3.0	400	250	REU-19
AMO-FDC(263)-BO-10	5.5	400	250	REU-19
AMO-FDC(263)-BO-11	8.0	400	250	REU-19
AMO-FDC(263)-BO-12	10.0	400	250	REU-19
AMO-FDC(263)-BO-13	3.0	400	250	
AMO-FDC(263)-BO-14	5.5	400	250	
AMO-FDC(263)-BO-15	8.0	400	250	
AMO-FDC(263)-BO-16	10.0	400	250	

* REU-19 : Test fluid reused from fouling Run AMO-FDC(263)-19

BOILING TESTS with BARREL No. 1

P= 250 psig ; Tb= 400 F

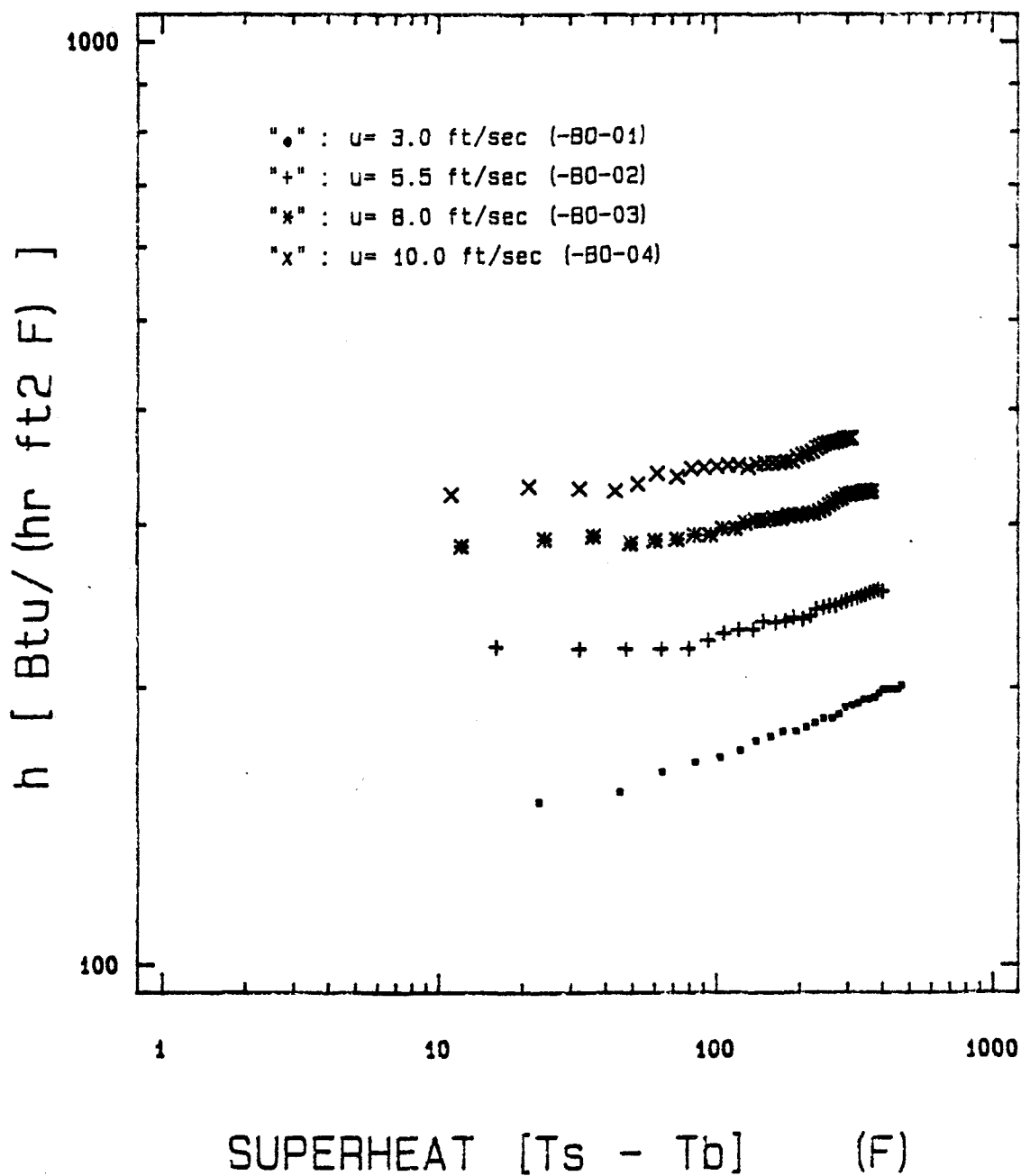


Figure 5.1 Heat transfer tests on crude oil from Barrel No. 1
 Runs AMO-FDC(263)-BO-01 through -BO-04
 (Fresh feed used)

occurring during the heat transfer tests, which would have influenced the values of the heat transfer coefficient.

Figure 5.2 is a plot of Runs -BO-05, -BO-09 (3.0 ft/sec) and Runs -BO-06, -BO-10 (5.5 ft/sec). At a velocity of 5.5 ft/sec, these two tests are in good agreement with each other over the whole range of superheats investigated. At 3.0 ft/sec, there are some differences between these two tests at low superheats but they agree well with each other at high superheats. The other four tests (Runs -BO-07, -BO-08, -BO-11 and -BO-12) are shown in Figure 5.3. Except for some small differences at low superheats, there is a good agreement between the data of runs not only for 8.0 ft/sec but also for 10.0 ft/sec. These results would indicate that no fouling occurred during the heat transfer tests. The same observation was obtained during the cleaning process of heater rod after Run -BO-08. A plot of Runs -BO-05 (3.0 ft/sec), -BO-06 (5.5 ft/sec), -BO-11 (8.0 ft/sec) and -BO-12 (10.0 ft/sec) is shown in Figure 5.4 and indicates that nucleate boiling occurs at superheats ($T_s - T_b$) above 120 °F for the crude oil in Barrel No. 2. Comparing Figure 5.4 with Figure 5.1 suggests that the crude oil samples of Barrel No. 1 and Barrel No. 2 are somewhat different.

Figure 5.5 is a plot of four tests (Runs -BO-13 through -BO-16) conducted on the fresh crude oil in Barrel No. 2. Nucleate boiling occurs at superheats above 80 °F. A comparison of Figure 5.4 and Figure 5.5 indicates that a certain amount of low boiling point component is perhaps lost when the test section is opened between runs (reusing the sample). Except for this point, there are no significant differences between these two plots.

In figure 5.5, it is also noted that at higher velocities of 5.5 and 8.0 ft/sec, the heat transfer coefficient goes through a minimum value from a transition regime to fully developed nucleate boiling. This phenomenon is possibly caused by transition from laminar flow to turbulent flow. It should be noted that $T_s - T_b$ may not be the true

BOILING TESTS with BARREL No. 2

P= 250 psig ; Tb= 400 F

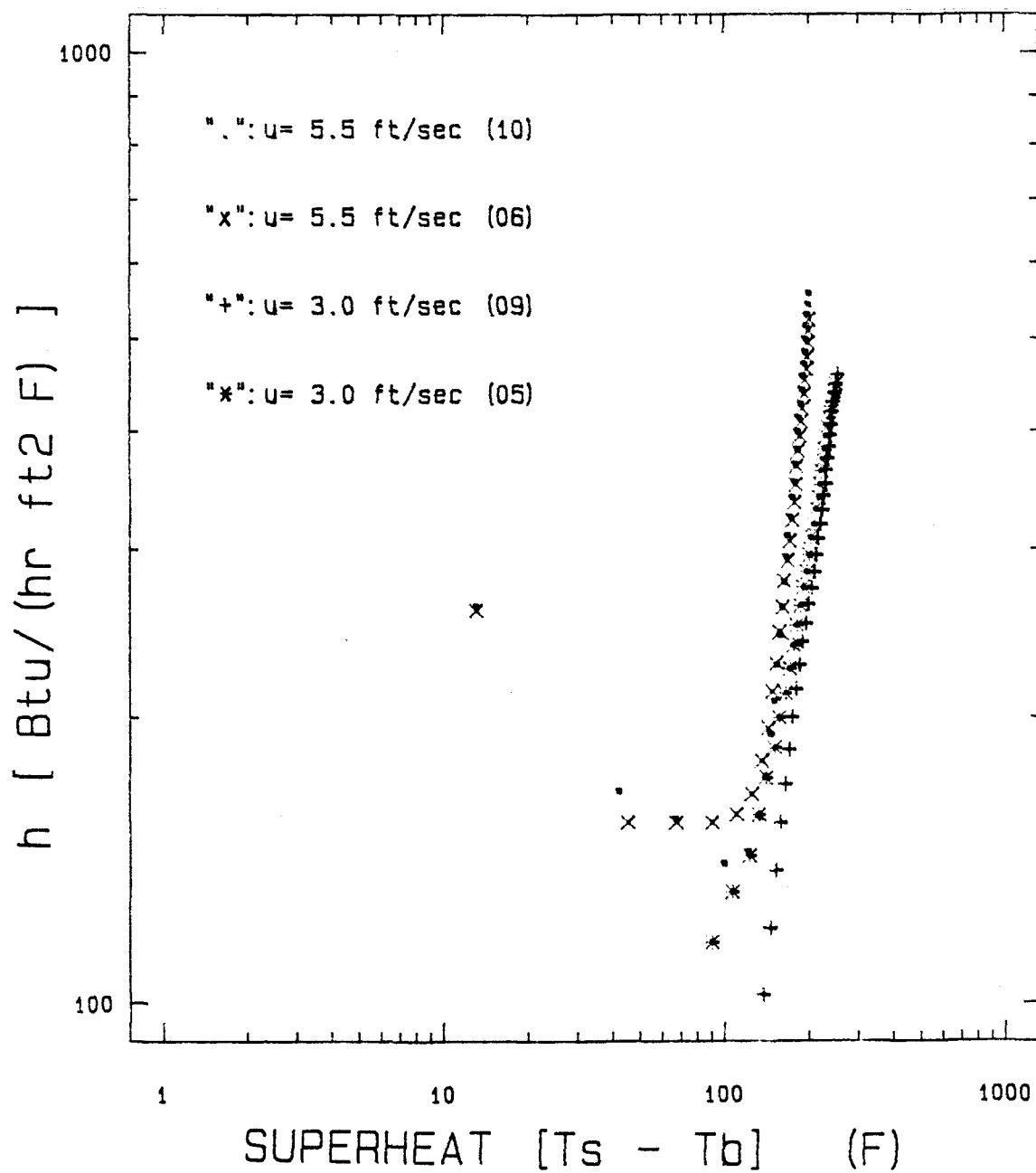


Figure 5.2 Heat transfer tests on crude oil from Barrel No. 2
Runs AMO-FDC(263)-BO-05, -BO-06, -BO-09 and -BO-10
(Reused oil)

BOILING TESTS with BARREL No. 2

P= 250 psig ; Tb= 400 F

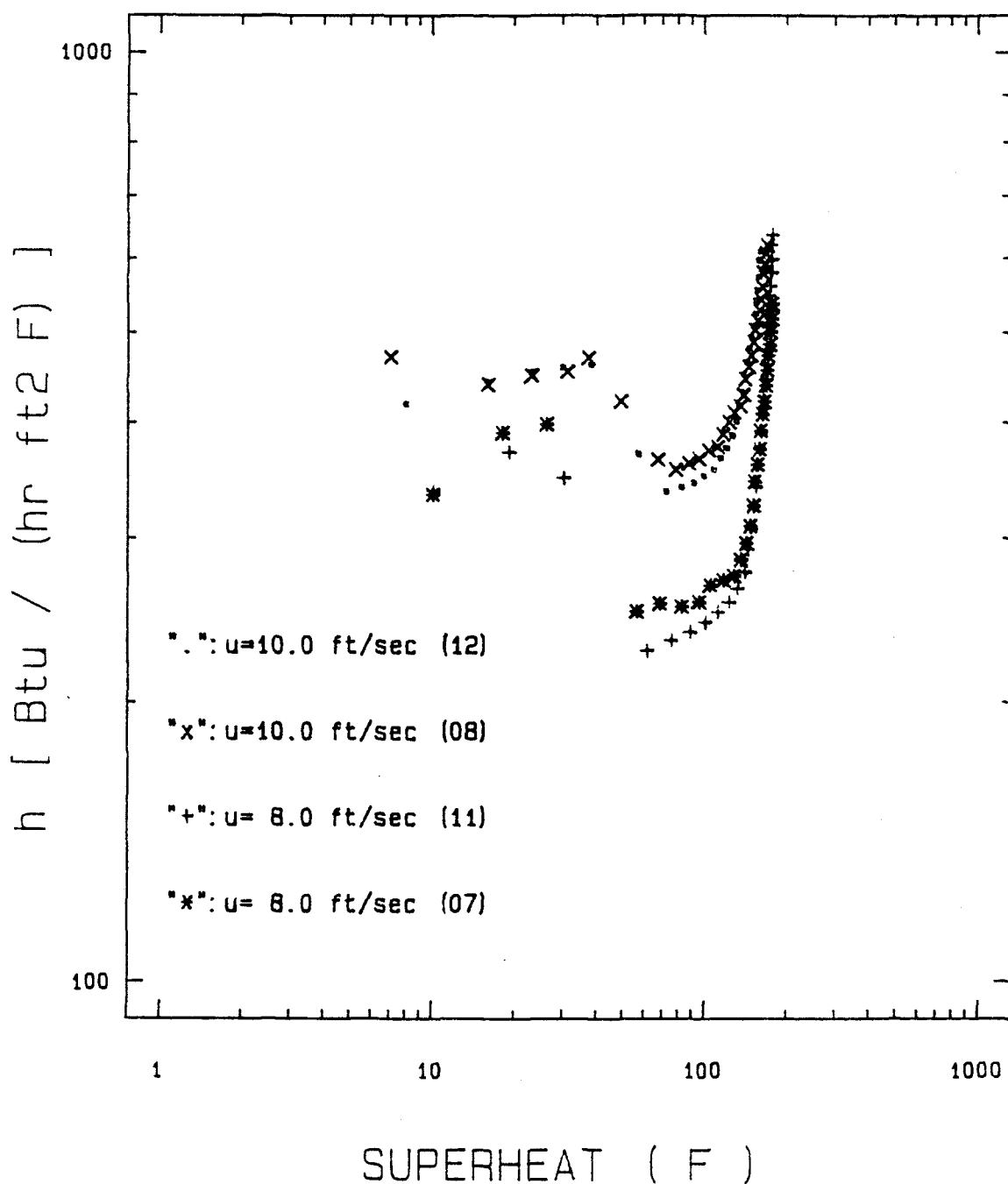


Figure 5.3 Heat transfer tests on crude oil from Barrel No. 2
 Runs AMO-FDC(263)-BO-07, -BO-08, -BO-11 and -BO-12
 (Reused oil)

BOILING TESTS with BARREL No. 2

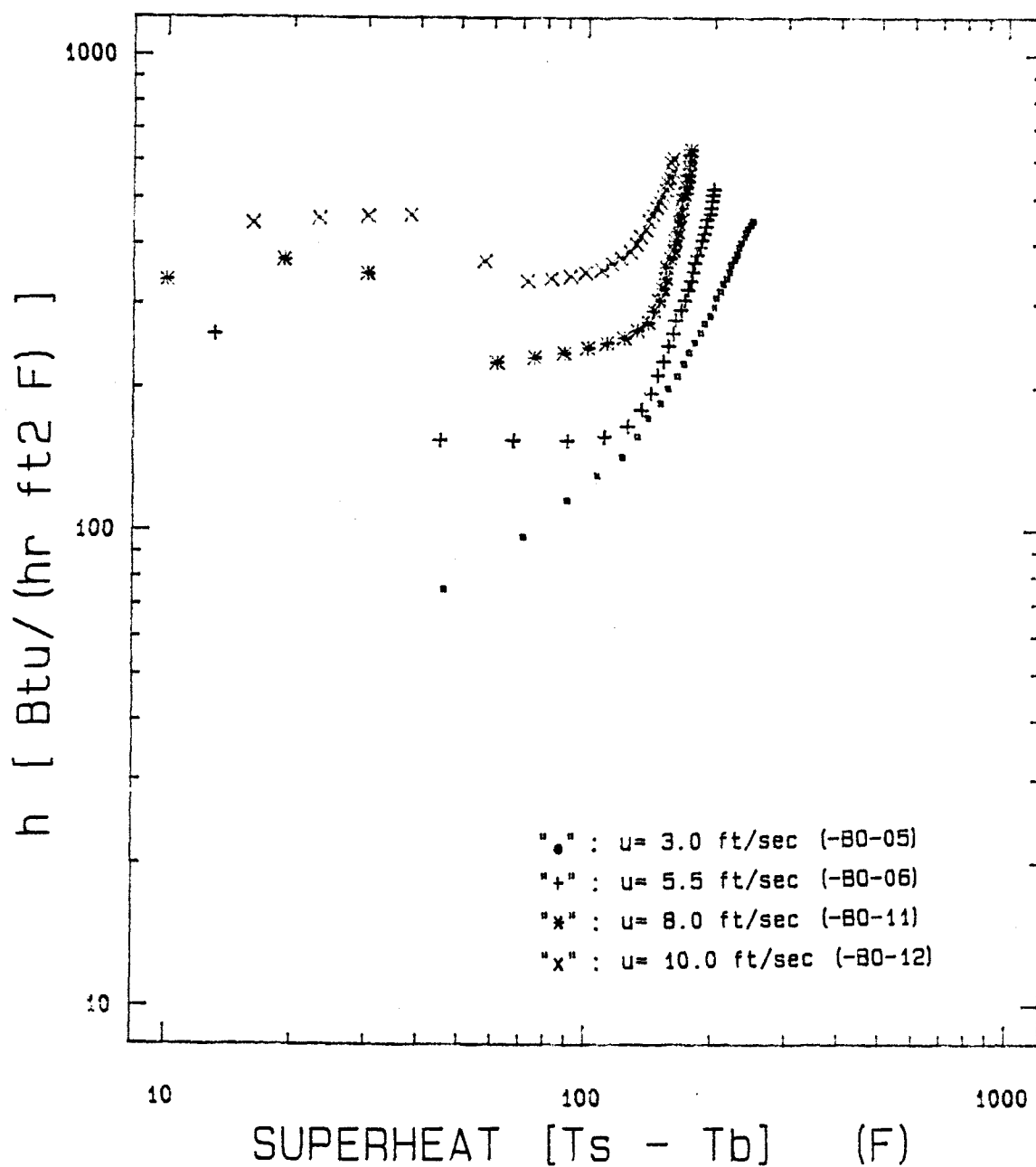
P= 250 psig ; T_b= 400 F

Figure 5.4 Heat transfer tests on crude oil from Barrel No. 2
 Runs AMO-FDC(263)-BO-05, -BO-06, -BO-11 and -BO-12
 (Reused oil)

BOILING TESTS with BARREL No. 2

P= 250 psig ; Tb= 400 F

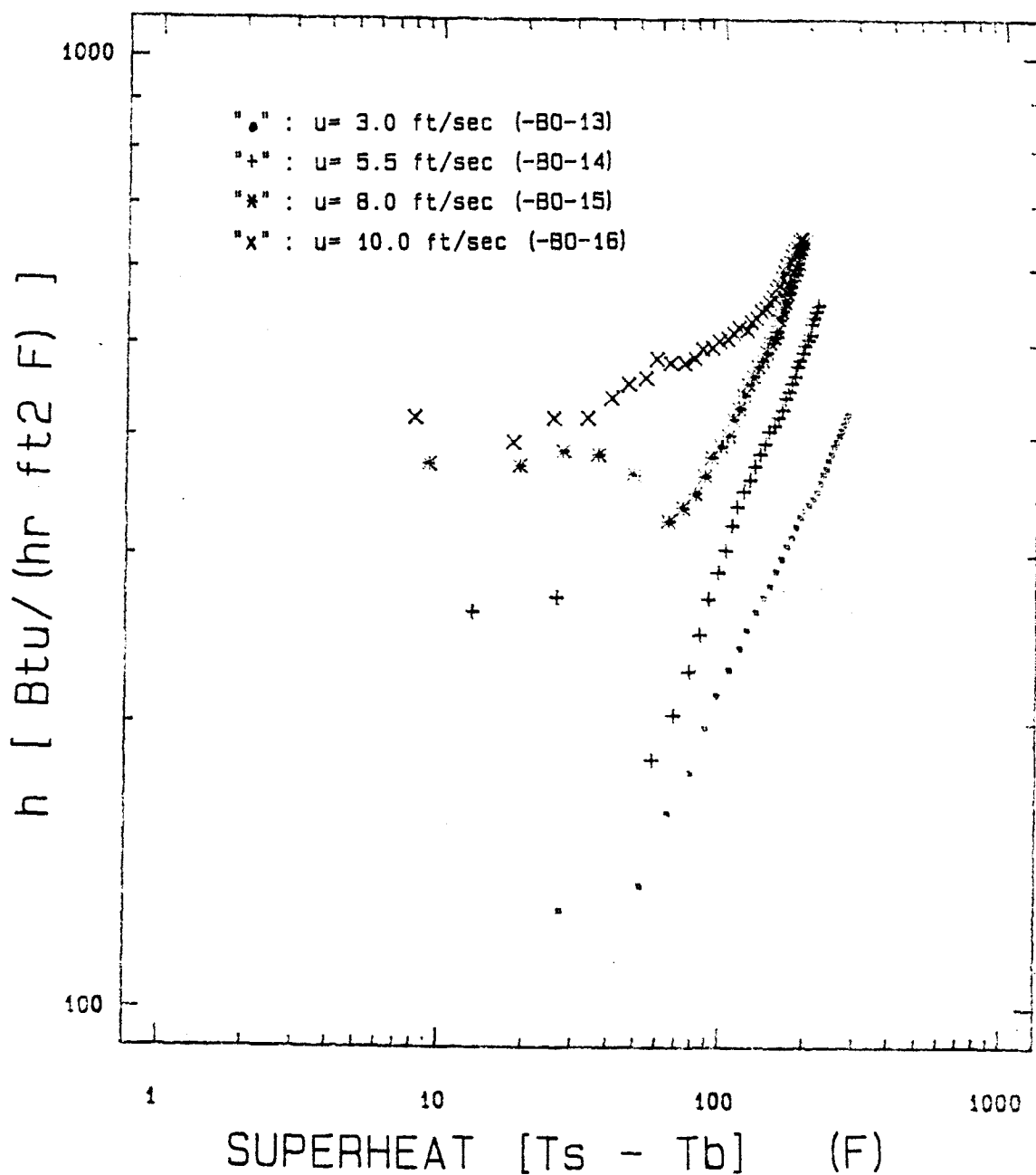


Figure 5.5 Heat transfer tests on crude oil from Barrel No. 2
 Runs AMO-FDC(263)-BO-13 through -BO-16
 (Fresh feed used)

superheat even though it is called as such here. The true superheat is the difference between the boiling point and the bulk temperature of the fluid.

5.2 Dry Bulk Tests on Amoco Crude Oil

Fifty seven dry bulk fouling tests were carried out with Amoco crude oil. Table 5.2 summarizes the results of these tests. Some inconsistencies of the initial heat transfer coefficients indicated that the crude oil sample from Barrel No. 1 was somewhat different from that from Barrel No. 2. A summary of the initial heat transfer coefficients for samples from these two barrels is given in Table 5.3. The initial heat transfer coefficients for samples from Barrel No. 2 are in reasonable agreement with these for samples from Barrel No. 3.

5.2.1 Fouling Tests with Barrel No. 1

Nine dry bulk tests were completed on the crude oil from Barrel No. 1 which was partially full. The operating conditions of these nine tests were the same as the boiling tests ($T_s = 400^\circ\text{F}$ and $P = 250$ psig). Heater surface temperatures and fluid velocities respectively ranged from 500°F to 651°F and 3.0 ft/sec to 8.0 ft/sec. The effects of velocity and surface temperature on fouling are discussed as follows:

5.2.1.1 Effect of Surface Temperature

At a velocity of 3.0 ft/sec, no fouling occurred at $T_s = 500^\circ\text{F}$ by reusing sample from a series of boiling tests (Runs -BO-01 through -BO-04). Increasing fouling occurred as the surface temperature was increased, in which no significant fouling occurred at $T_s = 549^\circ\text{F}$ but greater amounts of fouling were observed at $T_s = 600$ and 650°F . At 5.5 ft/sec,

Table 5.2 Summary of dry crude tests

Run No.	Time (hrs)	Velocity (ft/sec)	T _s (F)	T _b (F)	P (psig)	h _o (*)	Final R _f (**)	Remarks (***)
(Barrel No. 1)								
AMO-FDC(263)-01	40.00	3.0	500	400	250	138	-0.8	RH , NF
AMO-FDC(263)-02	116.00	3.0	549	400	250	142	5.7	REU, F
AMO-FDC(263)-03	61.00	3.0	599	400	250	158	10.1	REU, F
AMO-FDC(263)-04	84.00	3.0	600	400	250	142	47.2	F
AMO-FDC(263)-05	59.50	5.5	601	400	250	215	5.0	F
AMO-FDC(263)-06	65.50	5.5	650	400	250	229	-1.9	REU, NF
AMO-FDC(263)-07	74.50	3.0	650	400	250	133	71.4	F
AMO-FDC(263)-08	56.00	5.5	650	400	250	217	45.3	F
AMO-FDC(263)-09	54.25	8.0	651	400	250	320	30.5	F
(Barrel No. 2)								
AMO-FDC(263)-10	20.00	3.0	700	400	250	136	48.5	F
AMO-FDC(263)-11	97.50	5.5	699	400	250	355	8.7	F
AMO-FDC(263)-12	87.00	3.0	551	400	250	228	12.7	F
AMO-FDC(263)-13	7.45	8.0	702	400	250	339	16.9	F
AMO-FDC(263)-14	17.35	5.5	699	400	250	225	27.0	F
AMO-FDC(263)-15	20.35	8.0	599	400	250	508	26.6	F
AMO-FDC(263)-16	39.50	5.5	549	400	250	358	7.5	F
AMO-FDC(263)-17	90.00	5.5	551	400	250	194	5.5	REU, F
AMO-FDC(263)-18	353.00	5.5	551	400	250	181	40.0	REU, F
AMO-FDC(263)-19	54.50	3.0	499	400	250	119	18.8	F
AMO-FDC(263)-20	104.00	3.0	500	400	250	212	34.2	RH , F
AMO-FDC(263)-21	51.00	3.0	500	400	250	166	25.9	REU, F
AMO-FDC(263)-22	106.00	3.0	500	400	250	215	37.8	F
AMO-FDC(263)-23	66.50	3.0	500	400	250	100	10.9	REU, F
AMO-FDC(263)-24	40.50	10.0	500	400	250	397	-2.4	NF
AMO-FDC(263)-25	110.00	5.5	500	400	250	153	13.8	REU, F
AMO-FDC(263)-26	141.00	5.5	500	400	250	158	19.1	REU, F
AMO-FDC(263)-27	24.00	8.0	350	300	30	179	-2.7	NF
AMO-FDC(263)-28	35.25	8.0	400	300	30	209	-0.8	REU, NF
AMO-FDC(263)-29	25.00	8.0	450	400	155	390	0.5	REU, NF
AMO-FDC(263)-30	45.00	8.0	500	400	155	343	-0.9	REU, NF
AMO-FDC(263)-31	47.50	8.0	550	400	155	437	0.4	REU, NF
AMO-FDC(263)-32	62.25	8.0	600	400	155	499	16.4	REU, F
AMO-FDC(263)-32a	00.00	8.0	601	400	155	747	-----	REU

Table 5.2 Summary of dry crude tests (Continued)

Run No.	Time (hrs)	Velocity (ft/sec)	T _s (F)	T _b (F)	P (psig)	h _o (*)	Final R _f (**)	Remarks (***)
(Barrel No. 3)								
AMO-FDC(263)-33	24.00	8.0	350	300	30	197	0.7	NF
AMO-FDC(263)-34	24.00	8.0	400	300	30	214	0.6	REU,NF
AMO-FDC(263)-35	24.00	8.0	449	400	155	424	1.0	REU,NF
AMO-FDC(263)-36	40.25	8.0	500	400	155	418	0.0	REU,NF
AMO-FDC(263)-37	50.50	8.0	550	400	155	466	1.0	REU,NF
AMO-FDC(263)-38	99.90	8.0	600	400	155	478	27.0	REU, F
AMO-FDC(263)-38a	32.00	8.0	600	400	155	717	9.1	REU, F
AMO-FDC(263)-39	24.00	3.0	350	300	30	108	0.0	NF
AMO-FDC(263)-40	31.00	3.0	400	300	30	120	-0.9	REU,NF
AMO-FDC(263)-41	41.75	3.0	450	400	155	114	14.0	REU, F
AMO-FDC(263)-41a	53.50	3.0	449	400	155	95	12.7	REU, F
AMO-FDC(263)-42	44.00	3.0	475	400	155	93	24.3	REU, F
AMO-FDC(263)-43	24.00	5.5	350	300	30	143	-1.4	NF
AMO-FDC(263)-44	25.00	5.5	399	300	30	156	0.0	REU,NF
AMO-FDC(263)-45	43.00	5.5	450	400	155	173	1.1	REU,NF
AMO-FDC(263)-46	24.00	5.5	475	400	155	173	-0.3	REU,NF
AMO-FDC(263)-47	52.25	5.5	500	400	155	173	-6.4	REU,NF
AMO-FDC(263)-48	43.00	5.5	524	400	155	189	-19.2	REU,NF
AMO-FDC(263)-49	112.00	5.5	550	400	155	277	10.9	REU, F
AMO-FDC(263)-50	134.00	5.5	575	400	155	290	36.0	REU, F
AMO-FDC(263)-51	51.00	10.0	350	300	30	235	0.2	NF
AMO-FDC(263)-52	40.00	10.0	400	300	30	272	0.2	REU,NF
AMO-FDC(263)-53	24.00	10.0	450	400	155	488	0.0	REU,NF
AMO-FDC(263)-54	46.00	10.0	499	400	155	538	-0.2	REU,NF
AMO-FDC(263)-55	46.00	10.0	549	400	155	619	0.2	REU,NF
AMO-FDC(263)-56	70.00	10.0	601	400	155	726	1.2	REU, F
AMO-FDC(263)-57	171.00	10.0	625	400	155	667	7..5	REU, F

* Btu / (hr ft² °F)** hr ft² °F / Btu x 10⁴

*** REU : Test fluid reused from previous run.

RH : Test fluid reused from a series of boiling tests.

NF : No fouling.

F : Fouling.

Table 5.3 Initial heat transfer coefficients for dry bulk tests*

	Velocity (ft/sec)	Surface Temperature (T s)							
		350 F	400 F	450 F	500 F	550 F	600 F	650 F	700 F
Barrel No. 1	3.0				138 (1 R)	142 (2 R)	158 (3 R) 142 (4 F)	133 (7 F)	
	5.5						215 (5 F)	229 (6 R) 217 (8 F)	
	8.0						320 (9 F)		
Barrel No. 2	3.0				119 (19 F) 212 (20 R) 166 (21 R) 215 (22 F) 100 (23 R)	228 (12 F)			136 (10 F)
	5.5				153 (25 R) 158 (26 R)	358 (16 F) 194 (17 R) 181 (18 R)			355 (11 F) 225 (14 R)
	8.0	179 (27 F)	209 (28 R)	390 (29 R)	343 (30 R)	437 (31 R)	508 (15 F) 499 (32 R) 747 (32a R)		339 (13 F)
	10.0				397 (24 F)				

Table 5.3 Initial heat transfer coefficients for dry bulk tests* (Continued)

	Velocity (ft/sec)	Surface Temperature (T _s)									
		350 F	400 F	450 F	475 F	500 F	525 F	550 F	575 F	600 F	625 F
Barrel No. 3	3.0	108 (39 F)	120 (40 R)	114 (41 R) 95 (41a R)	93 (42 R)						
	5.5	143 (43 F)	156 (44 R)	173 (45 R)	173 (46 R)	173 (47 R)	189 (48 R)	277 (49 R)	290 (50 R)		
	8.0	197 (33 F)	214 (34 R)	424 (35 R)		418 (36 R)		466 (37 R)		778 (38 R) 717(38a R)	
	10.0	235 (51 F)	272 (52 R)	488 (53 R)		538 (54 R)		619 (55 R)		726 (56 R)	667 (57 R)

* Numbers in parentheses are the run numbers

R = reused feed. ; F = fresh feed.

no significant fouling was obtained at $T_s = 601^\circ\text{F}$ but serious fouling occurred at $T_s = 650^\circ\text{F}$. Figure 5.6 and Figure 5.7 show the effect of surface temperature on fouling at 3.0 and 5.5 ft/sec.

5.2.1.2 Effect of Velocity

There is an observable effect of velocity on fouling with the crude oil in Barrel No. 1. Figure 5.8 is a plot of the fouling results from Run -04 (3.0 ft/sec) and Run -05 (5.5 ft/sec) at a surface temperature of 600°F . Significant fouling occurred in both runs. After 60 hours, the fouling resistance at 5.5 ft/sec was about one fifth of that was obtained at 3.0 ft/sec. Similar effect of velocity (shown in Figure 5.9) was observed in another three runs (Runs -07 through -09) which were operated at $T_s = 650^\circ\text{F}$. The higher fouling occurred at the lower velocity. Reviewing Figure 5.8 and Figure 5.9, it is concluded that the effect of fluid velocity plays an important role on fouling, especially at a low surface temperature.

5.2.2 Fouling Tests with Barrel No. 2

Tests with Barrel No. 2 covered Runs -10 through -32a. Runs -10 through -26 were operated at the same conditions as Barrel No. 1 ($T_b = 400^\circ\text{F}$ and $P = 250$ psig). In order to determine the threshold surface temperature for the initiation of fouling at a velocity of 8.0 ft/sec, a series of runs (Runs -27 through -32a) were conducted to different operating conditions.

5.2.2.1 Effect of Surface Temperature

At 8.0 ft/sec, the effect of surface temperature is shown in Figure 5.10. Both runs (Runs -13 and -15) were conducted on the fresh sample from Barrel No.2. Fouling for Run -13 ($T_s = 702^\circ\text{F}$) was initially slow but increased rapidly to become greater than that for Run -15 ($T_s = 599^\circ\text{F}$). Figure 5.11 shows the fouling results for Runs -14, -16, and -

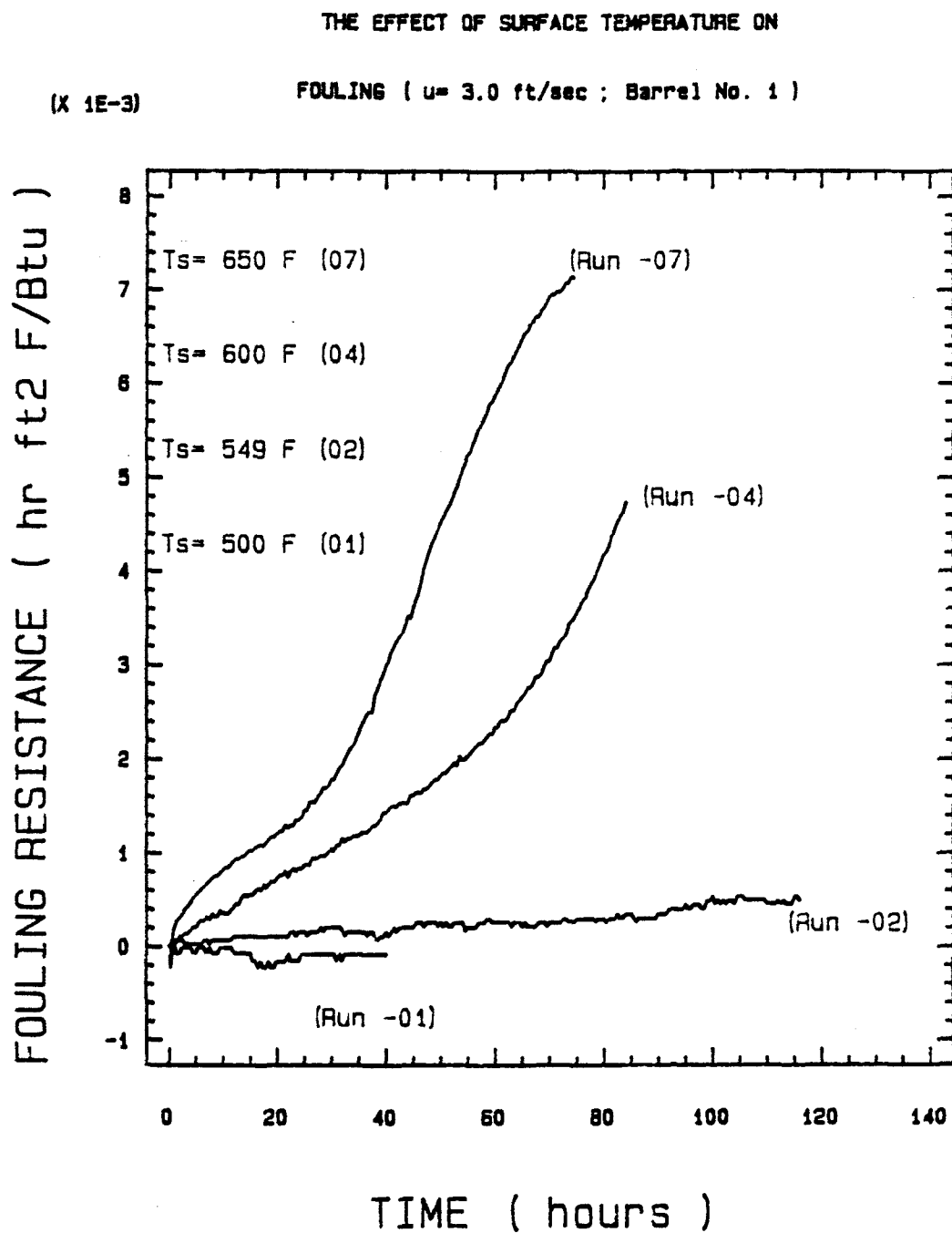


Figure 5.6 Effect of surface temperature on fouling from Barrel No. 1
Comparison of Runs AMO-FDC(263)-01, -02, -04 and -07

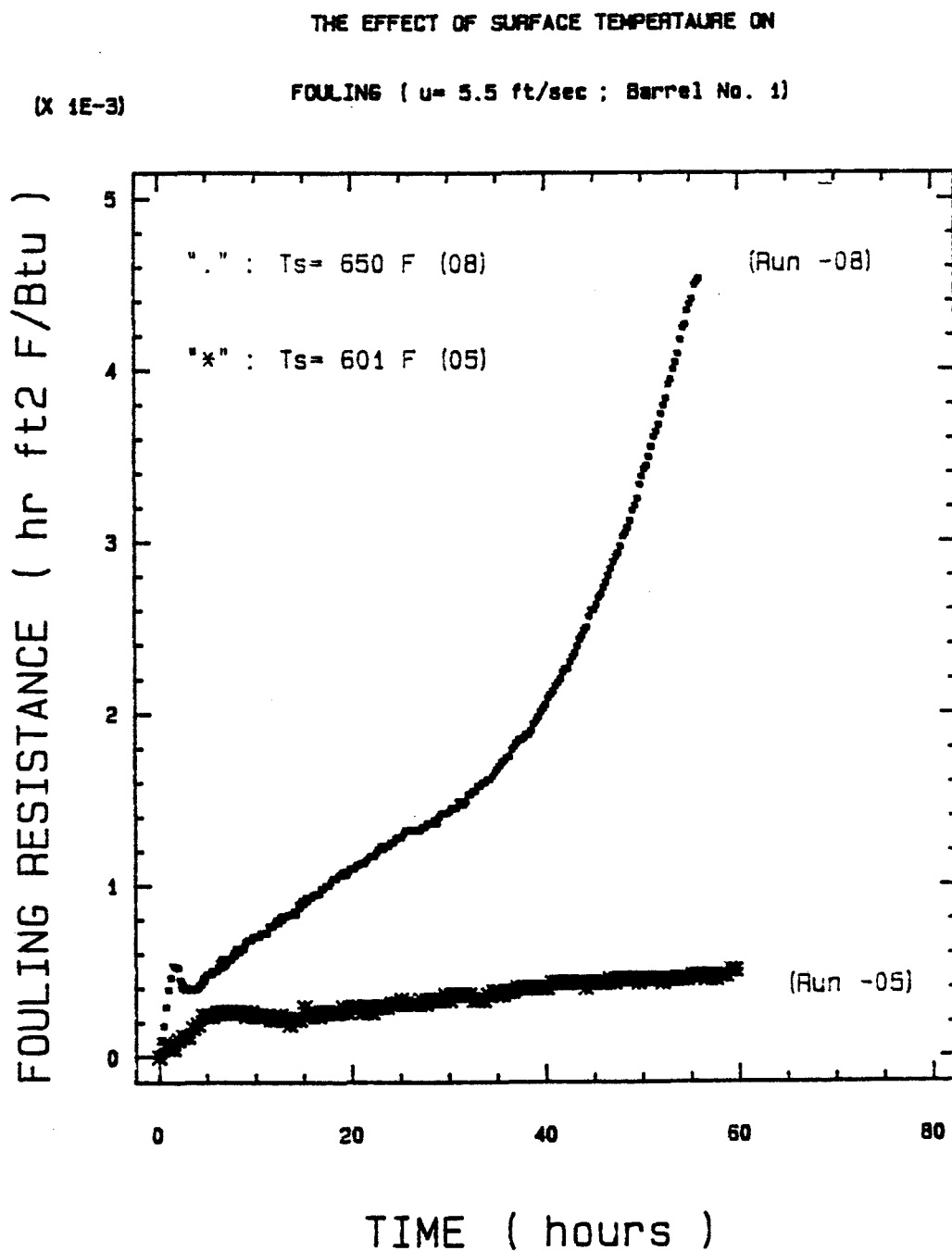


Figure 5.7 Effect of surface temperature on fouling from Barrel No. 1
Comparison of Runs AMO-FDC(263)-05 and -08

THE EFFECT OF VELOCITY ON FOULING

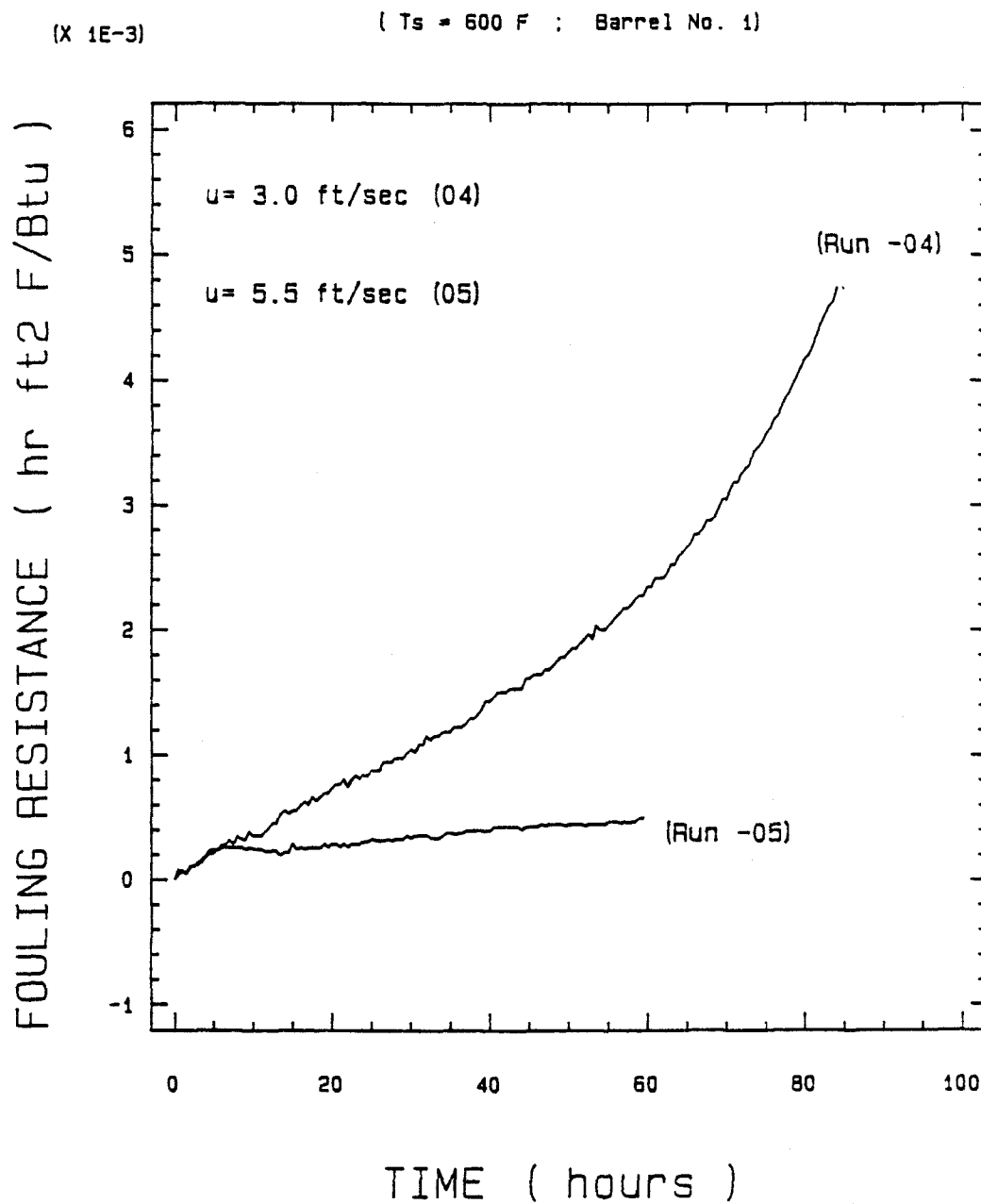


Figure 5.8 Effect of velocity on fouling from Barrel No. 1
Comparison of Runs AMO-FDC(263)-04 and -05

THE EFFECT OF VELOCITY ON FOULING

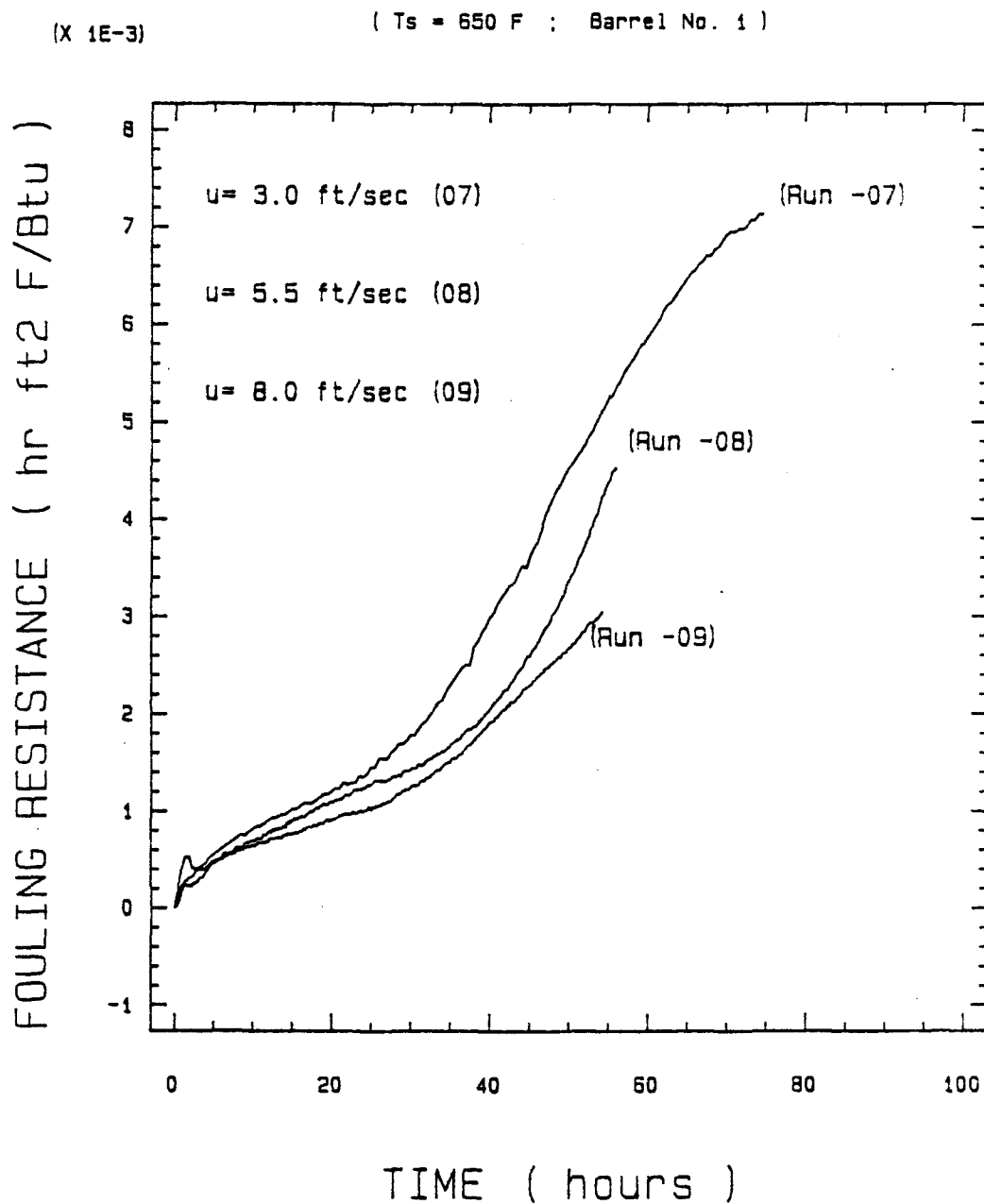


Figure 5.9 Effect of velocity on fouling from Barrel No. 1
Comparison of Runs AMO-FDC(263)-07, -08 and -09

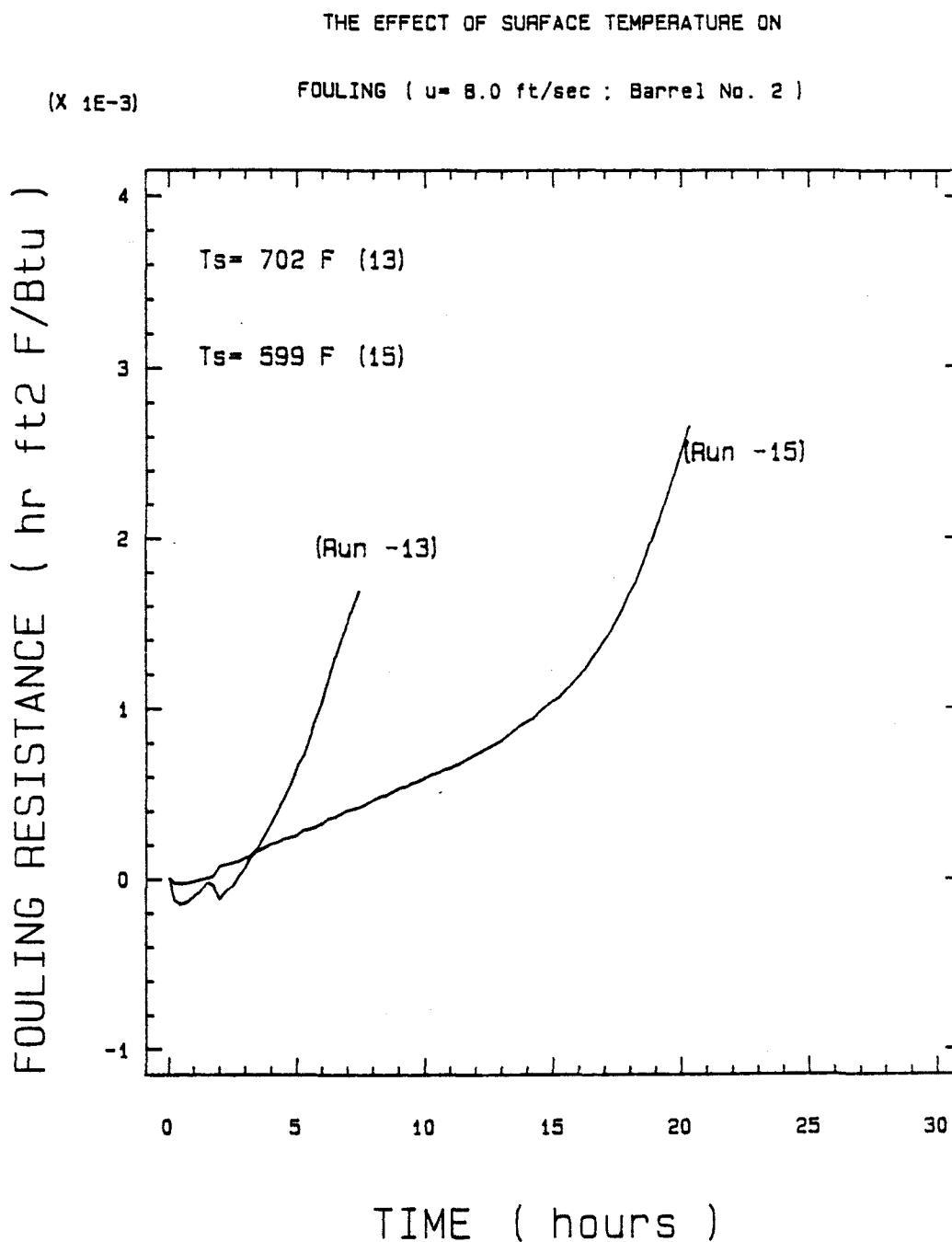


Figure 5.10 Effect of surface temperature on fouling from Barrel No. 2
Comparison of Runs AMO-FDC(263)-13 and -15

25. Runs -14 and -16 were completed on fresh samples but Run -25 utilized sample from Run -24 for which no fouling occurred. Figure 5.11 and Figure 5.10 show that the higher the surface temperature the greater the that fouling occurs.

5.2.2.2 Effect of Velocity

The effect of velocity on fouling is shown in Figure 5.12 and Figure 5.13. At $T_s = 700^\circ\text{F}$ (Figure 5.12), three tests at different velocities (3.0, 5.5 and 8.0 ft/sec) with fresh samples were conducted. As shown in Figure 5.12, fouling for Run -13 (8.0 ft/sec) was initially slow but increased rapidly and became greater than Run -10 (3.0 ft/sec) after 5.5 hours. The shape of the fouling curve is concave upward which indicates an increasing fouling rate with time. This would suggest that the chemical reaction fouling may be catalyzed by the initial deposit on the heat transfer surface. Another possible reason is that at a high surface temperature, a cracking process for some high molecular weight hydrocarbons occurs where some low molecular weight hydrocarbons (foulants) will be produced. Examining the fouling curves, fouling rates increase with time and then decrease with time as the curves reach their points of reflection. In such cases, the effect of velocity may not be consistent with the usual assumption that fouling decreases as velocity increases.

Figure 5.13 is a plot of the results from Runs -22 (3.0 ft/sec), -25 (5.5 ft/sec) and -24 (10.0 ft/sec) which were operated at $T_s = 500^\circ\text{F}$. Run -22 and Run -24 were studied on fresh samples but Run -25 utilized sample from Run -24 for which no fouling occurred after 40 hours duration. It is shown that fouling is strongly influenced by velocity at a low surface temperature. Considerable fouling occurred at 3.0 ft/sec, but no fouling was obtained at 10.0 ft/sec. At a surface temperature of 550°F , the effect of velocity on fouling is also shown in Figure 5.14. In this case, there appears to be no significant effect of velocity.

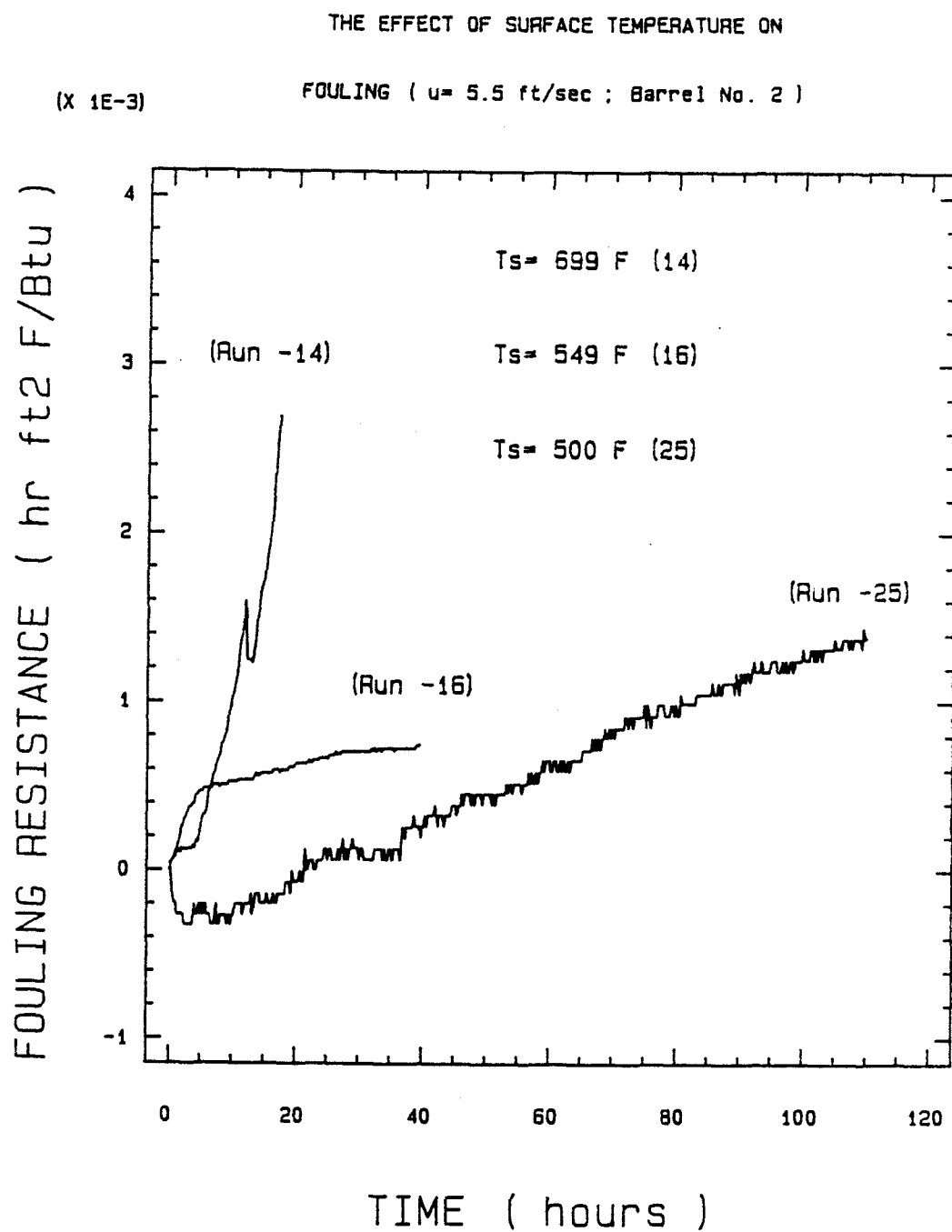


Figure 5.11 Effect of surface temperature on fouling from Barrel No.2
Comparison of Runs AMO-FDC(263)-14, -16 and -25

THE EFFECT OF VELOCITY ON FOULING

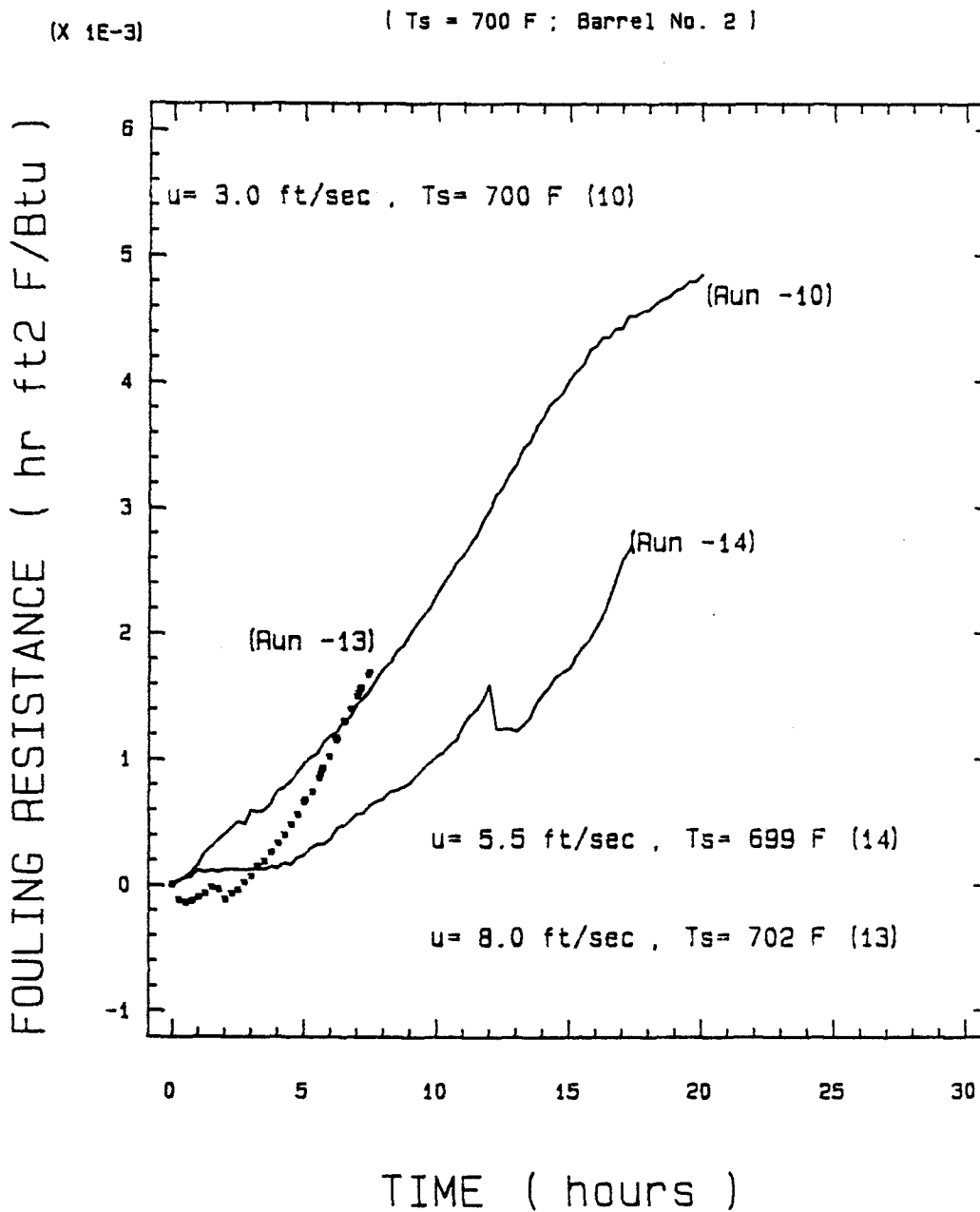


Figure 5.12 Effect of velocity on fouling from Barrel No. 2
Comparison of Runs AMO-FDC(263)-10, -13 and -14

THE EFFECT OF VELOCITY ON FOULING

(Ts = 500 F ; Barrel No. 2)

(X 1E-3)

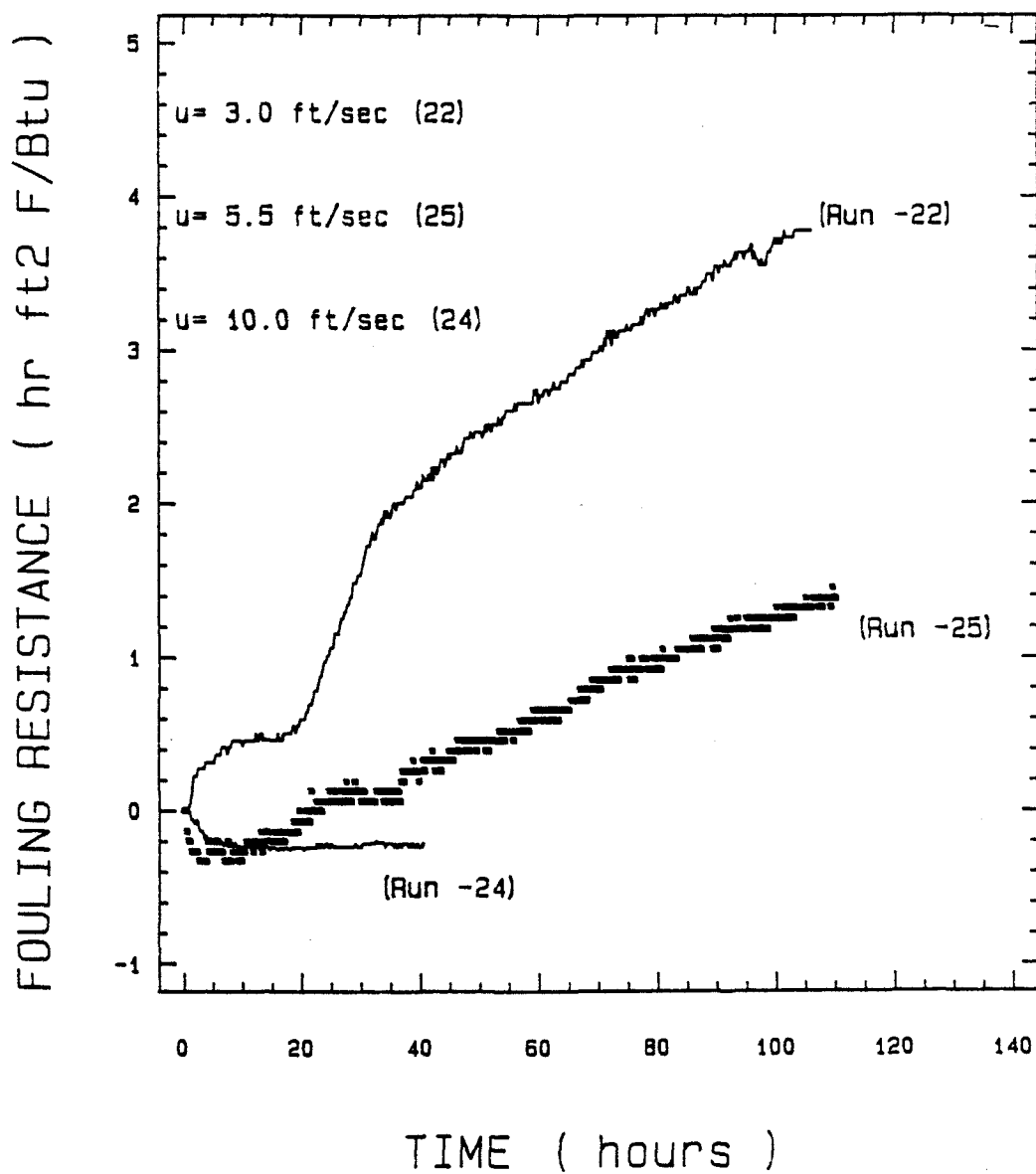


Figure 5.13 Effect of velocity on fouling from Barrel No. 2
Comparison of Runs AMO-FDC(263)-22, -24 and -25

THE EFFECT OF VELOCITY ON FOULING

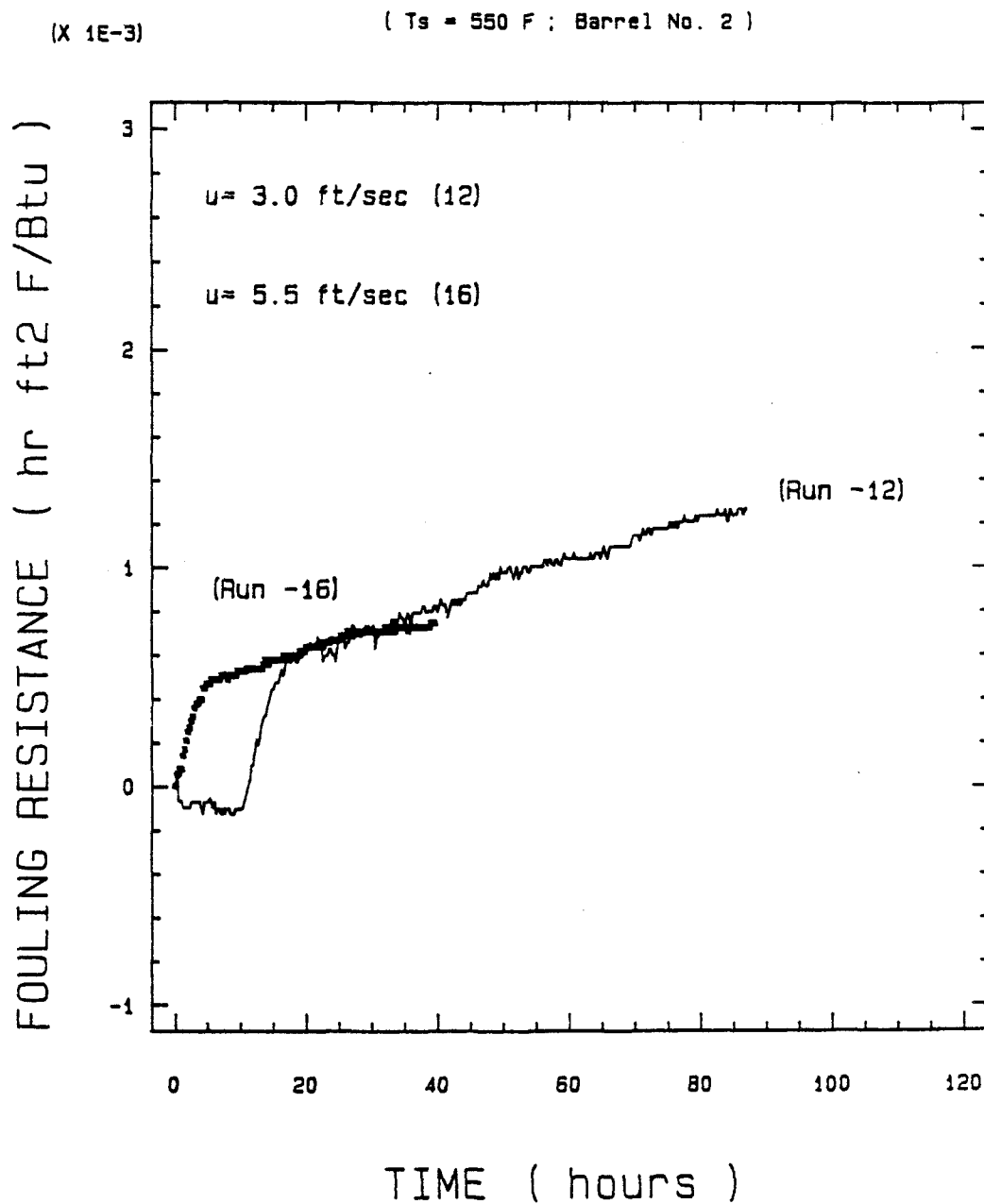


Figure 5.14 Effect of velocity on fouling from Barrel No. 2
Comparison of Runs AMO-FDC(263)-12 and -16

5.2.2.3 Determination of Threshold Fouling Temperature for Sample from Barrel No. 2

From the results of all the dry bulk tests conducted on Barrel No. 2, it is concluded that the threshold surface temperature for initial fouling ($P = 250$ psig and $T_b = 400$ °F) was between 450 and 500 °F at 3.0 and 5.5 ft/sec. At 8.0 ft/sec, a series of tests (Runs -27 through -32a) was conducted to determine the threshold surface temperature for initial fouling. The tests were operated at pressures of 30 psig (bulk temperature = 300 °F) and 155 psig (bulk temperature = 400 °F). Run -27 used fresh feed and all subsequent tests reused sample from the previous run. The circulation system was not opened until fouling occurred (Run -32). No fouling was observed at $T_s = 550$ °F but significant fouling occurred at $T_s = 600$ °F (shown in Figure 5.15). It is concluded that the initial surface temperature for fouling at 8.0 ft/sec was 550 to 600 °F. Run -32a was a repeat of Run -32 after the heater had been removed, cleaned and replaced. No fouling data were obtained because the initial heat transfer coefficient was very high (747 versus 499 for Run -32) when Run -32a was initiated, so the run was not continued.

5.2.3 Fouling Tests with Barrel No. 3

The dry bulk tests conducted on samples from Barrel No. 3 covered Runs -33 through -57. In general, four series of tests were used for the determination of the threshold surface temperature for the initiation of fouling at four different velocities of 3.0, 5.5, 8.0 and 10.0 ft/sec. The circulation system was not opened until fouling occurred.

5.2.3.1 Threshold Temperature at 8.0 ft/sec

Runs -33 through -38a repeated Runs -27 through -32a (on samples from Barrel No. 2) and were conducted at the same operating conditions. No fouling occurred until at a

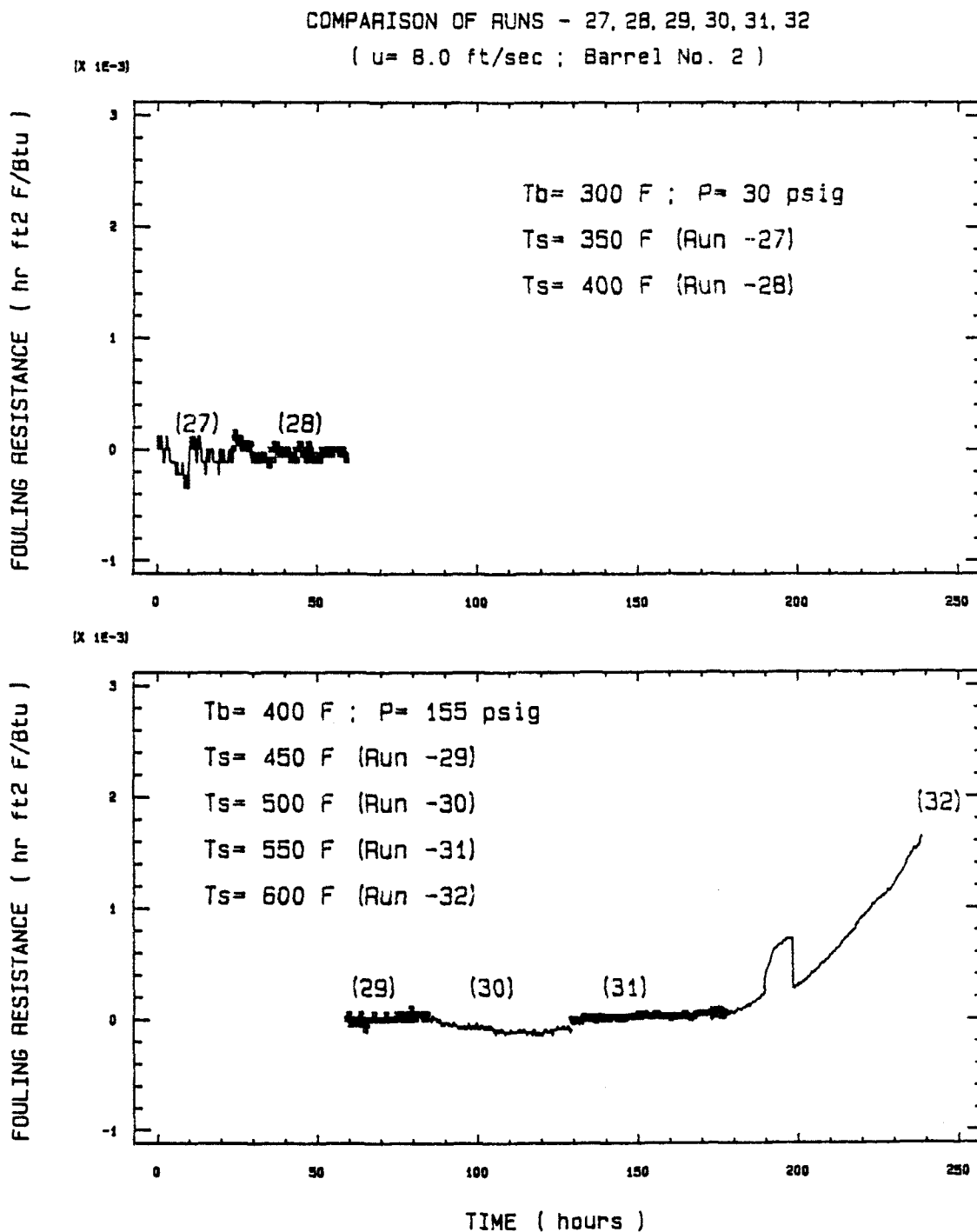


Figure 5.15 Determination of threshold fouling temperature for oil from Barrel No. 2
Comparison of Runs AMO-FDC(263)-27 through -32 (8.0 ft/sec)

surface temperature of 550 °F was reached. Fouling was very small at $T_s = 550$ °F but was significant at $T_s = 600$ °F. The results are shown in Figure 5.16. The results for this series of tests agree well with those for Runs -27 through -32a from Barrel No. 2 (shown in Figure 5.15). Run -38a was studied on sample from Run -38 and repeated Run -38 after the heater had been removed, cleaned and replaced. Regarding the initial heat transfer coefficients, the same phenomenon was observed as with Runs -32 and -32a. Run -38 had a much lower initial heat transfer coefficient than Run -38a (478 versus 717). These values are very close to those obtained for Runs -32 and 32a, respectively. The reason for these differences in the initial heat transfer coefficients is not explained but probably due to the surface condition of the heater, or the existence of fully developed nucleate boiling caused by a cracking process which would produce more low boiling components at a high surface temperature.

5.2.3.2 Threshold Temperature at 3.0 ft/sec

Runs -39 through -42 were operated at 3.0 ft/sec and were used to determine the threshold surface temperature of initial fouling for this velocity. The results of these tests are plotted in Figure 5.17. No fouling was observed at $T_s = 400$ °F but significant fouling occurred at $T_s = 450$ °F. Hence, the threshold surface temperature for fouling is between 400 and 450 °F at 3.0 ft/sec. Run -41a is a repeat of Run -41 ($T_s = 450$ °F) reusing the oil from Run -41. The fouling behaviors are nearly identical in both runs.

5.2.3.3 Threshold Temperature at 5.5 ft/sec

Runs -43 through -50 were conducted at 5.5 ft/sec and were used to determine the threshold surface temperature of fouling for this velocity. The results of this series tests are shown in Figure 5.18. No fouling was observed at a surface temperature of 524 °F (Run -48) but fouling significantly occurred at $T_s = 550$ °F (Run -49). It is also noted that very

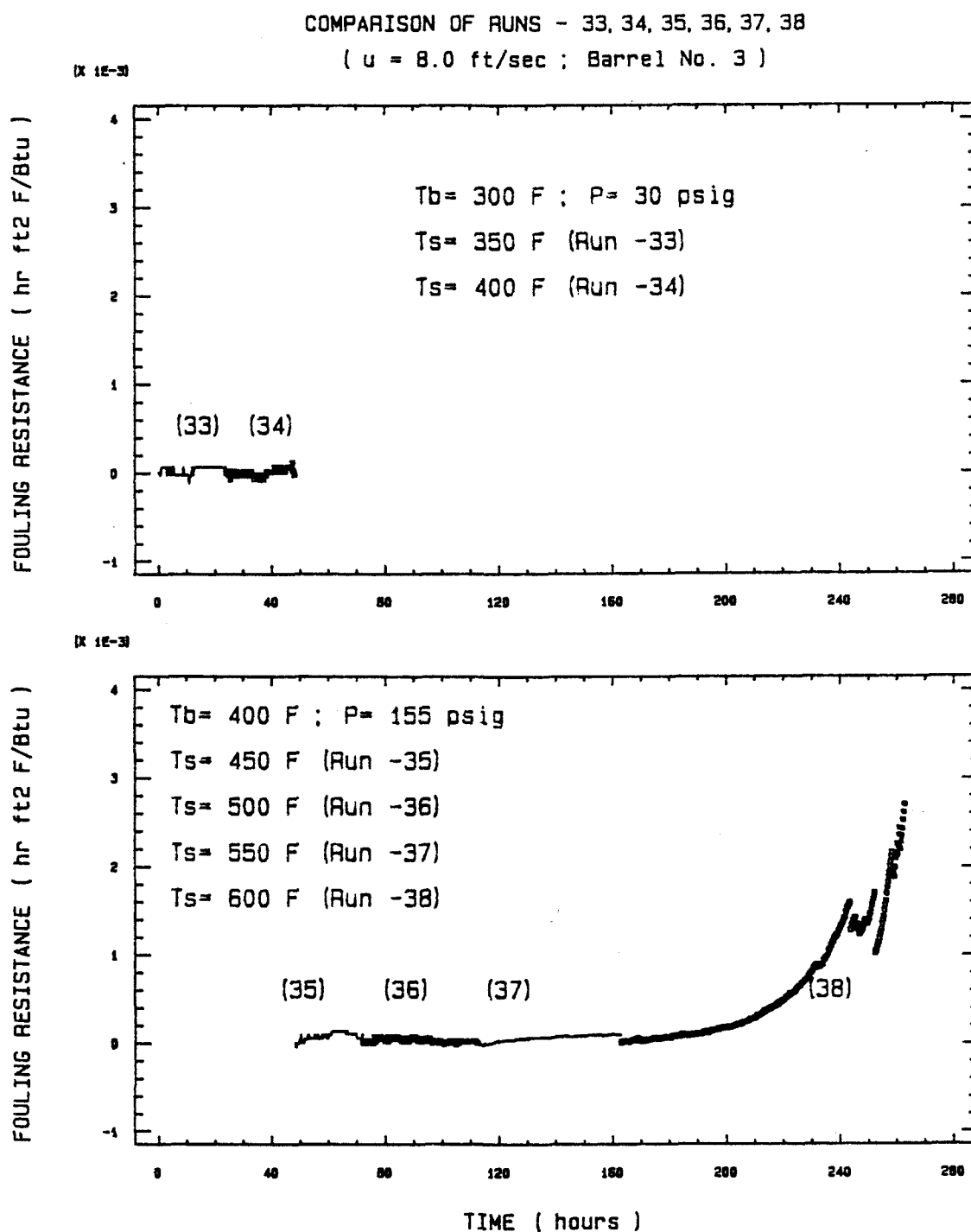


Figure 5.16 Determination of threshold fouling temperature for oil from Barrel No. 3
Comparison of Runs AMO-FDC(263)-33 through -38 (8.0 ft/sec)

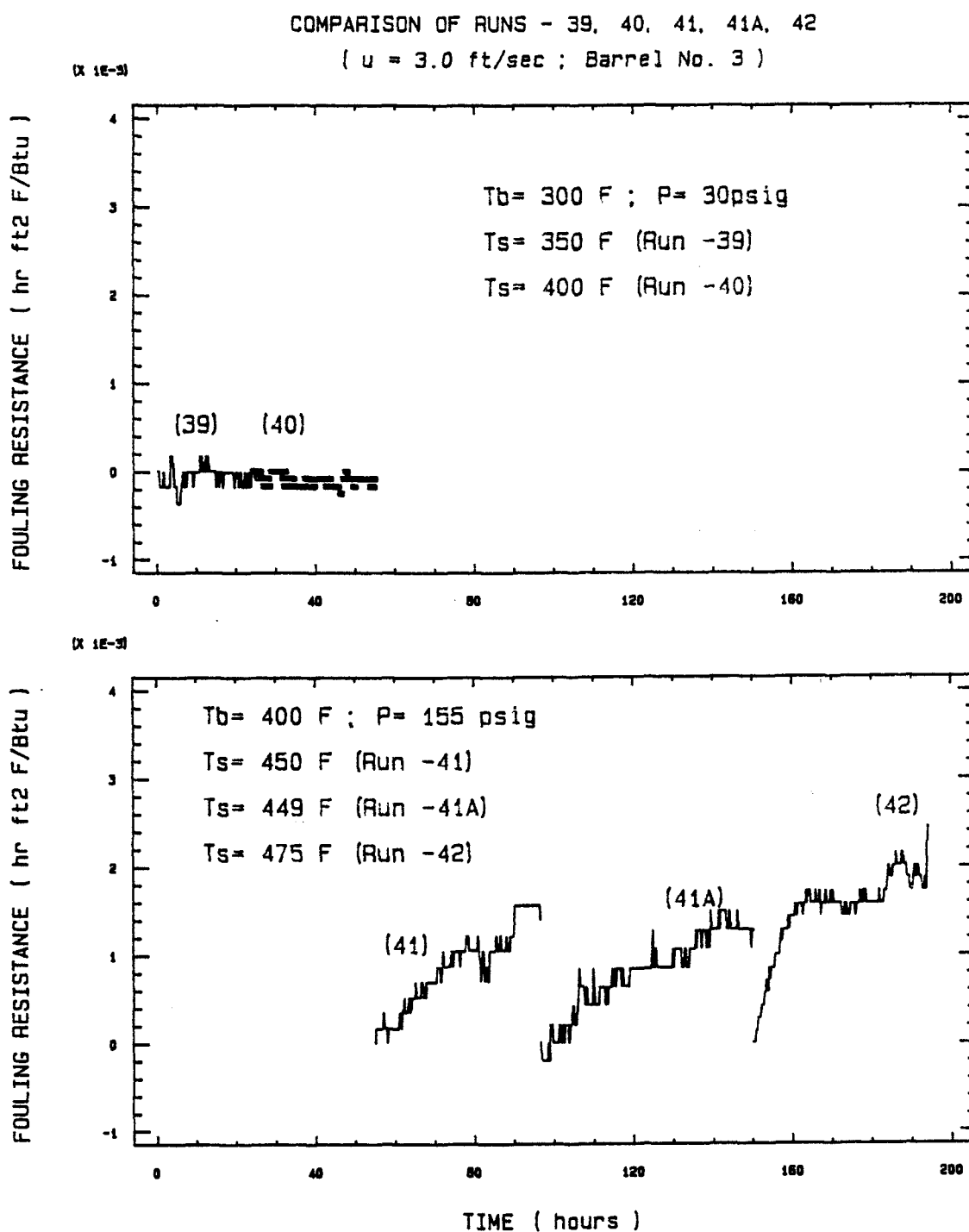


Figure 5.17 Determination of threshold fouling temperature for oil from Barrel No. 3
Comparison of Runs AMO-FDC(263)-39 through -42 (3.0 ft/sec)

large negative fouling resistances are observed in Runs -47 and -48. This phenomenon is apparently caused by a continuously increasing heat transfer coefficient (for unexplained reasons) during these two runs with no fouling or very little fouling occurring. From the results, it is concluded that the threshold surface temperature of initial fouling is between 524 and 550 °F at 5.5 ft/sec.

5.2.3.4 Threshold Temperature at 10.0 ft/sec

Runs -51 through -57 are all at 10.0 ft/sec and are used to determine the threshold surface temperature of initial fouling. The results are shown in Figure 5.19. No fouling was observed until a surface temperature of 601 °F was reached. The fouling resistance is very small (only $0.00012 \text{ hr ft}^2 \text{ °F/Btu}$) after 70 hours at $T_s = 601 \text{ °F}$ (Run -56). Significant fouling occurred at $T_s = 625 \text{ °F}$. It is concluded from this series of tests that the threshold surface temperature for initiating fouling at 10.0 ft/sec is about 600 °F.

5.2.4 Threshold Surface Temperature for Amoco Crude Oil from Barrel No.2 and Barrel No. 3

Runs -10 through -57 were conducted on samples from Barrel No. 2 and Barrel No. 3. At a pressure of 30 psig, no fouling occurred at surface temperatures of 350 and 400 °F for four different velocities (3.0, 5.5, 8.0 and 10.0 ft/sec). At a pressure of 155 psig, the threshold surface temperatures for the initiation of fouling at different velocities are as follows: 400 - 450 °F at 3.0 ft/sec, 525 - 550 °F at 5.5 ft/sec, 550 - 600 °F at 8.0 ft/sec and about 600 °F at 10.0 ft/sec. This conclusion is shown in Figure 5.20. Some tests (Runs -10 through -26) were completed at a pressure of 250 psig. The results of these tests ($P = 250 \text{ psig}$) are not significantly different from those obtained at $P = 155 \text{ psig}$.

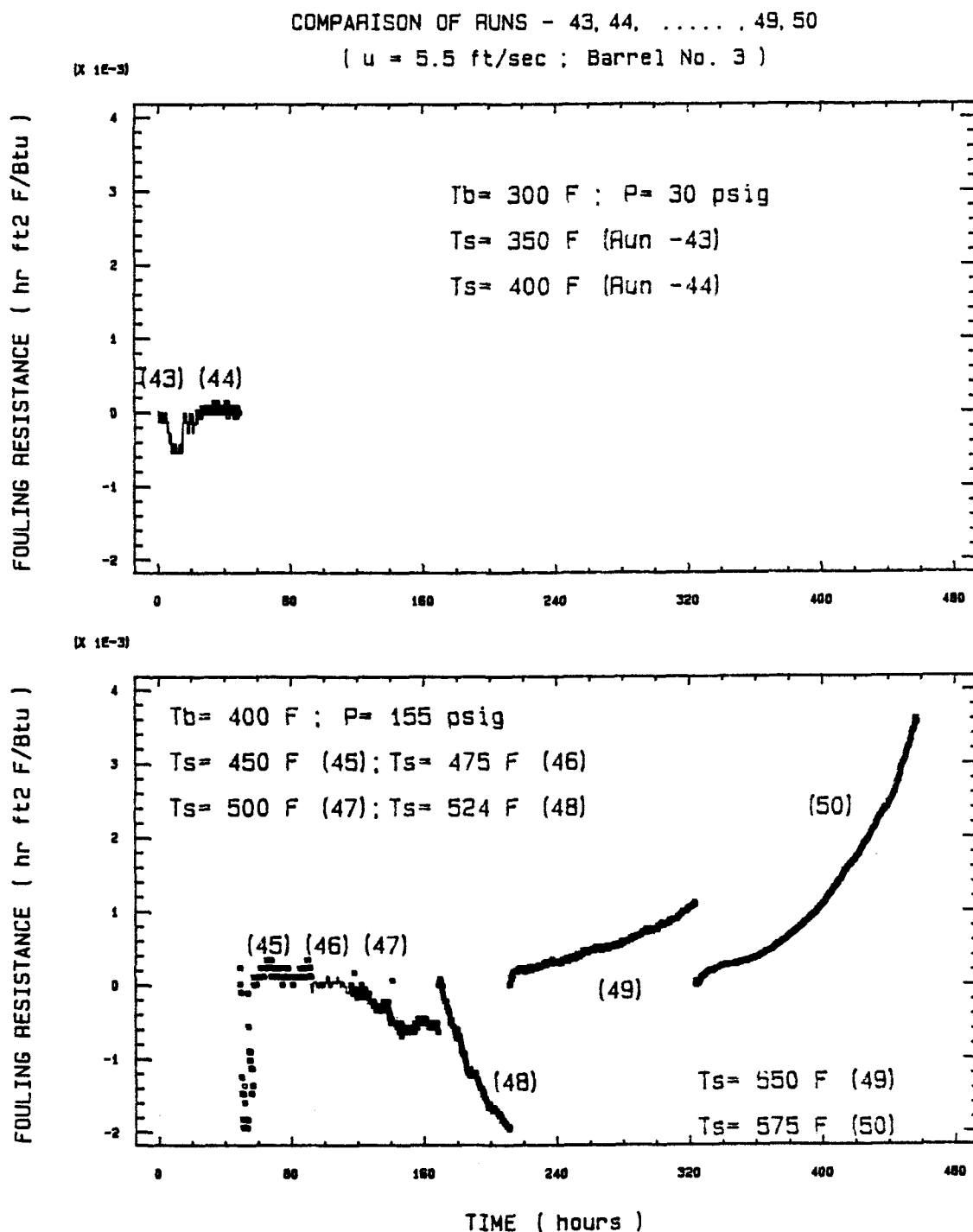


Figure 5.18 Determination of threshold fouling temperature for oil from Barrel No. 3
Comparison of Runs AMO-FDC(263)-43 through -50 (5.5 ft/sec)

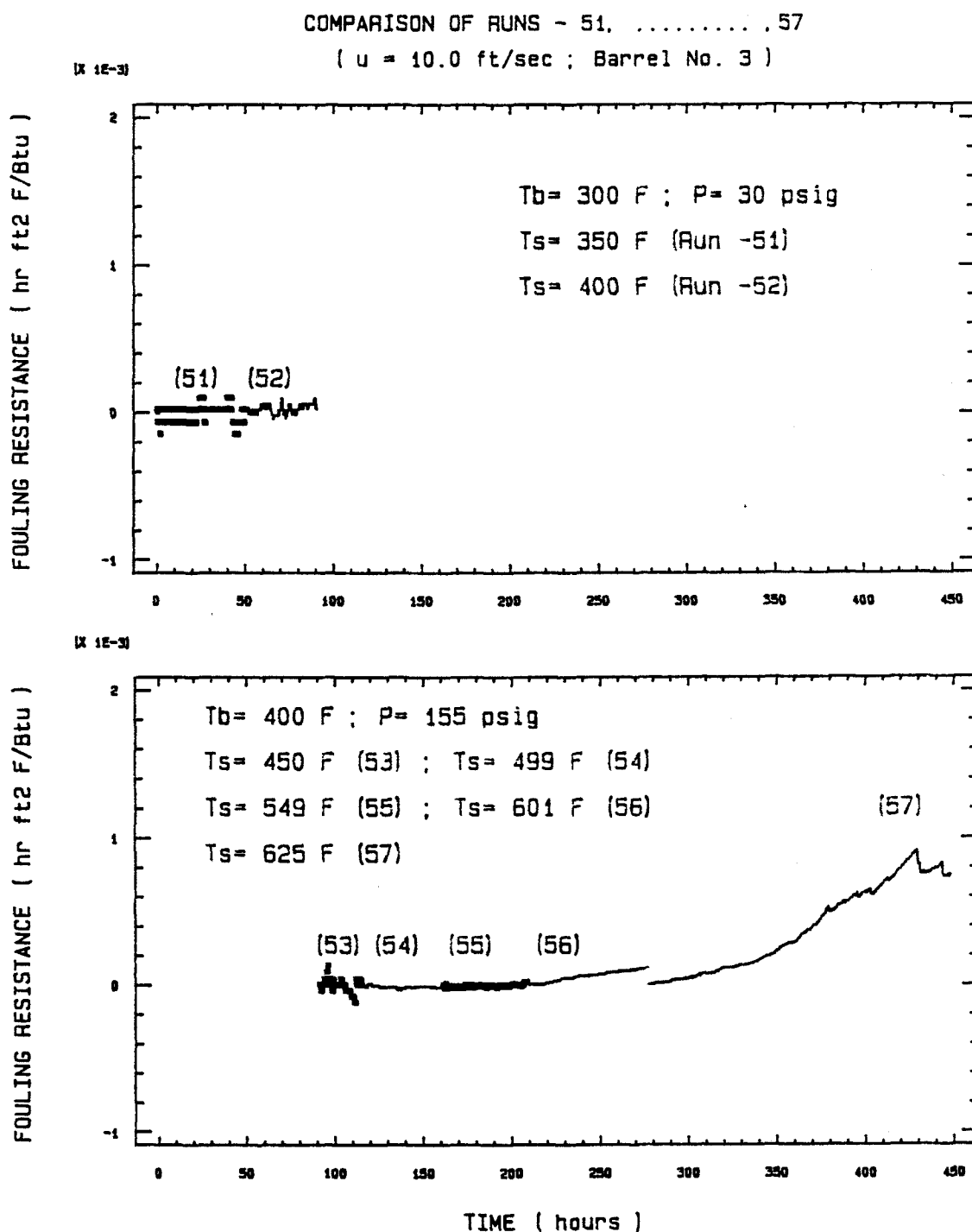


Figure 5.19 Determination of threshold fouling temperature for oil from Barrel No. 3
Comparison of Runs AMO-FDC(263)-51 through -57 (10.0 ft/sec)

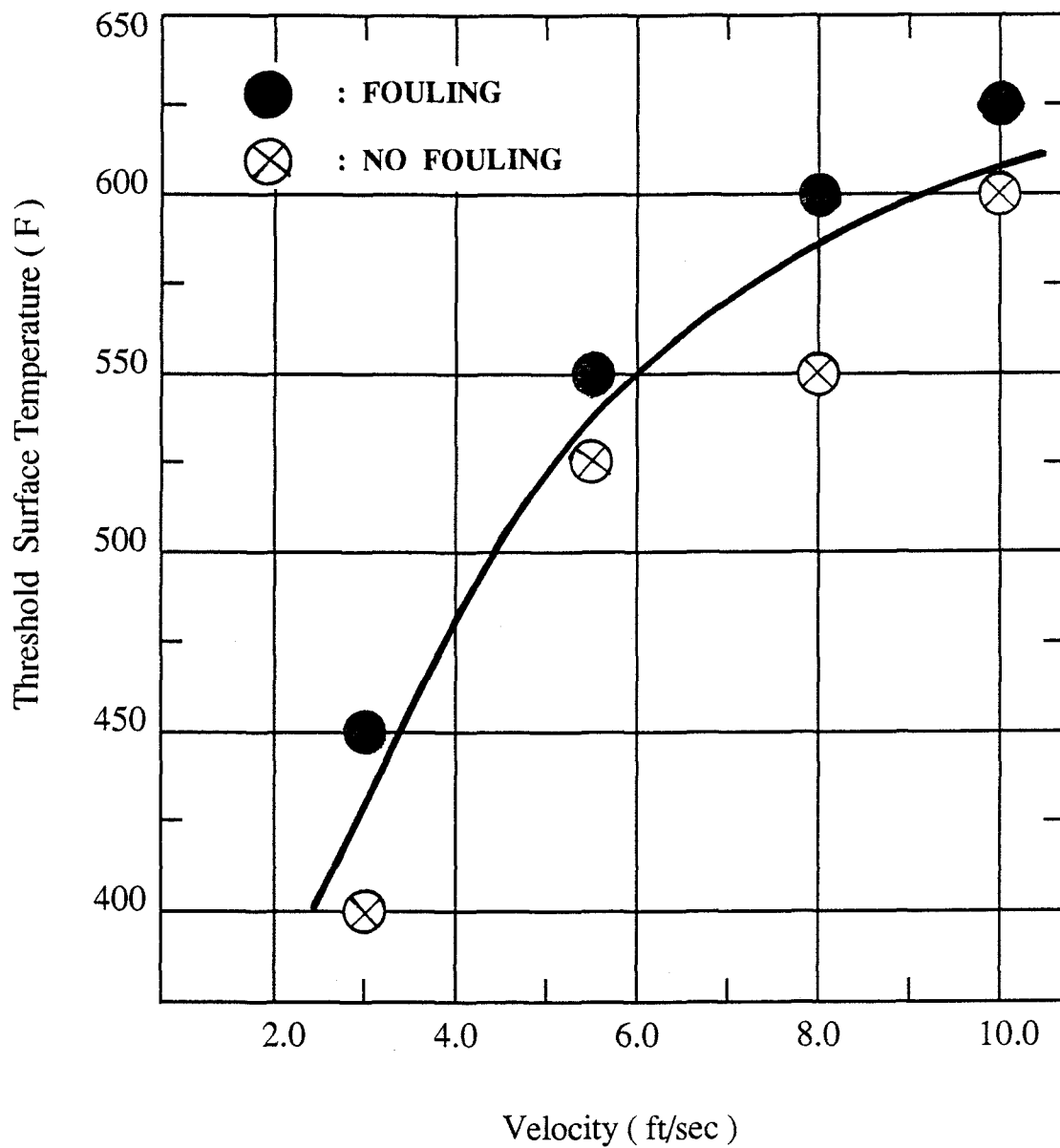


Figure 5.20 The effect of velocity on the threshold surface temperature from Barrel No. 2 and Barrel No. 3

5.3 Wet Bulk Tests on Amoco Crude Oil

Totally, 10 wet bulk tests (Runs -58 through -67) were completed on samples from Barrel No. 3. A certain amount of desalter brine supplied by Amoco Oil Company (weight percentage = 0.8 %) was added to each run. The purpose of these wet bulk tests was to determine the effect of the presence of liquid desalter brine in the crude oil. The desalter brine in the effluent from the desalter which essentially removes any brine that is in the crude oil.

The circulation system was not opened until fouling occurred. At a velocity of 5.5 ft/sec, Run -58 and Run -60 were conducted on fresh samples. Run -59, Run -61 and Run -62 reused the samples from the previous runs. Same procedures were made at 8.0 ft/sec (Runs -63 through -67), in which Runs -63 and -65 used fresh samples and the other runs were investigated on the reused samples from the previous runs. The results of these tests are shown in Figure 5.21 (5.5 ft/sec) and Figure 5.22 (8.0 ft/sec).

Table 5.4 shows a summary of the wet bulk tests. The tests are categorized as wet wall tests (given the notation -WW-) and semi-dry wall tests (given the notation -SDW-). In the wet wall tests (Runs FDC(263)-WW-58, -WW-60, -WW-63 and -WW-65), the bulk temperature of the crude oil is such that it is less than the boiling temperature of the salt-saturated brine so that the salts remain dissolved and an aqueous phase exists. Also, the weight percent of brine in the crude oil (0.8%) is greater than the water solubility in the crude oil at the surface temperature of the heater. No fouling was observed for these tests. This means that there is sufficient water present in the crude oil to keep the salts dissolved.

In the semi-dry wall tests (Runs AMO-FDC(263)-SDW-59, -SDW-61, -SDW-62, -SDW-64, -SDW-66 and -SDW-67), the bulk temperature is such that it is less than the boiling temperature of the salt-saturated brine but the weight fraction of brine in the crude oil is less than the water solubility in the crude oil at the surface temperature of the heater so

Table 5.4 Summary of wet crude tests

(Barrel No. 3) Run No.	Time (hrs)	Velocity (ft/sec)	T _s (F)	T _b (F)	P (psig)	Final Rf (*)	Remarks (**)
AMO-FDC(263)-WW-58	46.0	5.5	350	300	85	- 1.1	NF
AMO-FDC(263)-SDW-59	105.0	5.5	400	300	135	16.1	REU, F
AMO-FDC(263)-WW-60	48.0	5.5	350	300	285	0.0	NF
AMO-FDC(263)-SDW-61	92.0	5.5	400	300	285	13.2	REU, F
AMO-FDC(263)-SDW-62	72.0	5.5	425	300	285	11.1	REU, F
AMO-FDC(263)-WW-63	42.0	8.0	349	300	85	- 1.5	NF
AMO-FDC(263)-SDW-64	144.0	8.0	400	300	135	12.9	REU, F
AMO-FDC(263)-WW-65	64.0	8.0	349	300	285	-11.2	NF
AMO-FDC(263)-SDW-66	119.0	8.0	399	300	285	7.7	REU, F
AMO-FDC(263)-SDW-67	76.0	8.0	425	300	285	16.1	REU, F

* $\text{hr ft}^2 \text{ } ^\circ\text{F} / \text{Btu} \times 10^4$

** REU : Test fluid reused from previous run

NF : No fouling

F : Fouling

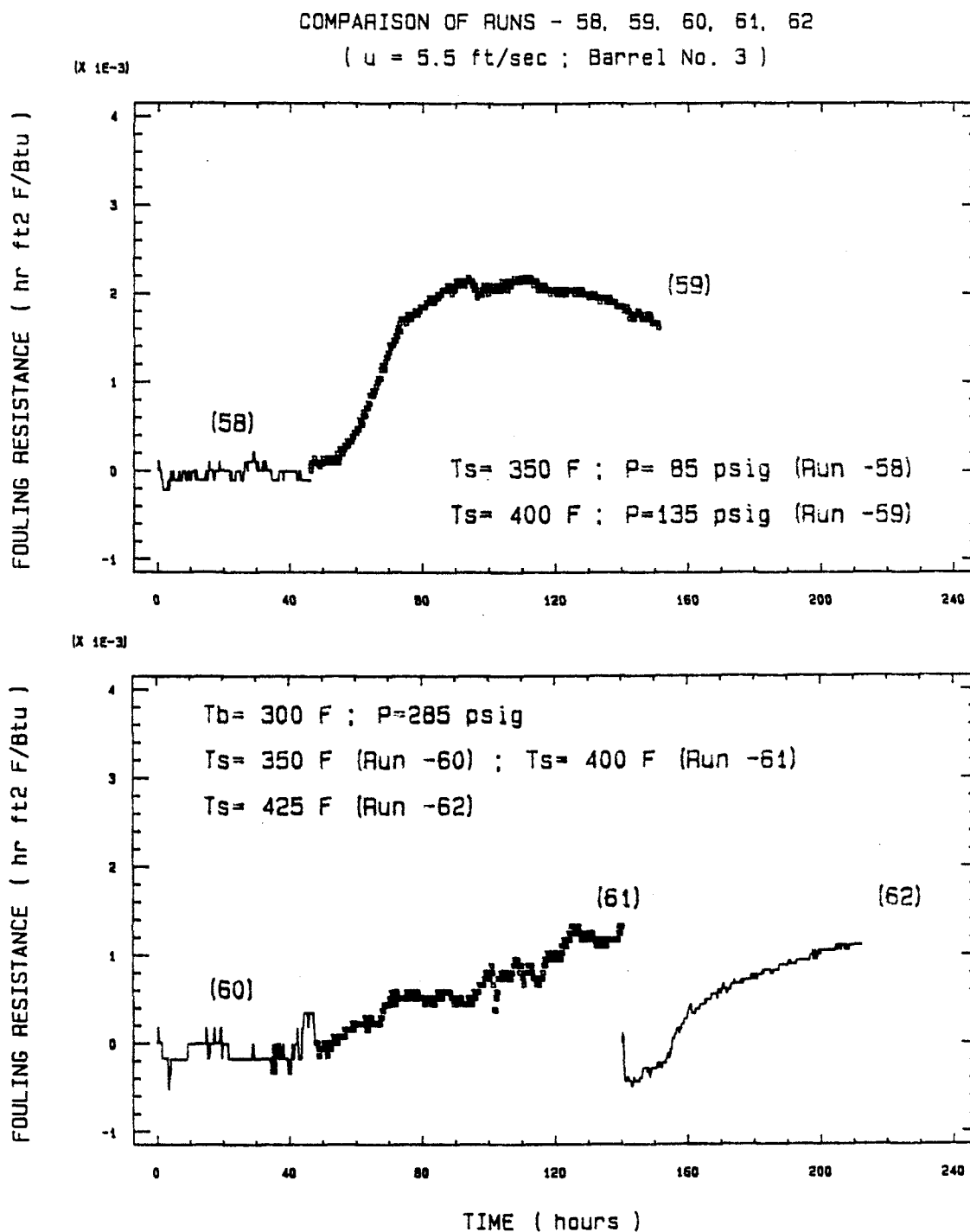


Figure 5.21 Determination of threshold fouling temperature for wet bulk test from Barrel No. 3. Comparison of Runs AMO-FDC(263)-58 through -62 (5.5 ft/sec)

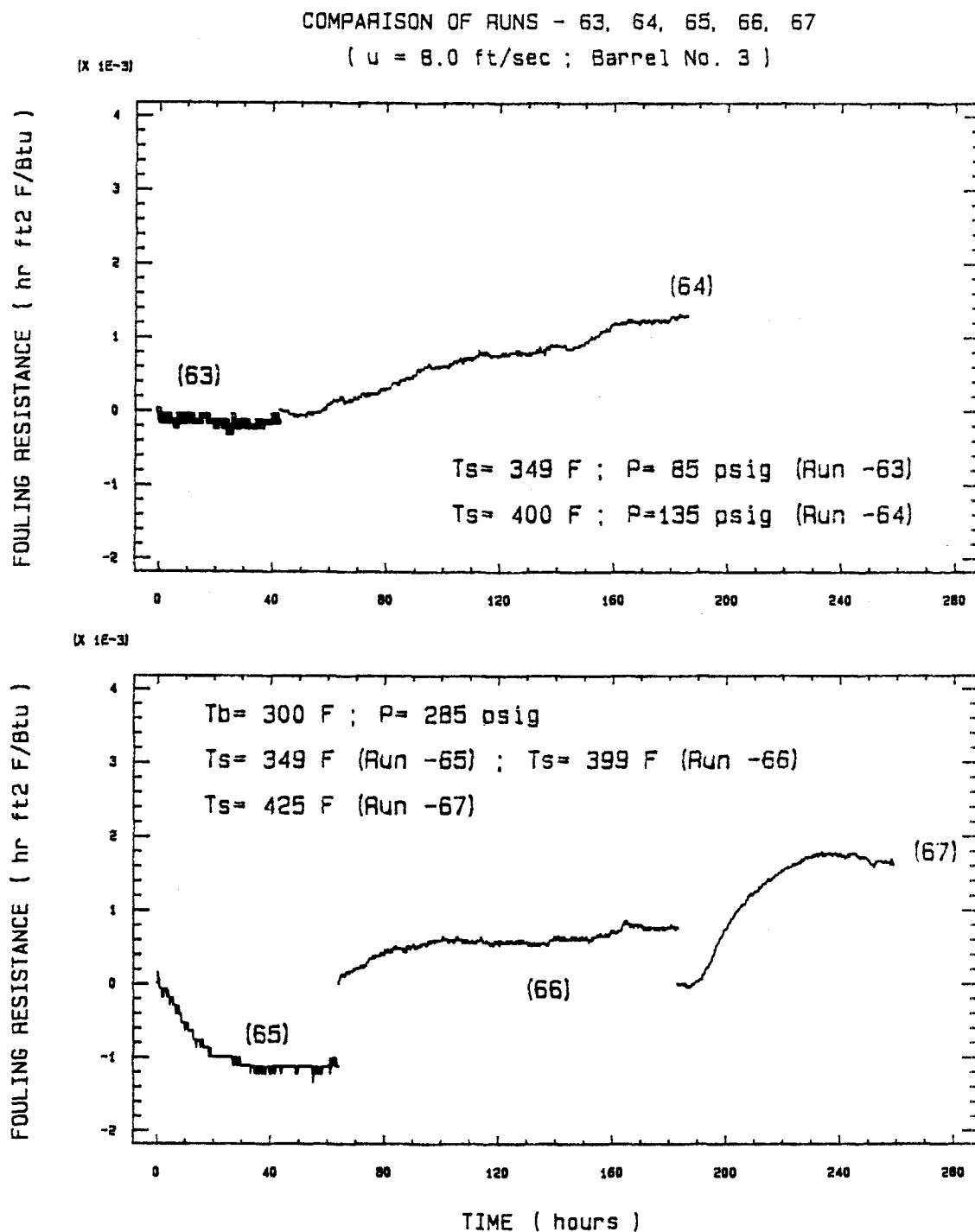


Figure 5.22 Determination of threshold fouling temperature for wet bulk test from Barrel No. 3. Comparison of Runs AMO-FDC(263)-63 through -67 (8.0 ft/sec)

that the brine is dissolved or boiled to extinction at the surface of the heater. The salts then are deposited on the heat transfer surface. Considerable fouling was observed for all of the semi-dry wall tests.

The wet bulk tests are also delineated by the condition no brine boiling at the wall (Runs -WW-60, -SDW-61, -SDW-62, -WW-65, -SDW-66 and -SDW-67) in which the heater surface temperature is less than the boiling point of the salt-saturated brine and by the brine boiling at the wall (Runs -WW-58, -SDW-61, -WW-63 and -SDW-64) in which the heater surface temperature is greater than the boiling temperature of the salt-saturated brine. In either case, no fouling occurred in the wet wall tests and significant fouling occurred in the semi-dry wall tests.

5.4 Effect of Reusing the Sample with the Dry Bulk Test

Figure 5.23 and Figure 5.24 show the effect of reusing the sample on fouling. At a velocity of 5.5 ft/sec and a surface temperature of 550 °F, a series of tests was conducted (shown in Figure 5.23) where Run -16 used fresh sample but Runs -17 and -18 reused the oil from the previous test. It was observed that fouling decreased when the sample was reused from the previous run. After 39 hours, the fouling resistance for Run -16 (fresh) is greater than those for Run -17 (reused) and Run -18 (reused). Figure 5.24 is a plot of Runs -19 through -23 which are all at 3.0 ft/sec and $T_s = 500$ °F. Run -19 was conducted on fresh sample but the circulation system was opened twice. Run -20 reused sample from a series of boiling tests (Runs -BO-13 through -BO-16) without opening the system. Run -20 could be considered to be completed on fresh feed with an assumption of no fouling occurring during the boiling tests. Run -22 was conducted on fresh oil and Runs -21 and -23 respectively reused the sample from Run -20 and Run -22. The fouling curves for Runs

COMPARISON OF RUNS - 16, 17 AND 18

(X 1E-3)

Velocity = 5.5 ft/sec ; Ts = 550 F

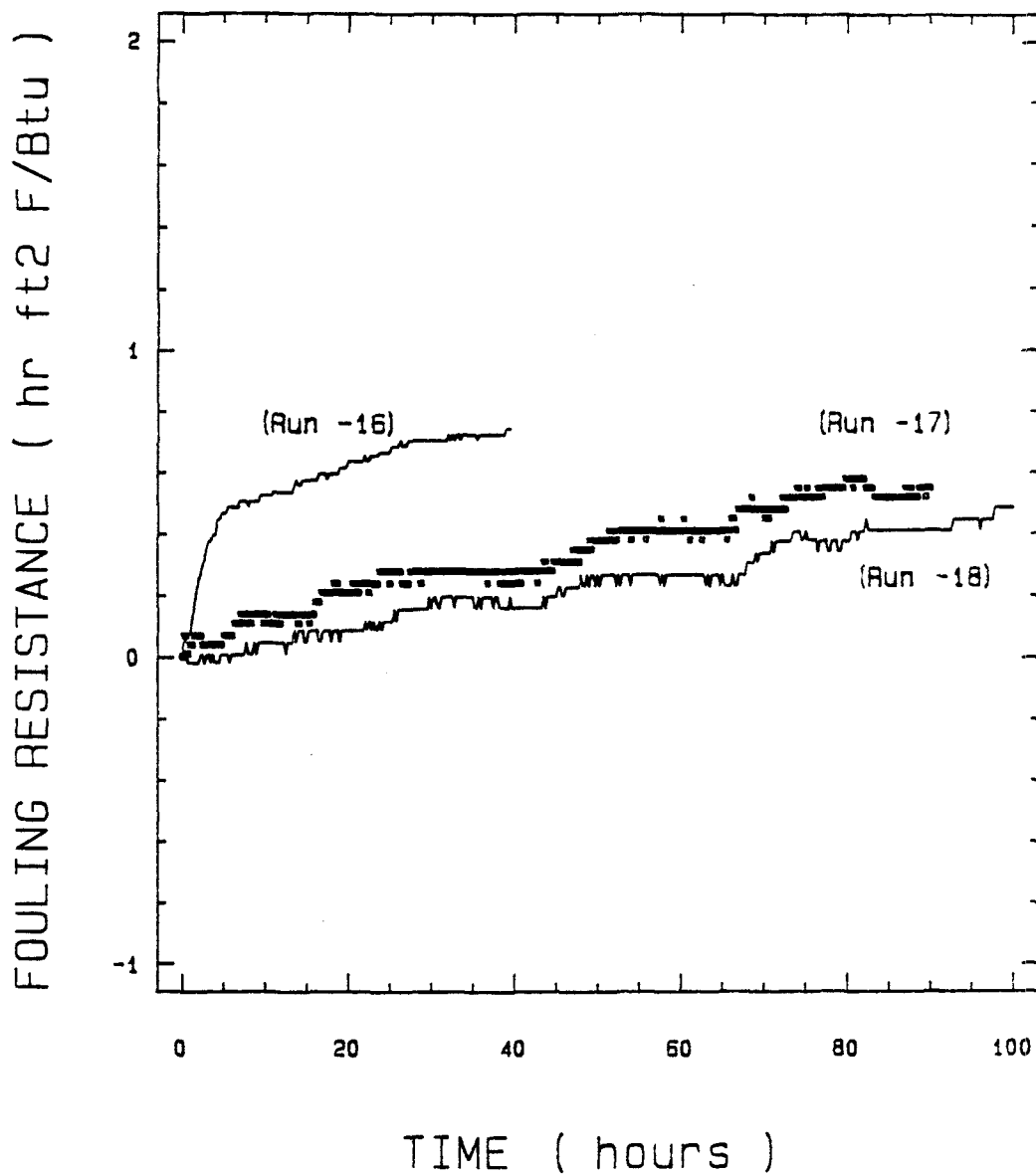


Figure 5.23 Effect of feed re-use on fouling from Barrel No. 2
Comparison of Runs AMO-FDC(263)-16, -17 and -18
(5.5 ft/sec)

COMPARISON OF RUNS -19, -20, -21, -22 & -23

(X 1E-3)

Velocity = 3.0 ft/sec ; Ts = 500 F

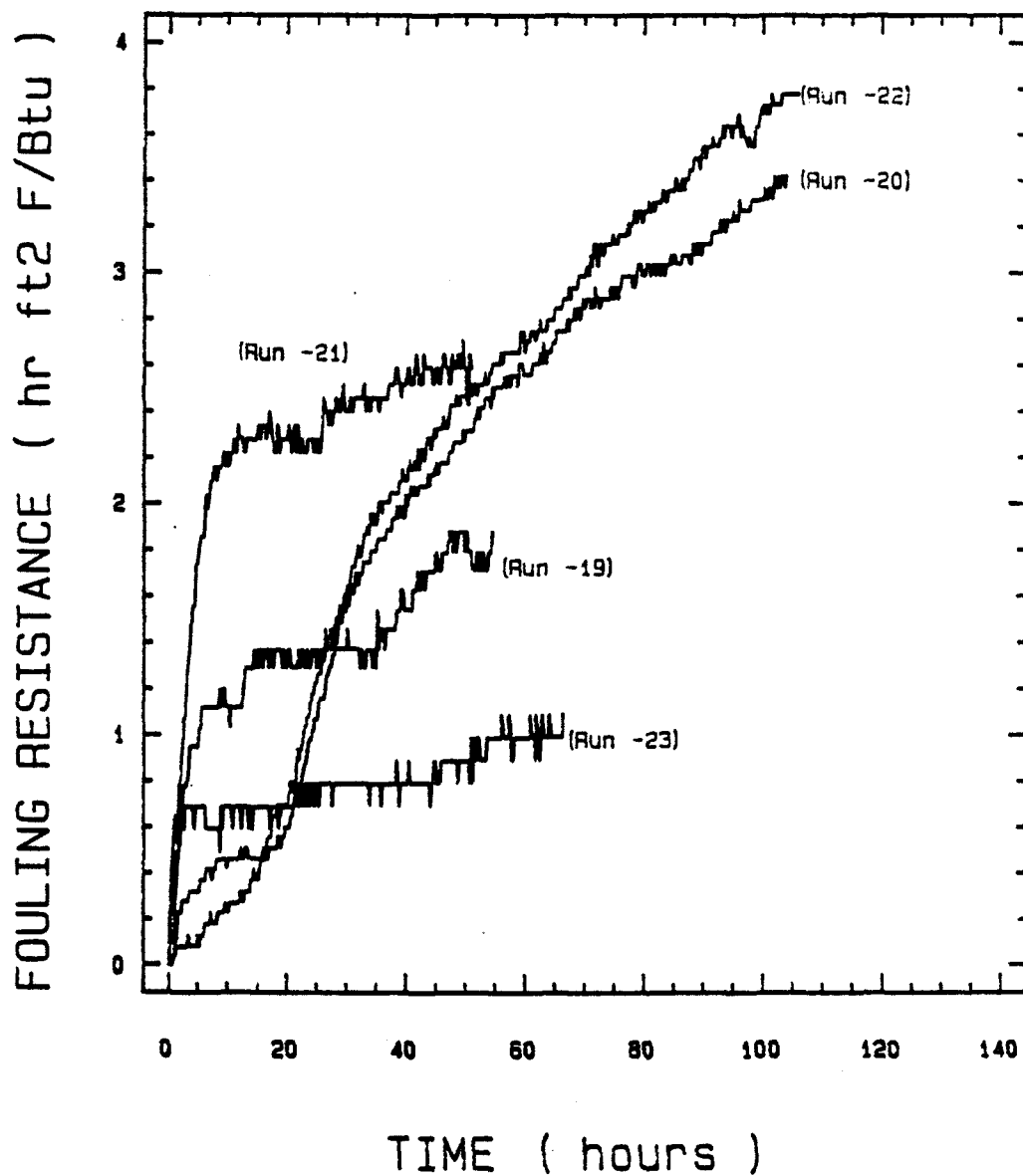


Figure 5.24 Effect of feed re-use on fouling from Barrel No. 2
Comparison of Runs AMO-FDC(263)-19 through -23
(3.0 ft/sec)

-20 and -22 (both fresh feed) are almost identical but quite different from the other three fouling curves on this figure.

There are also the differences in the initial heat transfer coefficient between fresh and reused samples. At a low surface temperature, a certain amount of low boiling point component will be lost when the system is opened. Hence, the initial heat transfer coefficient will be reduced with reusing sample. These phenomena are observed in some fouling tests which are as follows: Runs -19 (i.e., its original value is about 210), -20, -21, -22, -23 (at 3.0 ft/sec and $T_s = 500$ °F), Runs -16, -17, -18 (at 5.5 ft/sec and $T_s = 550$ °F) and Runs -41, -41a (at 3.0 ft/sec and $T_s = 450$ °F). At a higher surface temperature of 600 °F, the initial heat transfer coefficients were increased for Runs -32a and -38a which were conducted on reused samples from Runs -32 and -38. Although the circulation system is opened (some low boiling point components will be lost), the initial heat transfer coefficient is found to be much greater than the value obtained in the previous run. This phenomenon is probably caused by a cracking process (usually occurs at high temperatures) which will produce some low boiling point components during a fouling test. Hence, total amounts of low boiling point components will be increased even though a certain amount of these is lost when the system is opened.

5.5 Fouling Deposit Characteristics

The fouling deposit was a thin, carbonaceous layer on the heat transfer surface. The fouling deposit near the heat transfer surface is harder and more difficult to remove than the deposit near the liquid-solid interface. For the dry bulk tests, the fouling deposit is softer and easier to remove when operating at a low surface temperature than when operating at a high surface temperature even though the fouling resistances for both runs may be the same. In general, Lacquer Thinner dissolves most parts of the fouling deposits.

may be the same. In general, Lacquer Thinner dissolves most parts of the fouling deposits. It is difficult to remove the harder parts of deposits near the heater surface although it can be removed with wet/dry sand paper.

For the wet bulk tests, the fouling deposits were all hard for six runs for which fouling occurred. The deposits contained some white deposits near the heater surface. This phenomenon is quite different from the dry bulk test. The white deposits are probably caused by the precipitation of inorganic salts dissolved in brine.

CHAPTER 6

CONCLUSIONS AND RECOMMENDATIONS

6.1 Conclusions

The fouling behavior of Amoco Crude Oil (FDC.263, 400+) were investigated in this study. The effects of fluid velocity, surface temperature and brine on chemical reaction fouling have been studied. A systematic investigation was also undertaken to determine the threshold surface temperature for the initiation of fouling at different velocities. As a consequence of the discussions in Chapter 5, it is concluded as follows:

1. Fouling appears to be strongly affected by minor (almost indistinguishable) difference in the test fluid. At $u = 3.0$ ft/sec and $T_s = 500$ °F, significant fouling was obtained for crude oil from Barrel No. 2 but no fouling occurred for crude oil from Barrel No. 1.
2. With one exception, fouling was found to decrease with an increase of fluid velocity. The effect of velocity on fouling is specially strong at lower surface temperatures but becomes weaker at higher surface temperatures (above the threshold surface temperature for the initiation of fouling).
3. The higher the surface temperature greater the fouling was obtained at each velocity in all cases.
4. For Barrel No. 2 and Barrel No. 3, the threshold surface temperatures for the initiation of fouling are 400 - 450 °F (3.0 ft/sec), 525 - 550 °F (5.5 ft/sec), 550 - 600 °F (8.0 ft/sec) and 600 - 625 °F (10.0 ft/sec). For Barrel No. 1, the threshold temperatures are about 550 °F (3.0 ft/sec) and 600 °F (5.5 ft/sec).

5. In general, sample reused from a previous test in which fouling occurred shows less fouling when tested at the same conditions. The initial heat transfer coefficient is usually lower as well.
6. The initial shape of the fouling curves is generally concave upward which indicates fouling rates increase with time. This is probably due to a catalytic reaction on the heat transfer surface or a change of composition (caused by a cracking process) during the fouling test.
7. For the 10 wet bulk tests conducted in which desalter brine is added to the crude oil, no fouling was observed during the wet wall tests ($w > S_g$). However, significant fouling was observed for the semi-dry wall tests ($w < S_g$). For the wet wall tests, the salt in the brine remains in solution. For the semi-dry wall tests, the brine is dissolved or boiled to extinction at the wall and the salt is deposited on the wall.

6.2 Recommendations for Future Work

In order to make this investigation more complete, some recommendations for future work are as follows:

1. Repeat the fouling study at different bulk temperatures. This investigation will show the effect of bulk temperature on fouling.
2. The effect of boiling on fouling is still not well known for the dry bulk test. In order to determine the boiling effect, repeat the fouling tests with a high system pressure where no boiling occurs.
3. Repeat the wet bulk test changing the brine percentage in the crude oil. It may probably give more detailed information for the wet wall test and the semi-dry wall test.

4. It is also recommended to use heater rods with different diameters or different heated lengths (more than 3 inches) in further study.

BIBLIOGRAPHY

1. Standards of The Tubular Exchanger Manufacturers Association (T.E.M.A.), 7th Ed., New York, 1988.
2. Somerscales, E.F.C., "Fouling of Heat Transfer Surfaces: An Historical Review", Heat Transfer Eng., vol. 11, no. 1, pp. 19-36, 1990
3. Taborek, J., Aoki, T., Ritter, R.B., Palen, J.W. and Knudsen, J.G., "Fouling: The Major Unsolved Problem in Heat Transfer", Chem. Eng. Prog., vol. 68, no. 2, pp. 59-67, 1972.
4. Taborek, J., Aoki, T., Ritter, R.B., Palen, J.W. and Knudsen, J.G., "Predictive Methods for Fouling Behavior", Chem. Eng. Prog., vol. 68, no. 7, pp. 69-78, 1972.
5. Knudsen, J.G., "Fouling of Heat Exchangers: Are We Solving the Problem?", Chem. Eng. Prog., vol. 80, no. 2, pp. 63-69, 1984.
6. Pritchard, A.M., "Fouling - Science or Art ? An Investigation of Fouling and Antifouling Measures in the British Isles", in Fouling of Heat Transfer Equipment, Somerscales, E.F.C., and Knudsen, J.G., (eds), Hemisphere, Washington, pp. 513-523, 1981.
7. Van Nostrand, W.L., Leach, S.H., and Haluska, J.L., "Economic Penalties Associated with the Fouling of Refinery Heat Transfer Equipment", in Fouling of Heat Transfer Equipment, Somerscales, E.F.C. and Knudsen, J.G., (eds), Hemisphere, Washington, pp. 619-643, 1981.
8. Smith, S.A. and Driks, J.A., "Costs of Heat Exchanger Fouling in the U.S. Industrial Sector", in Industrial Heat Exchangers, Hayes, A.J., Liang, W.W., Richlen, S.L. and Tabb, E.S., (eds), American Society for Metals, pp. 339-344, 1985.
9. Lemmert, M. and Chawla, J.M., "Influence of Flow Velocity on Surface Boiling Heat Transfer Coefficient", in Heat Transfer in Boiling, Hahne, E. and Grigull, U., (eds),

- Hemisphere, Washington, pp. 237-247, 1977.
10. Kenning, D.B.R. and Hewitt, G.F., "Boiling Heat Transfer in the Annular Flow Regime", Proc. 8th Int. Heat Transfer Conf., vol. 5, pp. 2185-2190, 1986.
 11. Steiner, D. and Ozawa, M., "Flow Boiling Heat Transfer in Horizontal Vertical Tubes" in Heat Exchangers Theorey and Prattice, Taborek, J., Hewitt, G.F. and Afgan, N., (eds), Hemisphere, Washington, pp. 19-34, 1983.
 12. Berenson, P.J., "Experiments on Pool-Boiling Heat Transfer", Int. J. Heat Mass Transfer, vol. 5, pp. 985-999, 1962.
 13. Roy Chowdhury, S.K. and Winterton, R.H.S., "Surface Effects in Pool Boiling", Int. J. Heat Mass Transfer, vol. 28, no. 10, pp. 1881-1889, 1985.
 14. Insinger, T.H., Jr and Bliss, H., "Transmission of Heat to Boiling Liquids", Tran. Am. Inst. Chem. Engrs., 36, pp. 491-516, 1940.
 15. Al-Roubaie, S.M.A., Burton, H. and Skudder, P.J., "The Effect of Surface Tension on the Deposition of Solids from Milk on Heated Surfaces", in Fouling of Heat Transfer Equipment, Somerscales, E.F.C. and Knudsen, J.G., (eds), Hemisphere, Washington, pp. 477-482, 1981.
 16. Epstein, N., "Fouling in Heat Exchangers", in Fouling of Heat Transfer Equipment, Somerscales, E.F.C. and Knudsen, J.G., (eds), Hemisphere, Washington, pp. 701-743, 1981.
 17. Hasson, D., "Precipitation Fouling", in Fouling of Heat Transfer Equipment, Somerscales, E.F.C. and Knudsen, J.G., (eds), Hemisphere, Washington, pp. 527-568, 1981.
 18. Marschall, E., "Precipitation Fouling", in Fouling of Heat Transfer Equipment, Somerscales, E.F.C. and Knudsen, J.G., (eds), Hemisphere, Washington, pp. 689-693, 1981.
 19. Gudmundsson, J.S., "Particulate Fouling", in Fouling of Heat Transfer Equipment, Somerscales, E.F.C. and Knudsen, J.G., (eds), Hemisphere, Washington, pp. 357-

- 387, 1981.
20. Beal, S.K., "Particulate Fouling", in Fouling of heat Transfer Equipment, Somerscales, E.F.C. and Knudsen, J.G., (eds), Hemisphere, Washington, pp. 675-679, 1981.
 21. Bott, T.R., "Fouling Due to Solidification", in Fouling of Heat Transfer Equipment, Somerscales E.F.C. and Knudsen, J.G., (eds), Hemisphere, Washington, pp. 201-226, 1981.
 22. Lund, D. and Sandu, C., "Chemical Reaction Fouling Due to Foodstuffs", in Fouling of Heat Transfer Equipment, Somerscales, E.F.C. and Knudsen, J.G., (eds), Hemisphere, Washington, pp. 437-476, 1981.
 23. Froment, G.F., "Fouling of Heat Transfer Surfaces by Coke Formation in Petrochemical Reactors", in Fouling of Heat Transfer Equipment, Somerscales, E.F.C. and Knudsen, J.G., (eds), Hemisphere, Washington, pp. 411-436, 1981.
 24. Lister, D.H., "Corrosion Products in Power Generating Systems", in Fouling of Heat Transfer Equipment, Somerscales, E.F.C. and Knudsen, J.G., (eds), Hemisphere, Washington, pp. 135-200, 1981.
 25. Somerscales, E.F.C., "Corrosion Fouling", in Fouling in Heat Exchanger Equipment, Chenoweth, J.M. and Impagliazzo, M., (eds), A.S.M.E., HTD-vol.17, pp. 17-27, 1981.
 26. Characklis, W.G., "Microbial Fouling: A Process Analysis", in Fouling of Heat Transfer Equipment, Somerscales, E.F.C. and Knudsen, J.G., (eds), Hemisphere, Washington, pp. 251-291, 1981.
 27. Watkinson, A.P., "Final Report: Critical Review of Organic Fluid Fouling", Energy and Environmental Systems Division, Argonne National Laboratory, Illinois, 1988.
 28. Watkinson, A.P. and Epstein, N., "Particulate Fouling of Sensible Heat Exchangers", Proc. 4th Int. Heat Transfer Conf., vol.1, p. HE 1.6, 1970.
 29. Scarborough, C.E., Cherrington, D.C., Diener, R. and Golan, L.P., "Coking of Crude Oil at High Heat Flux Levels", Chem. Eng. Prog., vol. 75, no. 7, pp. 41-46, 1979.

30. Oufer, L., "Fouling Characteristics of Organic Fluids", Ph.D. Thesis in Chemical Engineering, Oregon State University, Corvallis, OR 97331, February 1990.
31. Smith, J.D., "Fuel for the Supersonic Transport - Effects of Deposits on Heat Transfer to Aviation Kerosine", IEC Proc. Des. Dev., vol. 8, no. 3, pp. 299-308, 1969.
32. Vranos, A., Marteney, P.J. and Knight, B.A., "Determination of Coking Rate in Jet Fuel", in Fouling of Heat Transfer Equipment, Somerscales, E.F.C. and Knudsen, J.G., (eds), Hemisphere, Washington, pp. 489-499, 1981.
33. Crittenden, B.D., Hout, S.A. and Alderman, N.J., "Model Experiments of Chemical Reaction Fouling", Chem. Eng. Res. Des., vol. 65, pp. 165-170, 1987.
34. Hausler, R.H. and Thalmeyer, C.E., "Fouling and Corrosion in Feed Effluent Exchangers - Discussion of a Test Method", Proc. Am. Pet. Inst. Refining Dept., vol. 54, p. 163, 1975.
35. Eaton, P. and Lux, R., "Laboratory Fouling Test Apparatus for Hydrocarbon Feedstocks", in Fouling in Heat Exchanger Equipment, Suitor, J.W. and Pritchard, A.M., (eds), A.M.S.E., HTD-vol. 35, pp. 33-42, 1984.
36. Crittenden, B.D. and Kthater, E.M.H., "Fouling from Vaporizing Kerosene", in Fouling in Heat Exchanger Equipment, Suitor, J.W. and Pritchard, A.M., (eds), A.M.S.E., HTD-vol. 35, pp. 57-64, 1984.
37. Somerscales, E.F.C., "Introduction and Summary: The Fouling of Heat Transfer Equipment", in Fouling of Heat Transfer Equipment, Somerscales, E.F.C. and Knudsen, J.G., (eds), Hemisphere, Washington, pp. 1-27, 1981.
38. Epstein, N., "Fouling of Heat Exchangers", in Heat Exchanger - Theory and Practice, Taborek, J., Hewitt, G.F. and Afgan, N., (eds), Hemisphere, Washington, pp. 795-815, 1983.
39. Epstein, N., "Thinking about Heat Transfer Fouling: A 5x5 Matrix", Heat Transfer Eng., vol. 4, no. 1, pp. 43-56, 1983.
40. Watkinson, A.P., "Chemical Reaction Fouling of Organic Fluids", in Fouling von

- Wärmeübertragungsflächen (Fouling of Heat Exchanger Surfaces), Bohnet, M., (preprints), GVC·VDI- Gesellschaft Verfahrenstechnik und Chemieingenieurwesen, Postfach 11 39, D-4000 Dusseldorf 1, West Germany, pp. 4.1 - 4.20, April 1990.
41. Crittenden, B.D., Kolaczowski, S.T/ and Hout, S.A., "Modeling Hydrocarbon Fouling", Chem. Eng. Res. Des., vol. 65, pp. 171-179, 1987.
 42. Nelson, W.L., "Fouling of Heat Transfer Exchangers", Refiner and Natural Gasoline Manufacturer, vol. 13, no. 8, pp. 273-298, 1934.
 43. Sundaram, K.M. and Froment, G.F., "Kinetics of Coke Deposition in the Thermal Cracking of Propane", Chem. Eng. Sci., vol. 34, pp. 635-644, 1979.
 44. Crittenden, B.D. and Kolaczowski, S.T., "Mass Transfer and Chemical Kinetics in Hydrocarbon Fouling", Proc. Conf. Fouling - Science or Art ? Inst. Corr. Sci. and Tech./IChemE, pp. 169-187, 1979.
 45. Paterson, W.R. and Fryer, P.J., "A Reaction Engineering Approach to the Analysis of Fouling", Chem. Eng. Sci., vol. 43, no. 7, pp. 1714-1717, 1988.
 46. Bott, T.R. and Gudmundsson, J.S., "Ripped Sillica Deposit in Heat Exchanger Tubes", 6th Int. Heat Transfer Conf., Hemisphere, Washington, vol. 4, pp. 373-378, 1978.
 47. Hasson, D., "Scale Prevention by Annular Flow of an Immiscible Liquid along the walls of a Heated Tube", 6th Int. Heat Transfer Conf., Hemisphere, Washington, vol. 4, pp. 391-396, 1978.
 48. Turakhia, M., Characklis, W.G. and Zelter, N., "Fouling of Heat Exchanger Surface: Measurement and Diagnosis", Heat Transfer Eng., vol. 5, pp. 93-100, 1984.
 49. Crittenden, B.D. and Alderman, N.J., "Negative Fouling Resistance: The Effect of Surface Roughness", Chem. Eng. Sci., vol. 43, no. 4, pp. 829-839, 1988.
 50. Knudsen, J.G., "Apparatus and Techniques for Measurement of Fouling of Heat Transfer Surfaces", in Fouling of Heat Transfer Equipment, Somerscales, E.F.C. and Knudsen, J.G., (eds), Hemisphere, Washington, pp. 57-81, 1981.
 51. Wilson, E.E., "A Basis for Rational Design of Heat Transfer Apparatus", Trans.

- A.S.M.E., vol. 37, p. 47, 1915.
52. Wiegand, J.H., "Discussion of Paper by McMillen and Larson", Trans. AIChE, vol. 41, p. 147, 1945.
53. Cole, R., "Nucleate - Boiling Heat Transfer, a General Survey", in Boiling Phenomena, Van Stralen, S. and Cole, R., (eds), Hemisphere, Washington, pp. 155 - 193, 1979.
54. Stephan, K., "Bubble Formation and Heat Transfer in Natural Convection Boiling", in Heat Transfer in Boiling, Hahne, E. and Grigull, U., (eds), Hemisphere, Washington, pp. 3 - 18, 1977.
55. Collier, J.G., "Pool Boiling", in Hemisphere Handbook of Heat Exchanger Design, Hewitt, G.F., (ed), Hemisphere, New York, pp. 2.7.2-1 - 2.7.2-6, 1990.
56. Collier, J.G., "Pool Boiling", in Hemisphere Handbook of Heat Exchanger Design, Hewitt, G.F., (ed), Hemisphere, New York, p. 2.7.2-7. 1990.
57. Knudsen, J.G., "Fouling in Heat Exchangers", in Hemisphere Handbook of Heat Exchanger Design, Hewitt, G.F., (ed), Hemisphere, New York, p. 3.17.2-1, 1990.
58. Knudsen, J.G. and Katz, D.L., "Fluid Dynamics and Heat Transfer", McGraw-Hill, New York, p. 403, 1958.

APPENDICES

APPENDIX A

HEATER CALIBRATION

Table A.1 and Figure A.1 show the calibration results of the clean and fouled heater. The fouling resistance recorded at the end of this run, AMO-FDC(263)-38a, is equal to $9.1 \times 10^{-4} \text{ hr ft}^2 \text{ }^\circ\text{F/Btu}$. The changes between clean and fouled conditions can be determined as follows:

$$\begin{aligned} \text{Change of intercept} &= \text{Fouled} - \text{Clean} & (A.1) \\ &= 7.467 \times 10^{-4} - 4.647 \times 10^{-4} = 2.820 \times 10^{-4} \text{ (hr ft}^2 \text{ }^\circ\text{F/Btu)} \end{aligned}$$

$$\begin{aligned} \text{Change of slope (\%)} &= \frac{\text{Fouled} - \text{Clean}}{\text{Clean}} & (A.2) \\ &= \frac{3.222 \times 10^{-3} - 3.152 \times 10^{-3}}{3.152 \times 10^{-3}} = 2.2 \% \end{aligned}$$

Compared to the recorded value of $9.1 \times 10^{-4} \text{ (hr ft}^2 \text{ }^\circ\text{F/Btu)}$, the change of intercept ($2.82 \times 10^{-4} \text{ hr ft}^2 \text{ }^\circ\text{F/Btu}$) is relatively low. Since the difference between this two values is as large as $6.28 \times 10^{-4} \text{ (hr ft}^2 \text{ }^\circ\text{F/Btu)}$, the fouling deposit seems to be washed out partially by water during the calibration process.

Variation in slopes is only 2.2 % which means that there is no significant change in convection heat transfer coefficient (h) between the clean and fouled surface. This result indicates the previous assumption in Chapter 2.4.2 is reasonable. This small change is believed due to the experimental error or the increasing roughness in the heat transfer surface.

Table A.1 Calibration results for clean and fouled heater

At Clean Condition :

Flow Rate (GPM)	Power (Watts)	T _b (F)	T _w (F)	U (*)	1 / U (**)	^{0.8} 1 / V (***)
15.3	1000	59	173	1219	8.200E-04	1.127E-01
14.5	974	59	173	1188	8.419E-04	1.175E-01
13.8	952	59	172	1171	8.538E-04	1.227E-01
13.0	930	60	172	1154	8.663E-04	1.287E-01
12.1	902	60	172	1120	8.932E-04	1.359E-01
11.2	880	60	172	1092	9.155E-04	1.446E-01
10.2	850	60	173	1046	9.563E-04	1.559E-01
9.0	802	60	172	995	1.005E-03	1.726E-01
8.6	782	60	172	971	1.030E-03	1.790E-01
7.7	746	60	172	926	1.080E-03	1.958E-01
6.7	702	60	173	864	1.158E-03	2.194E-01
5.4	628	60	172	779	1.283E-03	2.591E-01
----- INTERCEPT ----- SLOPE ----- RSQRD ----- k / x -----						
4.647 E-04		3.152 E-03		9.994 E-01		2.152 E+03

At Fouled Condition :

Flow Rate (GPM)	Power (Watts)	T _b (F)	T _w (F)	U (*)	1 / U (**)	^{0.8} 1 / V (***)
15.3	1000	66	219	909	1.101E-03	1.131E-01
14.5	980	67	220	890	1.123E-03	1.175E-01
13.8	956	67	219	874	1.144E-03	1.227E-01
13.0	940	67	218	865	1.156E-03	1.287E-01
12.1	920	66	218	841	1.188E-03	1.359E-01
11.2	896	66	218	819	1.220E-03	1.446E-01
10.2	872	67	219	798	1.254E-03	1.559E-01
9.0	836	67	219	765	1.308E-03	1.727E-01
8.2	708	67	218	744	1.344E-03	1.850E-01
7.5	786	67	219	719	1.391E-03	1.993E-01
6.4	742	67	219	679	1.474E-03	2.259E-01
5.4	694	67	219	635	1.575E-03	2.591E-01
----- INTERCEPT ----- SLOPE ----- RSQRD ----- k / x -----						
7.467 E-04		3.222 E-03		9.987 E-01		1.339 E+03

* Btu / hr ft² °F** hr ft² °F / Btu*** 1 / (GPM)^{0.8}

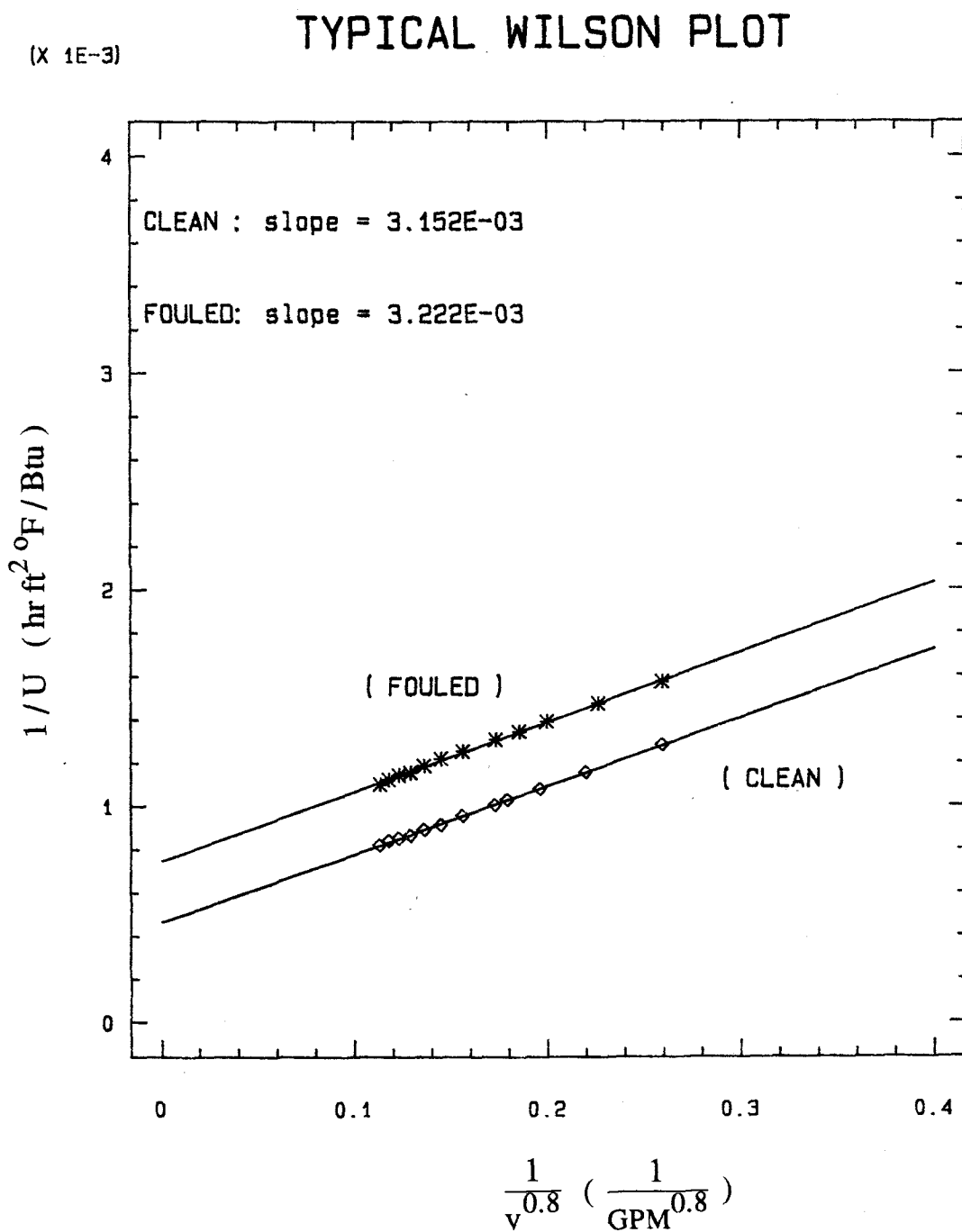


Figure A.1 Calibration results for clean and fouled heater

APPENDIX B

COMPUTER PROGRAM

The following computer program is used for the data acquisition, processing and monitoring the fouling process. In case of excessive temperatures of heater rod, this program also performs to shut the heater power off.

At a bulk temperature of 300 °F, totally 20 fouling tests (10 dry bulk tests and 10 wet bulk tests) were completed. In these 20 tests, it was very difficult to maintain the bulk temperature constant even though with no power input in the band heaters and silicon rubber heaters. The variation of bulk temperature is large in some experiments. In this situation, this program (Line 1630) was changed to use Equation (B.1) instead of Equation (2.24). Equation (B.1) is derived with considering the variation of bulk temperature and is given as follows:

$$R_f = \frac{T_{wf} - T_{wo} - T_{bf} + T_{bo}}{\left(\frac{q}{A}\right)_o} \quad (B.1)$$

The computer program is given below and is followed by an example output from the computer.

Computer program is as follows:

```

10 REM *****
20 REM *          VARIABLE DICTIONARY          999999999999 *
40 REM *   STAT = Heater status flag *
50 REM *   T = Measured variable array *
60 REM *   J = CHANNEL NUMBER *
70 REM *   TAVG = Averaged variable array *
80 REM *   SETHI = Upper heater setpoint *
90 REM *   SETLO = Lower heater setpoint *
100 REM *   TIME = Numerical value of present time *
110 REM *   SCTIME = Next scan time *
120 REM *   NSCAN = Current number of scans *
130 REM *   ITIME = Scan interval *
140 REM *
150 REM *****
160 REM *
170 REM *          CHANNEL ASSIGNMENTS
180 REM *
190 REM * CHANNEL 0 = BULK TEMP IN *
200 REM * CHANNEL 1 = BULK TEMP OUT *
210 REM * CHANNEL 2 = TANK TEMP *
220 REM * CHANNEL 3 = HEATER TEMP *
230 REM * CHANNEL 4 = FLOW RATE *
240 REM * CHANNEL 6 = HEATER POWER *
250 REM * CHANNEL 7 = MASS FLOW RATE *
260 REM *
270 REM *****
280 DIM HDATA(100,100),AVDATA#(10),AVDATA(10),TDATA(100),PDATA(100),FDATA(100)
290 DEF SEG=&H1F50:BLOAD "ADAPT.TSK",0
300 DEFINT A-Z
310 INIT=0:SLOWAD=45:TRIGGER=48:BASE=&H300:GAIN=256:TRIG=1:VALUE=29829
320 DAOUT=33: DIGOUT=24: DAUNI=0: DAMODE=1: HS=0: VALUE1=64
330 CALL INIT(BASE)
340 ON KEY(1) GOSUB 3130
350 KEY(1) ON
360 ON KEY(2) GOSUB 3390
370 KEY(2) ON
380 ON KEY(3) GOSUB 3470
390 KEY(3) ON
400 ON KEY(4) GOSUB 3310
410 KEY(4) ON
420 REM
430 REM Initialize program
440 REM
450 NSCAN=0
460 PTIME#=0
470 RTIME#=0
480 CHAHEAT=0
490 CHAPUMP=1
500 BITHEAT=1
510 BITPUMP=1
520 CALL DIGOUT(CHACHEAT,BITHEAT)
530 CALL DIGOUT(CHAPUMP,BITPUMP)
540 ON ERROR GOTO 540
550 ACS#=.002475
560 KX#=2024.5
570 RW#=1/KX#
580 PRINT "ENTER HEATER POWER (MILLIVOLTS)"
590 INPUT POWER#
600 POWER#=POWER#*25.115
610 PRINT "Enter upper temperature setpoint for heater (Deg F)"
620 INPUT SETHI#
630 PRINT "Press F5 when ready"
640 STOP
650 ON ERROR GOTO 0
660 OPEN "C:\FDC263.01" FOR OUTPUT AS #1
670 PRINT "ENTER THE SCAN INTERVAL IN MINUTES"
680 INPUT ITIME#
690 ITIME#=ITIME#*100
700 HH#=VAL(MID$(TIME$,1,2))
710 MM#=VAL(MID$(TIME$,4,2))
720 SS#=VAL(MID$(TIME$,7,2))
730 TIME#=HH#*10000+MM#*100+SS#

```

```

740 LRTIME#=TIME#
750 SCTIME#=ITIME#+TIME#
760 SCTIMEHH=INT(SCTIME#/10000)
770 SCTIMEMM=INT(SCTIME#/100)
780 SCTIMESS=SCTIME#-SCTIMEMM*100
790 SCTIMEDM=SCTIMEMM-SCTIMEHH*100
800 IF SCTIMEDM>=60 THEN SCTIME#=(SCTIMEHH+1)*10000+(SCTIMEDM-60)*100+SCTIMESS
810 IF SCTIME#>=240000! THEN SCTIME#=SCTIME#-240000!
820 REM
830 REM Collect base data
840 REM
850 CLS
860 BFLOW#=0
870 BTB#=0
880 BWATTS#=0
890 BTW#=0
900 BU#=0
920 BHPRED#=0
930 FOR BASE=0 TO 9
940 PRINT "COLLECTING BASE DATA #";BASE
950 GOSUB 1960
960 BFLOW#=BFLOW#+AVDATA#(7)
970 BTB#=BTB#+(AVDATA#(0)+AVDATA#(1))/2
980 BWATTS#=BWATTS#+AVDATA#(6)
990 BTW#=BTW#+AVDATA#(3)
1000 NEXT BASE
1010 BFLOW#=BFLOW#/(BASE)
1020 BTB#=BTB#/(BASE)
1030 TB#=BTB#
1040 BTW#=BTW#/(BASE)
1050 BWATTS#=BWATTS#/(BASE)
1060 BFLUX#=POWER#*139.017
1070 BU#=BFLUX#/(BTW#-BTB#)
1080 BH#=1/(1/BU#-RW#)
1090 TS#=BTW#-BFLUX#*RW#
1100 AVDATA#(3)=BTW#
1110 POWER=CINT(POWER#)
1120 TWSCAN#=BTW#
1130 VELB#=VEL#
1140 REM
1150 PRINT #1,"      FOULING DATA FOR RESID IN OIL - RUN AMO-FDC(263)-01":PRINT
1160 LPRINT "      FOULING DATA FOR RESID IN OIL - RUN AMO-FDC(263)-01":LPRINT
1170 PRINT #1," "
1180 LPRINT " "
1190 PRINT #1,"      INIT. H.T. COEFF. = ";CINT(BH#);"BTU/HR FT2 F"
1200 LPRINT "      INIT. H.T. COEFF. = ";CINT(BH#);"BTU/HR FT2 F"
1210 PRINT #1," "
1220 LPRINT " "
1230 PRINT #1,"      TIME      VELOCITY      POWER      TBULK      TWALL      TSURF      RESISTANCE"
1240 PRINT #1,"      HOURS      FT/SEC      WATTS      DEG F      DEG F      DEG F      HR FT2 F/BTU"
1250 PRINT #1,"      -----"
1260 LPRINT "      TIME      VELOCITY      POWER      TBULK      TWALL      TSURF      RESISTANCE"
1270 LPRINT "      HOURS      FT/SEC      WATTS      DEG F      DEG F      DEG F      HR FT2 F/BTU"
1280 LPRINT "      -----"
1290 PRINT #1," "
1300 LPRINT " "
1310 GOSUB 3040
1320 CLS
1330 REM
1340 REM Begin scan routine
1350 REM
1360 REM Determine next scan
1370 REM
1380 HH#=VAL(MID$(TIMES$,1,2))
1390 MM#=VAL(MID$(TIMES$,4,2))
1400 SS#=VAL(MID$(TIMES$,7,2))
1410 TIME#=HH#*10000+MM#*100+SS#
1420 IF SCTIME#>=240000! THEN SCTIME#=SCTIME#-240000!
1430 IF (TIME#>=SCTIME#) AND ((TIME#-SCTIME#)<10000) THEN GOSUB 2870
1440 GOSUB 1960
1450 REM
1460 REM End control routine

```

```

1470 REM
1480 TB#=(AVDATA#(0)+AVDATA#(1))/2
1490 TB=CINT(TB#)
1500 AVDATA(3)=CINT(AVDATA#(3))
1510 POWER=CINT(POWER#)
1560 TB#=TB
1570 AVDATA#(3)=AVDATA(3)
1580 POWER#=POWER
1600 FLUX#=POWER#*139.017
1610 U#=FLUX#/(AVDATA#(3)-TB#)
1620 XH#=BH#
1630 RF#=(AVDATA#(3)-BTW#)/FLUX#
1635 U2#=1/(RW#+RF#)
1640 TS#=AVDATA#(3)-(FLUX#/U2#)
1650 IF AVDATA#(6)=0 THEN RF#=0!
1660 IF AVDATA#(7)=0 THEN TS#=0 AND RF#=0
1670 POWER=CINT(POWER#)
1680 IF (AVDATA#(3)>SETHI#) THEN GOSUB 3880
1690 REM
1700 REM End scan routine
1710 REM
1720 PRINT "    DATE                      CURRENT TIME                      NEXT SCAN    "
1730 PRINT "-----"
1740 PRINT DATES$, "          ", TIMES$, "          ", SCTIME#
1750 PRINT
1760 PRINT "BULK          BULK          ROD          SURFACE"
1770 PRINT "TEMP1 (F)      TEMP2 (F)      TEMP (F)      TEMP (F)  "
1780 PRINT USING "###          "; AVDATA#(0), AVDATA#(1), AVDATA#(3), TS#
1790 PRINT
1800 PRINT "HEATER          FLOW          SURFACE          FOULING"
1810 PRINT "POWER (W)      RATE (LB/MIN)  VELOCITY (FT/S)  RESISTANCE  "
1820 MSK$="####          ###.##          ##.##          ##.#####"
1830 PRINT USING MSK$; POWER, AVDATA#(7), VEL#, RF#
1840 PRINT
1850 PRINT "UPPER          "
1860 PRINT "SETPPOINT (F)  "
1870 MSK$="###          "
1880 PRINT USING MSK$; SETHI#
1890 PRINT
1900 PRINT "*****"
1910 PRINT "          F1.....Change scan interval          "
1920 PRINT "          F2.....Terminate program              "
1930 PRINT "          F3.....Change heater setpoint          "
1940 PRINT "          F4.....Change heater power              "
1950 GOTO 1330
1960 REM
1970 REM Scan routine
1980 REM
1990 GAIN=64
2000 FOR N=0 TO 9
2010 AVDATA#(N)=0
2020 AVDATA(N)=0
2030 FDATA(N)=0
2040 NEXT N
2050 FOR J=0 TO 9
2060 FOR I=0 TO 9
2070 TDATA(I,J)=0
2080 NEXT I
2090 NEXT J
2100 FOR J=1 TO 2
2110 FOR I=0 TO 9
2120 CALL TRIGGER(TRIG, VALUE)
2130 CALL SLOWAD(J, GAIN, TDATA(I, J))
2140 NEXT I
2150 NEXT J
2160 FOR J=1 TO 2
2170 FOR I=1 TO 9
2180 AVDATA#(J)=AVDATA#(J)+TDATA(I, J)
2190 NEXT I
2200 NEXT J
2210 FOR J=1 TO 2
2220 AVDATA#(J)=AVDATA#(J)/(4095*GAIN*9)*1000
2230 NEXT J
2240 GAIN=1
2250 J=0
2260 AVDATA#(J)=0
2270 FOR I=0 TO 9
2280 CALL TRIGGER(TRIG, VALUE)

```

```

2290 CALL SLOWAD(J,GAIN,HDATA(I))
2300 NEXT I
2310 FOR I=1 TO 9
2320 AVDATA#(J)=AVDATA#(J)+HDATA(I)
2330 NEXT I
2340 AVDATA#(J)=AVDATA#(J)/(4095*GAIN*9)*1000
2350 AVDATA#(J)=AVDATA#(J)/100
2360 GAIN=1
2370 J=3
2380 AVDATA#(J)=0
2390 FOR I=0 TO 9
2400 CALL TRIGGER(TRIG,VALUE)
2410 CALL SLOWAD(J,GAIN,HDATA(I))
2420 NEXT I
2430 FOR I=1 TO 9
2440 AVDATA#(J)=AVDATA#(J)+HDATA(I)
2450 NEXT I
2460 AVDATA#(J)=AVDATA#(J)/(4095*GAIN*9)*1000
2470 AVDATA#(J)=AVDATA#(J)/10
2480 GAIN=1
2490 J=7
2500 FOR I=0 TO 9
2510 CALL TRIGGER(TRIG,VALUE)
2520 CALL SLOWAD(J,GAIN,FDATA(I))
2530 NEXT I
2540 FOR I=1 TO 9
2550 AVDATA#(J)=AVDATA#(J)+FDATA(I)
2560 NEXT I
2570 AVDATA#(J)=AVDATA#(J)/(4095*GAIN*9)*1000
2580 GAIN=1
2590 J=6
2600 FOR I=0 TO 9
2610 CALL TRIGGER(TRIG,VALUE)
2620 CALL SLOWAD(J,GAIN,PDATA(I))
2630 NEXT I
2640 FOR I=1 TO 9
2650 AVDATA#(6)=AVDATA#(6)+PDATA(I)
2660 NEXT I
2670 AVDATA#(6)=AVDATA#(6)/(4095*GAIN*9)*1000
2680 REM
2690 REM Convert thermocouple voltages
2700 REM
2710 GOSUB 3550
2720 REM
2730 REM Convert power voltages
2740 REM
2750 GOSUB 3720
2760 REM
2770 REM Convert flow voltages
2780 REM
2790 GOSUB 3790
2800 REM
2810 SPGR#=.832
2820 VEL#=AVDATA#(7)/(SPGR#*62.4*ACS#*60)
2850 CLS
2860 RETURN
2870 REM
2880 REM Record scan data
2890 REM
2900 RTIME#=RTIME#+ITIME#*60
2910 CLS
2920 PRINT "RECORDING DATA"
2930 HH#=VAL(MID$(TIMES$,1,2))
2940 MM#=VAL(MID$(TIMES$,4,2))
2950 SS#=VAL(MID$(TIMES$,7,2))
2960 LRTIME#=HH#*10000+MM#*100+SS#
2970 SCTIME#=SCTIME#+ITIME#
2980 SCTIMEHH=INT(SCTIME#/10000)
2990 SCTIME#MM=INT(SCTIME#/100)
3000 SCTIME#SS=SCTIME#-SCTIME#MM*100
3010 SCTIMEDM=SCTIME#MM-SCTIMEHH*100
3020 IF SCTIMEDM>=60 THEN SCTIME#=(SCTIMEHH+1)*10000+(SCTIMEDM-60)*100+SCTIME#SS
3030 IF SCTIME#>=240000! THEN SCTIME#=(SCTIME#-240000!)
3040 MSK$="###.##    .##    .###    .###    .###    .###    .###.#####"
3050 PRINT #1,USING MSK$;RTIME#;VEL#;POWER;TB#;AVDATA#(3);TS#;RF#
3060 LPRINT USING MSK$;RTIME#;VEL#;POWER;TB#;AVDATA#(3);TS#;RF#

```

```

3070 REM
3080 IF ITIME#=#15 THEN IF AVDATA#(3)>=TWSCAN#+10 THEN ITIME#=#3:GOTO 3100 ELS
E GOTO 3090
3090 IF ITIME#=#3 THEN IF AVDATA#(3)>=TWSCAN#+3 THEN GOTO 3100 ELSE ITIME#=#15

3100 GOSUB 3220
3110 TWSCAN#=AVDATA#(3)
3120 RETURN
3130 REM
3140 REM Change scan increment
3150 REM
3160 CLS
3170 PRINT
3180 PRINT
3190 PRINT
3200 PRINT "ENTER SCAN INTERVAL IN MINUTES"
3210 INPUT ITIME#
3220 ITIME#=#ITIME#*100
3230 SCTIME#=#ITIME#+LRTIME#
3240 SCTIMEHH=INT(SCTIME#/10000)
3250 SCTIME#=#SCTIME#-SCTIMEHH*100
3260 SCTIMESS=SCTIME#-SCTIMEHH*100
3270 SCTIMEDM=SCTIME#-SCTIMEHH*100
3280 IF SCTIMEDM>=60 THEN SCTIME#=(SCTIMEHH+1)*10000+(SCTIMEDM-60)*100+SCTIMESS
3290 IF SCTIME#>=240000! THEN SCTIME#=#SCTIME#-240000!
3300 RETURN
3310 REM
3320 REM CHANGE HEATER POWER
3330 REM
3340 PRINT"ENTER NEW HEATER POWER (MILLIVOLTS)"
3350 INPUT POWER#
3360 POWER#=#POWER#*25.115
3370 RETURN
3380 REM
3390 REM Escape scan routine
3400 REM
3410 PRINT
3420 PRINT
3430 PRINT "Scan routine terminated"
3440 CLOSE
3450 STOP
3460 REM
3470 REM
3480 REM Change heater setpoint
3490 REM
3500 CLS
3510 PRINT "Enter new upper temperature setpoint for heater (Deg F)"
3520 INPUT SETHI#
3530 RETURN
3540 REM
3550 REM *****
3560 REM Thermocouple voltage to temperature conversion
3570 REM
3580 FOR N=0 TO 3
3590 IF (AVDATA#(N)+4.72)<0 THEN AVDATA#(N)=0
3600 IF AVDATA#(N)>-1.029 THEN GOTO 3620
3610 AVDATA#(N)=32.583*(AVDATA#(N)+5.02)^.949:GOTO 3630
3620 AVDATA#(N)=38.529*(AVDATA#(N)+4.72)^.8765
3630 NEXT N
3640 AVDATA#(1)=AVDATA#(1)+3
3650 AVDATA#(0)=AVDATA#(0)+2
3660 AVDATA#(3)=AVDATA#(3)+3
3700 RETURN
3710 REM
3720 REM *****
3730 REM Voltage to power conversion
3740 REM
3750 AVDATA#(6)=AVDATA#(6)*25.115
3760 IF AVDATA#(6)<0 THEN AVDATA#(6)=0
3770 RETURN
3780 REM *****
3790 REM
3800 REM Flowrate Conversion
3810 REM
3820 REM
3830 IF AVDATA#(7)<10 THEN AVDATA#(7)=0
3840 AVDATA#(7)=AVDATA#(7)*(55!/1001.5)*1.474

```

```
3860 RETURN
3870 REM *****
3880 REM
3890 BITHEAT=0
3900 CALL DIGOUT(CHAHEAT,BITHEAT)
3910 TIMHTOFF=RTIME#
3920 RETURN
3930 REM
3940 REM BITPUMP=0
3950 REM CALL DIGOUT(CHAPUMP,BITPUMP)
3960 REM GOTO 3450
3970 END
```


FOULING DATA FOR RESID IN OIL - RUN AMO-FDC(263)-01

INIT. H.T. COEFF. = 138 BTU/HR FT² F

TIME HOURS	VELOCITY FT/SEC	POWER WATTS	TBULK DEG F	TWALL DEG F	TSURF DEG F	RESISTANCE HR FT ² F/BTU
0.00	3.0	99	401	505	500	0.00000
0.50	2.9	99	398	502	500	-0.00023
1.00	3.0	99	402	506	500	0.00006
1.50	3.0	99	401	504	500	-0.00008
2.00	3.0	99	400	504	500	-0.00008
2.50	2.9	99	401	505	500	-0.00001
3.00	2.9	99	402	505	500	-0.00001
3.50	2.9	99	402	505	500	-0.00001
4.00	2.9	99	401	505	500	-0.00001
4.50	2.9	99	401	504	500	-0.00008
5.00	3.0	99	401	504	500	-0.00008
5.50	2.9	99	401	505	500	-0.00001
6.00	3.0	99	401	505	500	-0.00001
6.50	3.0	99	401	505	500	-0.00001
7.00	3.0	99	401	504	500	-0.00008

APPENDIX C

RESULTS OF HEAT TRANSFER TESTS

This appendix presents a computer program used for the calculations of the heat transfer tests followed by the results of sixteen tests. The indicated variables and their units are as follows:

u	: fluid velocity, ft/sec
P	: pressure, psig
POWER	: power input of heater rod, watts
FLUX	: heat flux (q/A), Btu/hr ft ²
TBULK (TB)	: bulk temperature of test fluid, °F
TWALL	: wall temperature of heater rod, °F
TSURF	: surface temperature of heater rod, °F
SUPERHEAT	: superheat ($T_s - T_b$), °F
h	: convection heat transfer coefficient, Btu/hr ft ² °F

The copmputer program used for calculation of heat transfer test is as follows:

```

10 CLS
20 REM>>>>-----PROGRAM BOIL -----<<<<
30 REM>>>>  CALCULATES BOILING DATA FOR ORGANIC FOULING UNIT      <<<<
40 REM>>>>-----<<<<
50 PRINT"                                INSTRUCTIONS":PRINT
60 PRINT"  THESE INSTRUCTIONS APPEAR WHEN YOU EXECUTE PROFGRAM, i.e. <RUN>"
70 PRINT
80 PRINT"  1. LIST 190 AND PUT IN CORRECT FILE NAME":PRINT
85 PRINT"  2. LIST 195 AND PUT IN CORRECT FILE NAME FOR OUTPUT":PRINT
90 PRINT"  3. LIST 260 AND PUT IN CORRECT VALUE OF RW (=x/k)":PRINT
100 PRINT"  4. LIST 340 AND PUT IN CORRECT RUN NUMBER":PRINT
110 PRINT"  5. WHEN STEPS 1 TO 3 HAVE BEEN COMPLETED PRESS <RUN>. THESE"
120 PRINT"    INSTRUCTIONS WILL REAPPEAR WITH AN INDICATION THAT"
130 PRINT"    EXECUTION HAS BEEN INTERRUPTED AT STATEMENT 150":PRINT
140 PRINT"    PRESS <CONT> TO CONTINUE EXECUTION":PRINT:PRINT
150 STOP
160 CLS
170 DIM FLOW$(500),WATTS$(500),TBI$(500),TBO$(500),TB$(500),TW$(500)
180 DIM U$(500),XH$(500),FLUX$(500),TS$(500),VEL$(500),DT$(500)
190 OPEN "BOIL263.01" FOR INPUT AS #1
195 OPEN "RESBOIL.01"FOR OUTPUT AS #2
200 K=0
210 IF EOF(1) THEN 250
220 K=K+1
230 INPUT #1,WATTS$(K),TBI$(K),TBO$(K),TW$(K)
240 GOTO 210
250 N=K
260 RW#=1/2917
265 ACS#=.002475
340 PRINT #2, " BOILING DATA FOR RESID IN OIL - RUN AMO-FDC(263)-BO-01
      TB=400 F    u=3.0 ft/sec    P=250 psig
342 LPRINT "    BOILING DATA FOR RESID IN OIL - RUN AMO-FDC(263)-BO-01
      TB=400 F    u=3.0 ft/sec    P=250 psig
343 LPRINT" "
344 LPRINT" "
345 PRINT #2, " "
360 PRINT #2, " "
365 PRINT #2, " "
370 PRINT
380 FOR K = 1 TO N
385 REM FLOW$(K)=VEL$(K)*ACS#*448.8
390 FLUX$(K) = (WATTS$(K))*139.017
395 FLUX$(K) = (CINT(FLUX$(K)/10))*10
397 TB$(K) = .5*(TBI$(K)+TBO$(K))
400 U$(K) = FLUX$(K)/(TW$(K)-TB$(K))
410 XH$(K) = 1/(1/U$(K)-RW#)
430 TS$(K) = FLUX$(K)/XH$(K) + TB$(K)
435 DT$(K) = TS$(K)-TB$(K)
440 NEXT K
450 PRINT #2,"    POWER      FLUX      TBULK      TWALL      TSURF      SUPERHEAT      h
"
455 LPRINT "    POWER      FLUX      TBULK      TWALL      TSURF      SUPERHEAT      h "
460 PRINT #2,"    WATTS      BTU/HR FT2  DEG F    DEG F    DEG F    DEG F    BTU/HR
FT2 F"
465 LPRINT "    WATTS      BTU/HR FT2  DEG F    DEG F    DEG F    DEG F    BTU/HR FT2
F"
470 PRINT #2,"    -----
"
475 LPRINT"    -----
"
480 FOR K = 1 TO N
485 MSK$="#####   ###   ###   ###   ###   ####"
490 PRINT #2,USING MSK$;WATTS$(K),FLUX$(K),TB$(K),TW$(K),TS$(K),DT$(K),XH$(K)
495 LPRINT USING MSK$;WATTS$(K),FLUX$(K),TB$(K),TW$(K),TS$(K),DT$(K),XH$(K)
510 NEXT K
520 CLOSE #2
530 END

```

BOILING DATA FOR RESID IN OIL - RUN AMO-FDC(263)-BO-01
 TB=400 F u=3.0 ft/sec P=250 psig

POWER WATTS	FLUX BTU/HR FT2	TBULK DEG F	TWALL DEG F	TSURF DEG F	SUPERHEAT DEG F	h BTU/HR FT2 F
25	3480	400	424	423	23	150
50	6950	400	447	445	45	154
75	10430	400	468	464	64	162
100	13900	401	489	484	84	166
125	17380	401	510	504	103	168
150	20850	401	530	523	122	171
175	24330	401	549	540	139	175
200	27800	401	568	558	157	177
225	31280	402	587	576	174	179
250	34750	402	608	596	194	179
275	38230	402	626	612	211	181
300	41710	402	644	629	228	183
325	45180	402	662	646	244	185
350	48660	402	682	665	263	185
375	52130	402	698	680	278	187
400	55610	402	714	694	292	190
425	59080	403	732	711	309	191
450	62560	402	750	728	326	192
475	66030	402	766	743	341	194
500	69510	402	784	759	358	194
525	72980	402	801	775	374	195
550	76460	402	816	789	387	197
575	79930	402	832	804	402	199
600	83410	402	850	820	419	199
625	86890	402	870	839	438	199
650	90360	402	887	855	453	199
675	93840	402	903	870	468	201

BOILING DATA FOR RESID IN OIL - RUN AMO-FDC(263)-BO-02
 TB=400 F u=5.5 ft/sec P=250 psig

POWER WATTS	FLUX BTU/HR FT2	TBULK DEG F	TWALL DEG F	TSURF DEG F	SUPERHEAT DEG F	h BTU/HR FT2 F
25	3480	400	417	416	16	221
50	6950	400	434	432	32	220
75	10430	400	451	447	47	220
100	13900	400	468	463	63	220
125	17380	400	485	479	79	220
150	20850	400	500	493	93	225
175	24330	400	515	506	106	229
200	27800	400	530	520	120	231
225	31280	401	547	536	135	231
250	34750	401	560	548	147	236
275	38230	401	577	563	163	235
300	41710	401	592	577	177	236
325	45180	401	606	590	189	238
350	48660	401	623	606	205	237
375	52130	401	637	619	218	239
400	55610	402	650	630	229	243
425	59080	402	665	644	243	244
450	62560	402	679	657	255	245
475	66030	402	694	671	269	245
500	69510	402	708	683	282	247
525	72980	402	722	696	294	248
550	76460	402	736	709	307	249
575	79930	402	750	722	320	250
600	83410	402	764	734	332	251
625	86890	403	778	747	344	252
650	90360	403	792	760	357	253
675	93840	403	805	772	369	254
700	97310	403	819	785	382	255
725	100790	403	836	800	397	254

BOILING DATA FOR RESID IN OIL - RUN AMO-FDC(263)-BO-03
 TB=400 F u=8.0 ft/sec P=250 psig

POWER WATTS	FLUX BTU/HR FT2	TBULK DEG F	TWALL DEG F	TSURF DEG F	SUPERHEAT DEG F	h BTU/HR FT2 F
25	3480	400	413	412	12	284
50	6950	401	427	425	24	289
75	10430	401	440	436	36	291
100	13900	401	454	449	49	286
125	17380	401	467	461	60	288
150	20850	401	480	473	72	289
175	24330	401	493	484	83	292
200	27800	401	506	496	95	292
225	31280	402	518	507	105	297
250	34750	402	531	519	117	297
275	38230	402	542	528	127	301
300	41710	402	554	539	138	303
325	45180	401	566	550	149	303
350	48660	401	578	561	160	305
375	52130	401	591	573	172	304
400	55610	401	602	582	181	307
425	59080	401	615	594	193	306
450	62560	401	627	605	204	307
475	66030	401	639	616	215	308
500	69510	401	651	626	225	308
525	72980	401	662	636	235	310
550	76460	401	673	646	245	312
575	79930	401	683	655	254	315
600	83410	402	695	665	263	317
625	86890	403	706	675	272	319
650	90360	403	717	685	282	320
675	93840	403	727	694	291	323
700	97310	403	739	705	302	323
725	100790	403	750	714	311	324
750	104260	403	762	725	322	324
775	107740	403	773	735	332	325
800	111210	403	784	745	342	326
825	114690	403	796	755	352	325
850	118160	403	807	765	362	326

BOILING DATA FOR RESID IN OIL - RUN AMO-FDC(263)-BO-04
 TB=400 F u=10.0 ft/sec P=250 psig

POWER WATTS	FLUX BTU/HR FT2	TBULK DEG F	TWALL DEG F	TSURF DEG F	SUPERHEAT DEG F	h BTU/HR FT2 F
25	3480	399	411	410	11	323
50	6950	400	423	421	21	330
75	10430	400	435	431	32	328
100	13900	400	447	442	43	326
125	17380	400	458	452	52	332
150	20850	400	468	461	61	341
175	24330	400	480	471	72	338
200	27800	400	490	480	81	345
225	31280	400	501	490	90	346
250	34750	400	512	500	100	347
275	38230	400	523	509	110	348
300	41710	399	533	518	120	348
325	45180	399	545	529	130	346
350	48660	399	555	538	139	349
375	52130	399	566	548	149	350
400	55610	399	577	557	159	350
425	59080	399	588	567	169	350
450	62560	399	599	577	178	351
475	66030	399	610	587	188	351
500	69510	401	621	596	196	355
525	72980	401	631	605	205	357
550	76460	401	641	614	213	358
575	79930	402	652	624	222	360
600	83410	402	661	631	230	363
625	86890	402	671	640	238	365
650	90360	402	680	648	246	367
675	93840	402	690	657	255	368
700	97310	402	701	667	265	368
725	100790	402	711	675	273	369
750	104260	402	721	684	282	370
775	107740	402	730	692	290	372
800	111210	403	741	702	299	372
825	114690	403	752	711	308	372

BOILING DATA FOR RESID IN OIL - RUN AMO-FDC(263)-BO-05
 TB=400 F u=3.0 ft/sec P=250 psig

POWER WATTS	FLUX BTU/HR FT2	TBULK DEG F	TWALL DEG F	TSURF DEG F	SUPERHEAT DEG F	h BTU/HR FT2 F
25	3480	400	448	446	46	75
50	6950	401	475	472	71	97
75	10430	401	495	490	90	116
100	13900	401	513	507	106	131
125	17380	401	530	522	122	143
150	20850	401	542	532	132	158
175	24330	401	552	541	140	173
200	27800	401	563	550	150	186
225	31280	401	571	557	156	200
250	34750	401	580	564	164	212
275	38230	401	588	571	170	225
300	41710	401	595	576	175	238
325	45180	401	602	581	180	250
350	48660	401	609	587	186	262
375	52130	401	615	591	190	274
400	55610	401	622	597	196	284
425	59080	402	628	601	200	296
450	62560	402	633	604	202	309
475	66030	402	639	609	207	319
500	69510	402	644	612	210	331
525	72980	402	650	617	215	340
550	76460	402	655	620	218	351
575	79930	402	659	622	220	363
600	83410	402	664	626	224	373
625	86890	402	669	629	227	382
650	90360	402	672	631	229	395
675	93840	402	677	634	232	404
700	97310	402	682	638	236	413
725	100790	402	686	640	238	424
750	104260	402	691	643	241	432
775	107740	402	696	647	245	440
800	111210	402	701	650	248	448

BOILING DATA FOR RESID IN OIL - RUN AMO-FDC(263)-BO-06
 TB=400 F u=5.5 ft/sec P=250 psig

POWER WATTS	FLUX BTU/HR FT2	TBULK DEG F	TWALL DEG F	TSURF DEG F	SUPERHEAT DEG F	h BTU/HR FT2 F
25	3480	399	414	412	13	259
50	6950	399	447	444	45	155
75	10430	400	472	467	67	155
100	13900	400	496	490	90	155
125	17380	400	518	510	110	158
150	20850	400	535	525	125	166
175	24330	400	546	535	135	180
200	27800	400	555	542	142	195
225	31280	400	561	547	147	213
250	34750	400	568	552	152	228
275	38230	400	573	556	156	246
300	41710	400	579	560	160	261
325	45180	400	583	562	162	278
350	48660	400	589	567	167	292
375	52130	400	594	570	170	306
400	55610	400	598	573	173	322
425	59080	400	603	576	176	336
450	62560	400	607	578	178	351
475	66030	401	611	581	180	367
500	69510	401	615	583	182	381
525	72980	401	619	586	185	395
550	76460	401	623	588	187	409
575	79930	401	627	590	189	422
600	83410	401	630	592	191	437
625	86890	401	633	593	192	452
650	90360	401	637	596	195	464
675	93840	402	641	598	196	478
700	97310	402	643	599	197	495
725	100790	402	646	600	198	509
750	104260	402	649	601	199	523

BOILING DATA FOR RESID IN OIL - RUN AMO-FDC(263)-BO-07
 TB=400 F u=8.0 ft/sec P=250 psig

POWER WATTS	FLUX BTU/HR FT2	TBULK DEG F	TWALL DEG F	TSURF DEG F	SUPERHEAT DEG F	h BTU/HR FT2 F
25	3480	400	412	410	10	334
50	6950	400	421	418	18	390
75	10430	400	431	426	26	398
100	13900	400	462	456	56	250
125	17380	400	476	468	68	255
150	20850	400	492	482	82	253
175	24330	400	506	495	95	256
200	27800	401	518	505	104	267
225	31280	400	530	516	116	270
250	34750	400	543	527	127	273
275	38230	400	552	535	135	284
300	41710	400	560	541	141	296
325	45180	400	567	546	146	309
350	48660	399	571	549	150	325
375	52130	399	574	550	151	345
400	55610	399	579	554	155	360
425	59080	399	584	557	158	374
450	62560	400	588	559	159	392
475	66030	400	592	562	162	408
500	69510	400	597	565	165	421
525	72980	401	601	568	167	438
550	76460	401	604	569	168	455
575	79930	401	607	570	169	472
600	83410	401	611	573	172	485
625	86890	401	614	574	173	501
650	90360	401	617	576	175	517
675	93840	401	619	576	175	536

BOILING DATA FOR RESID IN OIL - RUN AMO-FDC(263)-BO-08
 TB=400 F u=10.0 ft/sec P=250 psig

POWER	FLUX	TBULK	TWALL	TSURF	SUPERHEAT	h
WATTS	BTU/HR FT2	DEG F	DEG F	DEG F	DEG F	BTU/HR FT2 F

25	3480	400	409	407	7	470
50	6950	399	418	415	16	439
75	10430	399	427	422	23	449
100	13900	399	436	430	31	453
125	17380	399	444	436	37	469
150	20850	399	458	448	49	421
175	24330	399	477	466	67	364
200	27800	399	490	477	78	355
225	31280	399	500	486	87	361
250	34750	399	510	494	95	365
275	38230	399	519	502	103	373
300	41710	399	529	510	111	376
325	45180	401	538	517	116	388
350	48660	401	545	523	122	400
375	52130	401	552	528	127	410
400	55610	401	560	535	134	416
425	59080	401	566	539	138	428
450	62560	402	571	542	140	445
475	66030	402	576	546	144	459
500	69510	402	581	549	147	472
525	72980	402	585	552	150	488
550	76460	402	589	554	152	503
575	79930	401	593	556	155	514
600	83410	401	597	559	158	528
625	86890	401	601	561	160	542
650	90360	401	604	563	162	559
675	93840	401	606	563	162	579
700	97310	401	610	566	165	591
725	100790	401	613	567	166	607
750	104260	401	617	569	168	619

BOILING DATA FOR RESID IN OIL - RUN AMO-FDC(263)-BO-09
 TB=400 F u=3.0 ft/sec P=250 psig

POWER WATTS	FLUX BTU/HR FT2	TBULK DEG F	TWALL DEG F	TSURF DEG F	SUPERHEAT DEG F	h BTU/HR FT2 F
25	3480	400	451	449	49	71
50	6950	400	488	485	85	82
75	10430	401	525	520	120	87
100	13900	401	544	537	136	102
125	17380	401	554	546	145	120
150	20850	401	562	552	151	138
175	24330	401	570	558	157	155
200	27800	401	578	565	164	170
225	31280	401	585	570	169	185
250	34750	401	591	574	173	200
275	38230	401	598	580	179	214
300	41710	401	605	585	184	227
325	45180	401	611	589	188	240
350	48660	401	618	595	194	251
375	52130	401	624	599	198	263
400	55610	401	631	604	203	273
425	59080	401	637	609	208	284
450	62560	401	642	612	211	296
475	66030	402	648	616	214	308
500	69510	402	653	620	218	319
525	72980	402	658	623	221	330
550	76460	402	662	625	223	342
575	79930	402	667	629	227	352
600	83410	402	671	631	229	364
625	86890	402	676	634	232	374
650	90360	402	680	637	235	385
675	93840	402	684	639	237	396
700	97310	402	688	641	239	406
725	100790	402	691	643	241	419
750	104260	402	695	645	243	429
775	107740	403	700	648	246	438
800	111210	403	704	651	248	448
825	114690	403	708	653	251	458

BOILING DATA FOR RESID IN OIL - RUN AMO-FDC(263)-BO-10
 TB=400 F u=5.5 ft/sec P=250 psig

POWER WATTS	FLUX BTU/HR FT2	TBULK DEG F	TWALL DEG F	TSURF DEG F	SUPERHEAT DEG F	h BTU/HR FT2 F
25	3480	400	415	413	13	261
50	6950	401	446	443	42	167
75	10430	401	473	468	67	156
100	13900	401	507	500	99	140
125	17380	401	530	522	121	144
150	20850	401	544	534	133	157
175	24330	401	553	541	140	173
200	27800	401	559	546	145	192
225	31280	401	566	551	150	208
250	34750	402	571	554	153	227
275	38230	401	576	558	157	244
300	41710	401	581	561	160	261
325	45180	401	586	564	163	277
350	48660	401	590	567	166	294
375	52130	401	594	569	168	310
400	55610	401	599	572	171	324
425	59080	401	603	575	174	340
450	62560	401	608	578	177	353
475	66030	401	612	580	179	368
500	69510	401	616	583	182	382
525	72980	401	619	584	183	399
550	76460	401	623	586	185	412
575	79930	401	627	589	188	426
600	83410	401	630	590	189	441
625	86890	402	634	592	190	456
650	90360	402	638	595	193	469
675	93840	402	641	596	194	483
700	97310	402	644	597	195	498
725	100790	402	646	598	196	515
750	104260	402	649	599	197	529
775	107740	403	653	601	199	542
800	111210	403	656	603	200	557

BOILING DATA FOR RESID IN OIL - RUN AMO-FDC(263)-BO-11
 TB=400 F u=8.0 ft/sec P=250 psig

POWER WATTS	FLUX BTU/HR FT2	TBULK DEG F	TWALL DEG F	TSURF DEG F	SUPERHEAT DEG F	h BTU/HR FT2 F
25	3480	400	412	410	10	337
50	6950	400	422	419	19	372
75	10430	400	435	430	30	348
100	13900	400	468	461	61	227
125	17380	400	483	475	75	233
150	20850	401	498	488	88	238
175	24330	401	512	500	100	244
200	27800	401	525	512	111	250
225	31280	401	538	523	122	256
250	34750	401	549	532	131	265
275	38230	401	558	540	139	276
300	41710	401	564	544	143	292
325	45180	401	570	548	147	307
350	48660	401	574	551	150	325
375	52130	401	579	554	153	341
400	55610	401	582	555	154	360
425	59080	402	587	559	157	376
450	62560	402	592	562	160	391
475	66030	402	595	563	161	409
500	69510	402	598	565	163	427
525	72980	402	601	566	164	445
550	76460	402	604	567	165	462
575	79930	402	607	569	167	479
600	83410	402	609	569	167	499
625	86890	402	613	571	169	513
650	90360	402	616	573	171	529
675	93840	402	618	573	171	548
700	97310	402	622	575	173	561
725	100790	402	624	576	174	580
750	104260	402	626	576	174	599
775	107740	403	628	576	173	621
800	111210	403	631	578	175	636

BOILING DATA FOR RESID IN OIL - RUN AMO-FDC(263)-BO-12
 TB=400 F u=10.0 ft/sec P=250 psig

POWER	FLUX	TBULK	TWALL	TSURF	SUPERHEAT	h
WATTS	BTU/HR FT2	DEG F	DEG F	DEG F	DEG F	BTU/HR FT2 F

25	3480	400	410	408	8	418
50	6950	400	419	416	16	443
75	10430	400	428	423	23	453
100	13900	400	437	430	30	458
125	17380	401	447	439	38	461
150	20850	401	467	457	57	369
175	24330	401	485	473	72	336
200	27800	401	496	483	82	340
225	31280	401	507	492	91	344
250	34750	401	517	500	99	350
275	38230	401	527	509	108	355
300	41710	401	535	515	114	366
325	45180	401	543	521	120	375
350	48660	401	550	527	126	387
375	52130	401	556	531	130	401
400	55610	401	561	534	133	417
425	59080	402	567	539	137	431
450	62560	402	571	541	139	450
475	66030	402	576	544	142	464
500	69510	402	580	547	145	480
525	72980	402	585	550	148	493
550	76460	402	589	552	150	508
575	79930	402	593	555	153	523
600	83410	402	596	556	154	541
625	86890	402	600	558	156	555
650	90360	402	603	560	158	573
675	93840	403	605	560	157	597
700	97310	403	609	562	159	610

BOILING DATA FOR RESID IN OIL - RUN AMO-FDC(263)-BO-13
 TB=400 F u=3.0 ft/sec P=250 psig

POWER WATTS	FLUX BTU/HR FT2	TBULK DEG F	TWALL DEG F	TSURF DEG F	SUPERHEAT DEG F	h BTU/HR FT2 F
25	3480	400	429	427	27	127
50	6950	400	455	452	52	135
75	10430	400	470	465	65	161
100	13900	400	485	478	78	178
125	17380	400	496	488	88	198
150	20850	401	508	498	97	214
175	24330	401	519	507	107	228
200	27800	401	530	517	116	240
225	31280	401	540	525	124	251
250	34750	401	550	533	133	262
275	38230	401	560	542	141	271
300	41710	401	570	550	149	279
325	45180	401	579	557	156	289
350	48660	401	588	564	163	298
375	52130	401	596	571	170	307
400	55610	401	605	578	177	314
425	59080	402	614	585	183	322
450	62560	402	622	592	190	330
475	66030	402	631	599	197	335
500	69510	402	640	606	204	340
525	72980	401	648	613	212	345
550	76460	401	656	619	218	351
575	79930	401	663	624	223	358
600	83410	401	669	629	228	366
625	86890	401	677	635	234	371
650	90360	401	684	640	239	378
675	93840	402	692	647	245	384
700	97310	402	698	651	249	391
725	100790	402	705	656	254	396
750	104260	402	712	662	260	402
775	107740	402	719	667	265	407
800	111210	402	725	671	269	413
825	114690	402	732	677	275	418
850	118160	403	739	682	279	423

BOILING DATA FOR RESID IN OIL - RUN AMO-FDC(263)-BO-14
 TB=400 F u=5.5 ft/sec P=250 psig

POWER WATTS	FLUX BTU/HR FT2	TBULK DEG F	TWALL DEG F	TSURF DEG F	SUPERHEAT DEG F	h BTU/HR FT2 F
25	3480	400	415	413	13	261
50	6950	400	429	426	26	271
75	10430	400	462	457	57	183
100	13900	400	475	468	68	204
125	17380	400	485	477	77	227
150	20850	400	494	484	84	248
175	24330	400	502	490	90	270
200	27800	400	510	497	97	288
225	31280	400	518	503	103	304
250	34750	401	525	508	108	323
275	38230	401	532	514	113	338
300	41710	400	539	519	119	351
325	45180	400	547	525	125	361
350	48660	400	554	530	130	373
375	52130	400	561	536	136	384
400	55610	400	568	541	141	394
425	59080	400	574	545	145	406
450	62560	400	582	552	152	412
475	66030	400	589	557	157	420
500	69510	400	596	562	162	428
525	72980	400	601	566	166	440
550	76460	400	608	571	171	447
575	79930	400	614	575	175	456
600	83410	400	620	580	180	464
625	86890	400	625	583	183	475
650	90360	400	631	587	187	482
675	93840	401	637	592	191	491
700	97310	401	642	595	194	500
725	100790	401	648	599	199	507
750	104260	401	654	604	203	513
775	107740	402	659	607	205	526
800	111210	402	664	610	208	534
825	114690	402	669	614	212	542
850	118160	402	674	617	215	550

BOILING DATA FOR RESID IN OIL - RUN AMO-FDC(263)-BO-15
 TB=400 F u=8.0 ft/sec P=250 psig

POWER WATTS	FLUX BTU/HR FT2	TBULK DEG F	TWALL DEG F	TSURF DEG F	SUPERHEAT DEG F	h BTU/HR FT2 F
25	3480	400	411	409	9	374
50	6950	400	422	419	19	373
75	10430	400	432	427	27	387
100	13900	400	443	436	36	383
125	17380	400	456	448	48	365
150	20850	400	474	464	64	326
175	24330	400	484	472	72	337
200	27800	400	493	480	80	349
225	31280	400	501	486	86	364
250	34750	400	508	491	91	381
275	38230	400	516	498	98	392
300	41710	400	524	504	104	402
325	45180	400	530	508	108	418
350	48660	400	537	513	113	429
375	52130	400	543	518	118	443
400	55610	400	549	522	122	455
425	59080	400	556	527	127	464
450	62560	400	562	532	132	475
475	66030	400	569	537	137	482
500	69510	400	575	541	141	492
525	72980	400	580	545	145	504
550	76460	400	587	550	150	510
575	79930	400	593	554	154	518
600	83410	400	597	557	157	532
625	86890	400	602	560	160	543
650	90360	401	607	563	163	555
675	93840	401	612	567	166	567
700	97310	401	617	570	169	576
725	100790	401	622	573	172	585
750	104260	401	627	577	176	594
775	107740	401	632	580	179	602
800	111210	401	637	583	182	610
825	114690	402	641	586	184	625
850	118160	402	646	589	187	632
875	121640	402	651	592	190	640

BOILING DATA FOR RESID IN OIL - RUN AMO-FDC(263)-BO-16
 TB=400 F u=10.0 ft/sec P=250 psig

POWER WATTS	FLUX BTU/HR FT2	TBULK DEG F	TWALL DEG F	TSURF DEG F	SUPERHEAT DEG F	h BTU/HR FT2 F
25	3480	400	410	408	8	418
50	6950	399	420	417	18	394
75	10430	399	429	424	25	418
100	13900	399	439	432	33	418
125	17380	399	447	439	40	439
150	20850	400	456	446	46	454
175	24330	401	465	453	53	461
200	27800	401	472	459	58	483
225	31280	401	481	466	65	478
250	34750	401	490	473	73	478
275	38230	401	498	480	79	484
300	41710	401	505	485	84	495
325	45180	400	513	491	91	496
350	48660	400	520	496	96	504
375	52130	400	528	503	103	507
400	55610	400	535	508	108	514
425	59080	400	542	513	113	521
450	62560	400	551	521	121	518
475	66030	400	557	525	125	528
500	69510	400	564	530	130	533
525	72980	400	570	535	135	542
550	76460	400	577	540	140	546
575	79930	400	583	544	144	554
600	83410	400	589	549	149	561
625	86890	400	594	552	152	572
650	90360	400	600	556	156	578
675	93840	400	605	560	160	588
700	97310	400	610	563	163	597
725	100790	401	616	567	166	606
750	104260	401	622	572	171	611
775	107740	402	628	576	174	620
800	111210	402	633	579	177	628
825	114690	402	639	584	182	632
850	118160	402	643	586	184	643
875	121640	402	649	590	188	646